I. SITE EFFECTS AND EXCITON STRUCTURE IN MOLECULAR CRYSTALS – BENZENE.

II. THE FIRST AND SECOND TRIPLET STATES OF SOLID BENZENE.

Thesis by

Elliot R. Bernstein

In Partial Fulfillment of the Requirements

For the Degree of

Doctor of Philosophy

California Institute of Technology

Pasadena, California

1968

(Submitted August 8, 1967)

ACKNOWLEDGMENT

That a large portion of this thesis is in many respects a joint effort is quite obvious; indeed the form of the thesis itself is in part to indicate just that. Many beneficial hours of discussion and learning were spent with Raoul Kopelman, Steve Colson, and Dino Tinti during the preparation of this material and the research itself. Steve and I have worked closely and fruitfully together for four years. I would like to thank my research advisor, Dr. G. Wilse Robinson for his enthusiastic support, encouragement, and instruction throughout the work.

The experimental procedures involved here could never have been accomplished if not for Bill Schuelke and Tony Stark of the Machine Shop and Learco Minghetti and Erich Siegel of the Glass Shop. Their help in design and dexterity in construction of apparatus was invaluable.

The support of a Woodrow Wilson National Fellowship in 1963-64 is gratefully acknowledged.

I. Site Effects and Exciton Structure in Molecular Crystals – Benzene.

II. The First and Second Triplet States of Solid Benzene.

by Elliot R. Bernstein

Abstract

The effect of intermolecular coupling in molecular energy levels (electronic and vibrational) has been investigated in neat and isotopic mixed crystals of benzene. In the isotopic mixed crystals of C_6H_6, C_6H_5D, m-$C_6H_4D_2$, p-$C_6H_4D_2$, sym-$C_6H_3D_3$, C_6D_5H, and C_6D_6 in either a C_6H_6 or C_6D_6 host, the following phenomena have been observed and interpreted in terms of a refined Frenkel exciton theory: a) Site shifts; b) site group splittings of the degenerate ground state vibrations of C_6H_6, C_6D_6, and sym-$C_6H_3D_3$; c) the orientational effect for the isotopes without a trigonal axis in both the $^1B_{2u}$ electronic state and the ground state vibrations; d) intrasite Fermi resonance between molecular fundamentals due to the reduced symmetry of the crystal site; and e) intermolecular or intersite Fermi resonance between nearly degenerate states of the host and guest molecules. In the neat crystal experiments on the ground state vibrations it was possible to observe many of these phenomena in conjunction with and in addition to the exciton structure.

To theoretically interpret these diverse experimental data, the concepts of interchange symmetry, the ideal mixed crystal, and site wave functions have been developed and are presented in detail. In the interpretation of the exciton data the relative signs of the intermolecular coupling constants have been emphasized, and in the limit of the

ideal mixed crystal a technique is discussed for locating the exciton band center or unobserved exciton components. A differentiation between static and dynamic interactions is made in the Frenkel limit which enables the concepts of site effects and exciton coupling to be sharpened. It is thus possible to treat the crystal induced effects in such a fashion as to make their similarities and differences quite apparent.

A calculation of the ground state vibrational phenomena (site shifts and splittings, orientational effects, and exciton structure) and of the crystal lattice modes has been carried out for these systems. This calculation serves as a test of the approximations of first order Frenkel theory and the atom-atom, pair wise interaction model for the intermolecular potentials. The general form of the potential employed was $V(\underset{\sim}{r}) = Be^{-Cr} - A/r^6$; the force constants were obtained from the potential by assuming the atoms were undergoing simple harmonic motion.

In part II the location and identification of the benzene first and second triplet states ($^3B_{1u}$ and $^3E_{1u}$) is given.

TABLE OF CONTENTS

To

Barbara

"riverrun, past Eve and Adam's, ..."

PART I

Electronic and Vibrational Exciton Structure in Crystalline Benzene*

ELLIOT R. BERNSTEIN, STEVEN D. COLSON,
RAOUL KOPELMAN,† and G. WILSE ROBINSON

Gates and Crellin Laboratories of Chemistry,‡
California Institute of Technology, Pasadena, California 91109

(Received 10 April 1967)

ABSTRACT

Although much work has been done on vibrational and electronic excitons in crystalline benzene, emphasis in the past has mostly been placed on "splittings" rather than on the magnitudes and relative signs of the intermolecular interaction energies (i.e., matrix elements or coupling constants) causing these splittings. Not only do the splittings and associated polarization studies in neat (pure) crystals shed light on these interaction energies, but also important in this regard are band-to-band ($\underset{\sim}{k} \neq \underset{\sim}{0}$) transitions in neat crystals; and orientational effects, site splittings, shifts, and resonance pair spectra in isotopic mixed crystals. Using a diversity of these kinds of complimentary experimental results, we shall in future papers present new information about magnitudes and relative signs of many of the pertinent coupling

* Supported in part by the National Science Foundation.

† Present address: Department of Chemistry, University of Michigan, Ann Arbor, Michigan 48104.

‡ Contribution No. 3512.

constants for vibrational and electronic excitons in crystalline benzene. The purpose of this particular paper is to lay a consistent theoretical framework for the discussion of these experimental papers. Emphasis will be placed on $\underset{\sim}{k} \neq \underset{\sim}{0}$ states, isotopic mixed crystals, and translationally equivalent interactions, as well as the Davydov splittings. The <u>interchange group</u> concept is introduced in order to simplify the theoretical analysis. From the four possible interchange groups $\underset{\sim}{D}_2$, $\underset{\sim}{C}_{2v}^{a}$, $\underset{\sim}{C}_{2v}^{b}$, $\underset{\sim}{C}_{2v}^{c}$, the $\underset{\sim}{D}_2$ group is found to be the most convenient for the classification of benzene exciton functions. A differentiation between <u>static</u> and <u>dynamic</u> interactions is made in the limit of Frenkel excitons, and the concepts of <u>site distortion energy</u> and the <u>ideal mixed crystal</u> are introduced to aid in this distinction. Data pertaining to site shifts and splittings and resonance and quasiresonance interaction terms for the $^1B_{2u}$ electronic exciton band and the vibrational $\nu_{12}(b_{1u})$, $\nu_{15}(b_{2u})$ and $\nu_{18}(e_{1u})$ exciton bands are discussed in order to illustrate the theoretical concepts.

I. INTRODUCTION

The benzene molecule has long served as a prototype for the study of π-electron systems. The benzene crystal has been of similar importance in the study of intermolecular interactions. The experimental investigation of vibrational[1] and electronic[2] transitions in solid benzene paralleled the theoretical development of symmetry considerations[3] and exciton theory[4] for molecular crystals. Several review articles discuss much of this past work.[5] More recently, a powerful approach to the investigation of exciton interactions, first mentioned by Hiebert and Hornig,[6] using off-resonance techniques in isotopic mixed crystals, has been utilized[7] in the study of the electronic exciton structure of benzene.

Certainly for vibrational excitons and probably for those electronic excitons associated with the lowest singlet and triplet states of benzene, the Frenkel limit applies. Even though the theory of Frenkel excitons has been discussed many times before, both in general and with particular reference to the benzene crystal, the presently available literature on this subject has many shortcomings for our purposes. Not only is there the usual wide range of notational differences, but unfortunately there have been a number of confusing or incorrect statements made. Most confusion seems to arise in the symmetry classification of the crystal wave functions, the Davydov "D-term", the approximations leading to closed-form expressions for eigenfunctions and eigenvalues of $\underset{\sim}{k} \neq \underset{\sim}{0}$ states and transition probabilities involving these states, the meaning of site-group splittings, and the causes of breakdown of oriented-gas model polarization properties. It is partly for this reason that we undertake to redevelop and extend the subject. In doing this we develop the concepts of the <u>ideal mixed crystal</u> and the <u>site distortion energy</u>, and clarify the meaning of the Davydov D term. We further emphasize the possible shortcomings of a first-order theory.

One of the specific purposes of this paper is to emphasize the importance of discussing exciton interactions in terms of precisely defined exciton coupling constants rather than splittings, band shapes, or overall bandwidths. While it is possible to derive uniquely these characteristics of the exciton band from the coupling constants, the converse is not generally true. In particular, for the case of benzene, merely giving the splittings among the observed three Davydov components, as has been done for both electronic and vibrational bands, in no way fixes the magnitude or relative signs of the excitation exchange interactions responsible for this splitting. This is so because one transition from the totally symmetric ground state to one of the Davydov components is dipole-forbidden. It should be further noted that the relative signs of the coupling constants have significance only if the convention used in defining the crystal wave functions is given explicitly. The interchange group concept is introduced for this purpose. Not only do the magnitudes and signs of the coupling constants uniquely define the Davydov splittings, but they also give detailed information concerning the directional properties of the excitation exchange interaction. This provides a much more sensitive test of theoretical calculations, which in the past have been compared only to overall splittings, and thus presents a means of determining the origin of these interactions (i. e., in the case of electronic excitations, mixing with ion-pair exciton states,[8] octopole-octopole interactions,[4b] exchange interactions,[7] etc.).

Using the theory we illustrate, with specific examples from the benzene crystal spectra, how to extract the exciton coupling constants. The band structure of the $^1B_{2u}$ electronic state and a few ground state vibrational bands of C_6H_6 are discussed in detail. While the magnitudes and relative signs of the exciton coupling constants (see Sec. II-F) can be obtained from studies

with unpolarized light, assignments of each coupling constant to an interaction among a specific set of molecules in the crystal requires polarization properties of the transitions to be known. Because of the difficulty of identification of crystal faces in benzene, in addition to depolarization caused by cracking and straining at low temperatures, polarization assignments are more apt to be unreliable than those in other crystals of aromatic molecules. It is hoped that unambiguous polarized light experiments can be carried out in the near future, in order that reliable assignments of the coupling constants can be made.

II. THEORY

A. Site, Interchange, and Factor Group Symmetry

The symmetry of crystals can be considered as made up of the following types of operations: (1) site operations, describing the local "point" symmetry, where the "point" of interest usually is the center of the molecular building block; and (2) transport operations, carrying a given molecular unit into a physically identical location and orientation. The transport operations can be classified further into two categories: (a) the translational operations; and (b) the interchange operations. The latter includes both proper and improper rotations, screw rotations, and glide reflections. The so-called static field interactions are related to the site symmetry, while the dynamic interactions are related to the transport symmetry. Dynamic interactions have gone under names such as excitation exchange, resonance, or exciton interactions, or by the term "the coupling of oscillators".

In the case of the benzene crystal the space group is $D_{2h}^{15}(P_{bca})$, and there are four molecules per primitive unit cell occupying sites of inversion symmetry[9] (see Fig. 1). The site group is therefore C_i. The four sets of translationally inequivalent molecules corresponding to the four sites

per unit cell are labeled I, II, III, IV. The interchange operations in the benzene crystal are the screw axis rotations C_2^a, C_2^b, and C_2^c; and the glide plane reflections σ^a ($\equiv iC_2^a$), σ^b ($\equiv iC_2^b$), and σ^c ($\equiv iC_2^c$). Considering the translations as interchange-identity operations E, certain sets of the above mentioned operations generate groups of order four[10] which we call <u>interchange groups</u>. The four interchange operations associated with an interchange group permute the four sets of translationally inequivalent molecules among themselves. There are four possible interchange groups for the benzene crystal: $\underset{\sim}{C}_{2v}^a = \{E, C_2^a, \sigma^b, \sigma^c\}$; $\underset{\sim}{C}_{2v}^b = \{E, \sigma^a, C_2^b, \sigma^c\}$; $\underset{\sim}{C}_{2v}^c = \{E, \sigma^a, \sigma^b, C_2^c\}$; and $\underset{\sim}{D}_2 = \{E, C_2^a, C_2^b, C_2^c\}$. The particular set $\{E, C_2^a, C_2^b, C_2^c\}$ is unique in that it has the virtue that the right or left handedness of a coordinate system attached to a site is preserved upon such permutations. We therefore call the set $\underset{\sim}{D}_2$ the <u>proper interchange group</u> for the benzene crystal.

The <u>factor group</u> $\underset{\sim}{D}_{2h}$ for the benzene crystal is generated as the direct product of the site group and the interchange group, $\underset{\sim}{D}_2 \times \underset{\sim}{C}_i$ for the particular case of the proper interchange group. This relationship among site, interchange, and factor group symmetry holds, however, for all interchange groups, proper as well as improper. The space symmetry of the crystal is generated from the factor group symmetry and the translational symmetry; or, alternatively, from the site and transport symmetries, or the interchange and site-translation symmetry $\underset{\sim}{S}(\alpha^1)$ defined by Vedder and Hornig.[5b] The correlation among the benzene molecular point group and the site, interchange, and factor groups in the benzene crystal is depicted in Fig. 2. It should be noted that the only non-trivial symmetry of the molecule that is carried over to the site, and therefore to the factor and space groups, is inversion.

B. Generation of Exciton Functions

In the limit of the tight-binding (Frenkel) approximation for a crystal containing N molecules with four molecules per unit cell, we construct antisymmetrized functions representing localized electronic or vibrational excitation f on a particular molecule at a given site in the crystal,

$$\phi^{f}_{nq} = \mathcal{A}\chi^{f}_{nq} \prod_{n'\neq n}^{N/4} \chi^{o}_{n'q} \tag{1}$$

where $\mathcal{A}$ is the electronic antisymmetrizing operator, n labels the unit cell, q labels the site (I, II, III, IV) in the unit cell, and χ_{nq} is a crystal site function (see below). From these functions one can generate the one-site exciton functions in the Bloch representation,[3e]

$$\phi^{f}_{q}(\underset{\sim}{k}) = (N/4)^{-\frac{1}{2}} \sum_{n=1}^{N/4} \exp(i\underset{\sim}{k}\cdot\underset{\sim}{R}_{nq})\phi^{f}_{nq} \ , \tag{2}$$

where $\underset{\sim}{R}_{nq}$ denotes the position of the center of a molecule located at the qth site in the nth unit cell with respect to a common crystal origin, and $\underset{\sim}{k}$ is the reduced wave vector. It is convenient to write,

$$\underset{\sim}{R}_{nq} = \underset{\sim}{r}_{n} + \underset{\sim}{\tau}_{nq} \ , \tag{3}$$

with $\underset{\sim}{r}_{n}$ defining some convenient local origin in the nth unit cell and $\underset{\sim}{\tau}_{nq}$ being a vector from this local origin to site q (= I, II, III, IV) in this same unit cell. Note that because of translational symmetry, $\underset{\sim}{\tau}_{nq}$ is identical for all n. Therefore, we shall hereafter drop the subscript n.

Before going further one must be specific about the site numbering. One scheme is as good as another, but it is important to be consistent and always to state explicitly which convention is used, since the appearance

of the results depends on the numbering scheme used. Using the operations of the proper interchange group $\underset{\sim}{D}_2$, we define the numbering scheme for benzene as in Table I such that for $\underset{\sim}{k} = \underset{\sim}{0}$ [11]: $C_2^a \phi_I^f(\underset{\sim}{0}) \rightarrow \phi_{II}^f(\underset{\sim}{0})$; $C_2^b \phi_I^f(\underset{\sim}{0}) \rightarrow \phi_{III}^f(\underset{\sim}{0})$; and $C_2^c \phi_I^f(\underset{\sim}{0}) \rightarrow \phi_{IV}^f(\underset{\sim}{0})$. In the same way C_2^a "interchanges" sites III and IV, C_2^b "interchanges" sites II and IV, while C_2^c "interchanges" sites II and III. This is the same numbering scheme as used by Cox but is different from that of Ref. 4b and Ref. 7.

C. The Crystal Hamiltonian

We now proceed to determine the Hamiltonian matrix elements for the specific case of the benzene crystal. The manner in which one divides up the total crystal Hamiltonian H into a zero-order part and a perturbation Hamiltonian part depends upon the representation to be employed. In the tight-binding limit, where excitation is localized primarily at the site, it is convenient to divide H into a one-site Hamiltonian H^0 and an intersite interaction Hamiltonian H':

$$H^0 = \sum_{n=1}^{N/4} \sum_{q=1}^{IV} H^0(nq) \tag{4}$$

$$H' = \tfrac{1}{2} \sum_{n=1}^{N/4} \sum_{q=1}^{IV} \sum_{n'=1}^{N/4} \sum_{q'=1}^{IV} (1 - \delta_{nn'}\delta_{qq'}) H'(nq;n'q') \tag{5}$$

where $\delta_{nn'}\delta_{qq'} = 1$ for $n = n'$ and $q = q'$ simultaneously, and zero otherwise. The eigenfunctions of $H^0(nq)$ are just the crystal site functions χ_{nq} introduced in Eq. (1). It should be emphasized that Eq. (4) does not provide for multiple excitations of two or more sites, and therefore places at least a part (for example, the R^{-6} part) of the van der Waals energy in H'. Mixing with Wannier exciton states or ion-pair states must also come from H' when using the tight-binding representation.

Since the translational subgroup of the space group is Abelian, only one-dimensional irreducible representations occur.[12] Thus, as is well known, in the Bloch representation the Hamiltonian matrix describing the energy levels associated with a set of translationally equivalent molecules in a crystal contains no off-diagonal elements. The matrix is therefore diagonal in the reduced wave vector $\underset{\sim}{k}$, each diagonal element being characterized by one specific value of this "quantum number". If only a single non-degenerate excited state of the molecule is considered and if the crystal structure is such that there is only one molecule per unit cell, i.e., if all N molecules in the crystal are translationally equivalent, then the $N \times N$ Hamiltonian matrix simply consists of N diagonal terms of the type $\langle f, \underset{\sim}{k} | H | f, \underset{\sim}{k} \rangle$, where $f, \underset{\sim}{k}$ represents the function (and its complex conjugate) of Eq. (2) for a single $\underline{q}$, and where $H = H^0 + H'$.

If two molecular states, say f' and f'', in such a crystal are considered, then the Hamiltonian matrix consists of 2N diagonal terms, $\langle f', \underset{\sim}{k} | H | f', \underset{\sim}{k} \rangle$ and $\langle f'', \underset{\sim}{k} | H | f'', \underset{\sim}{k} \rangle$. Since in general $\phi_q^f(\underset{\sim}{k})$ need not be an exact eigenfunction of H because of the choice of χ_{nq}^f, there may be "configuration interaction" terms $\langle f', \underset{\sim}{k} | H | f'', \underset{\sim}{k} \rangle$, giving rise to a matrix consisting of N 2×2 blocks along the main diagonal. Many such singly excited configurations f', f'', $f''' \cdots$ may have to be considered. In addition, again depending upon the choice of representation, there may be <u>multiply excited configurations</u> of the crystal that must be included for energy or intensity calculations. For example, the doubly excited configurations constructed from localized excitation functions,

$$\phi_{n', n''}^{f'f''} = \mathcal{A} \chi_{n'}^{f'} \chi_{n''}^{f''} \prod_{n \neq n', n''}^{N} \chi_n^0 \tag{6}$$

(for one molecule per unit cell) may be very important in the consideration of van der Waals energies and spectral shifts through the matrix elements $\langle f'f'', \underset{\sim}{k} | H | 00, \underset{\sim}{k} \rangle$ and $\langle f'f'', \underset{\sim}{k} | H | f0, \underset{\sim}{k} \rangle$.

When there are 4 molecules per unit cell (4 different sets of translationally equivalent molecules) and the possibility exists of doubly degenerate molecular states, as in the benzene crystal, the Hamiltonian matrix is a little more complicated. Considering only a single, non-degenerate excited

state $\underline{f}$, the full $N \times N$ Hamiltonian matrix consists of $N/4$ 4×4 Hermitian submatrices, each submatrix labeled by a unique $\underset{\sim}{k}$, along the main diagonal. Off-diagonal elements within each submatrix arise because of interactions among the four sets of translationally inequivalent molecules (i.e., sites). Matrices of higher-order than four would have to be considered if $\underline{f}$ described a doubly degenerate molecular state (in which case the $N/4$ submatrices are 8×8) or if interaction of the $f^{\underline{th}}$ configuration with other singly or multiply excited configurations were to be included.

D. First-Order Frenkel Theory

Using the one-site exciton functions of Eq. (2) as zero-order functions, the first-order Hamiltonian matrix elements for the excited state of crystalline benzene, corresponding to the $f^{\underline{th}}$ excited state of the molecule, are,

$$\mathcal{L}^{f}_{qq'}(\underset{\sim}{k}) = \sum_{n'=1}^{N/4} \exp i\underset{\sim}{k}\cdot(\underset{\sim}{\tau}_{q'} - \underset{\sim}{\tau}_{q}) \exp i\underset{\sim}{k}\cdot(\underset{\sim}{r}_{n'} - r_{n}) \times \int \phi^{f*}_{nq} H \phi^{f}_{n'q'} dR. \tag{7}$$

It is convenient in Eq. (7) to separate the $\underset{\sim}{k}$ independent terms, for which $q = q'$ and $n = n'$, from the $\underset{\sim}{k}$ dependent terms, and write,

$$\mathcal{L}^{f}_{qq'}(\underset{\sim}{k}) = (\epsilon^{f} + D^{f})\delta_{qq'} + L^{f}_{qq'}(\underset{\sim}{k}), \tag{8}$$

where

$$\epsilon^{f} = \int \phi^{f*}_{nq} H^{o} \phi^{f}_{nq} dR \tag{9}$$

$$D^{f} = \int \phi^{f*}_{nq} H' \phi^{f}_{nq} dR. \tag{10}$$

Using an approximate Hamiltonian matrix, in which certain non-nearest translationally equivalent interactions are assumed negligible,[13] the normalized crystal eigenfunctions $\Psi^{f\alpha}(\underset{\sim}{k})$ may be expressed in terms of the representations $\underline{\alpha}$ of the $\underset{\sim}{D}_2$ interchange group. They are:

$$\Psi^{f\alpha}(\underset{\sim}{k}) = \tfrac{1}{2} \sum_{q=I}^{IV} a_q^{\alpha} \phi_q^{f}(\underset{\sim}{k}) \tag{11}$$

where the a_q^{α} are coefficients corresponding to the $\underline{\alpha}^{th}$ representation of $\underset{\sim}{D}_2$. For $\alpha = A$, $a_q^A = +1, +1, +1, +1$ when $q = I, II, III, IV$, respectively. Similarly, $a_q^{B_1} = +1, +1, -1, -1$; $a_q^{B_2} = +1, -1, +1, -1$; and $a_q^{B_3} = +1, -1, -1, +1$. In the particular case of $\underset{\sim}{k} = \underset{\sim}{0}$ one need not call upon the above approximation, and in our first-order tight-binding limit, the eigenfunctions may be written exactly:

$$\begin{aligned}
\Psi^{fA}(\underset{\sim}{0}) &= \tfrac{1}{2}(\phi_I^f(\underset{\sim}{0}) + \phi_{II}^f(\underset{\sim}{0}) + \phi_{III}^f(\underset{\sim}{0}) + \phi_{IV}^f(\underset{\sim}{0})) \\
\Psi^{fB_1}(\underset{\sim}{0}) &= \tfrac{1}{2}(\phi_I^f(\underset{\sim}{0}) + \phi_{II}^f(\underset{\sim}{0}) - \phi_{III}^f(\underset{\sim}{0}) - \phi_{IV}^f(\underset{\sim}{0})) \\
\Psi^{fB_2}(\underset{\sim}{0}) &= \tfrac{1}{2}(\phi_I^f(\underset{\sim}{0}) - \phi_{II}^f(\underset{\sim}{0}) + \phi_{III}^f(\underset{\sim}{0}) - \phi_{IV}^f(\underset{\sim}{0})) \\
\Psi^{fB_3}(\underset{\sim}{0}) &= \tfrac{1}{2}(\phi_I^f(\underset{\sim}{0}) - \phi_{II}^f(\underset{\sim}{0}) - \phi_{III}^f(\underset{\sim}{0}) + \phi_{IV}^f(\underset{\sim}{0}))
\end{aligned} \tag{12}$$

The functions $\Psi^{f\alpha}(\underset{\sim}{0})$ map into <u>gerade</u> or <u>ungerade</u> functions of the $\underset{\sim}{D}_{2h}$ factor group depending on whether χ^f is <u>gerade</u> or <u>ungerade</u>. The complete correlation diagram is given in Fig. 2.

It is important to note that the $\underset{\sim}{k} = \underset{\sim}{0}$ crystal function transformations under $\underset{\sim}{D}_2$ are independent of the symmetry $\underline{g}$ or $\underline{u}$ of the site function χ^f. This is not the case for the other three possible interchange groups, all of which contain two glide-plane reflection operations that change the sign of $\underline{u}$ functions but not of $\underline{g}$ functions, if right handed coordinate systems are used throughout.[10] This is an example of the kind of ambiguity that may arise when an improper interchange group is used. Group theoretically such improper groups are correct, but they can certainly lead to

confusion in practice. In any case, both for those who use the proper interchange group and for those who insist on using improper ones, it is important in molecular crystal spectroscopy that the convention, whatever it is, be stated explicitly. Even though the difference of results is only a matter of phasing, in order to compare calculated and experimental quantities it is important to know just what phase relation is used by any particular author!

It should perhaps be pointed out how not to form interchange or factor group representations. Symmetry elements present in the molecule but absent in the site have no significance in the crystal! Using them to find the interchange or factor group representations is definitely incorrect in principle and, at best, misleading in practice. This procedure, introduced by Davydov (see p. 43 of Ref. 4a), has consistently given wrong or inconsistent results for the benzene crystal; though usually the results have been correct for systems such as naphthalene and anthracene where there are only two molecules per unit cell. For instance, Davydov (p. 56 of Ref. 4a) gives only a pair of factor group components (and different ones at that!) for B_{1u} and B_{2u} electronic states of benzene even though he employs four molecules per unit cell. The reason that Davydov obtained incorrect results for benzene was not, as is often stated,[2e,4b] that he employed the old crystal structure, since that had the correct space group. It was because he tried to make use of the molecular point group operations in the crystal, where, except for those preserved by the site, they have no meaning.

In the paper of Fox and Schnepp,[4b] an attempt was made to follow Davydov's method of constructing factor group representations by using molecular point group operations. These authors did, however, use carefully selected coordinate systems on each molecule in conjunction with the refined crystal structure data of Cox.[9] They correctly found four factor group components for each nondegenerate state of molecular benzene in

agreement with Winston[3d]; but the crystal functions they obtained for the molecular B_{1u} state belonged to different factor group representations than those for the molecular B_{2u} state! Both B_{1u} and B_{2u} states, and for that matter all u states of benzene, have identical site and factor group representations and should therefore all be described by the same type of crystal wave function insofar as symmetry is concerned. It is easy to see from what we have presented here and in Section II-A that the treatment of Fox and Schnepp actually amounts to the use of the $\underset{\sim}{C}_{2v}^{b}$ interchange group for the $^1B_{1u}$ molecular electronic state, and the $\underset{\sim}{C}_{2v}^{c}$ interchange group for the $^1B_{2u}$ state. The use of such conventions is mathematically correct, but, unless they are stated explicitly, the meaning of the factor group wave functions and the relative signs (vide infra) of the coupling constants become obscure.

One last thing should be pointed out. The use of projection operators[14] does indeed guarantee that the crystal functions are eigenfunctions, but does not specify a convention, unless the phases of the functions used in this method are explicitly identified with certain interchange operations.[10]

E. Site Functions

For small site distortions, like those for crystalline benzene, distinguishing between site functions and molecule functions is not expected to make large differences in energy. It is, however, extremely important to differentiate between site functions and free-molecule functions when considering intensities and polarization properties of transitions. A breakdown of the

oriented gas model for intensities can occur because of site distortion even in the absence of large energy perturbations by intersite interactions. This model, for example, would be obviously inappropriate in cases where a weak or forbidden gas phase transition is greatly enhanced in the crystal. Such enhancement can occur even though the intermolecular forces causing the intensity enhancement are so weak that they do not cause a measurable breakdown of the first-order Frenkel limit with respect to energy.

Unfortunately, the concept of the site function as introduced by Winston and Halford[3c] and further discussed by Winston[3d] is somewhat ambiguous. These authors envisioned the distortion at the site as arising from a general "crystal field". This sort of language is convenient for many problems, and in particular for the discussion of the vibrational states of crystals, with which Winston and Halford were primarily concerned. For the vibrational problem it is easy to separate crystal field effects in H^0 from interaction terms in H'. One merely considers in H^0 a molecule in the crystal where not only the nuclei but also the electrons have been distorted. This leads to different equilibrium nuclear positions and different (intramolecular) force constants than in the free molecule; H', which also has the symmetry of the site, is written in terms of intermolecular force constants coupling these distorted molecules. For the electronic exciton problem, however, the crystal field idea does not allow a very clear separation of H^0 and H'. Which intermolecular interaction terms in H should be considered part of the "crystal field" and which should be included in H' ?

Three possible choices of electronic basis functions χ^f_{nq} come to mind: 1) the χ^f_{nq} could be eigenfunctions of a free, undistorted benzene molecule; 2) χ^f_{nq} could be eigenfunctions of a distorted benzene molecule in some "average field" of all the other molecules in the crystal; or 3) χ^f_{nq} could be eigenfunctions

of a free benzene molecule whose nuclear framework has been distorted to match that of the molecule in the crystal.

The first choice is undesirable since the symmetry of the terms in H^0 are higher than that of the crystal site. Terms in H' would have to contain the effect of the nuclear distortion on the electronic energies in addition to the usual interaction terms. The advantage of this approach, however, lies in the relative simplicity of the basis functions. It is the one that has been used in theoretical calculations. We shall not use this model here since one of our objectives is to emphasize the consequences of the low symmetry of the crystal site functions. It should be emphasized that the higher order effects of configuration interaction and van der Waals energy must be taken care of separately in this approach. Thus, a strictly first-order theory may be inadequate to explain "shifts" and other contributions to the crystal energies. Such contributions are expected to be particularly important for electronic excitation.

The second type of basis function may lead to the kind of ambiguity mentioned earlier since terms in H^0 representing the "crystal field" contain intermolecular interelectronic interactions usually included in H'. It would be desirable to choose H^0 to be an "effective Hamiltonian" such that the eigenvalues $\langle 0 | H^0 | 0 \rangle$ and $\langle f | H^0 | f \rangle$ already include the $\underset{\sim}{k}$-independent configuration interaction and van der Waals terms. However, such an effective Hamiltonian cannot be written down in terms of one-site functions as in Eq. (4); and to include multisite functions in H^0 would destroy the useful Frenkel exciton formalism upon which the above theoretical results are based. We therefore abandon this extreme approach in the case of vibrational and low-lying electronic states of benzene, which we feel lie very close to the Frenkel limit.

To employ a less extreme crystal field model, where only one-site terms appear in H^0 is possible, but difficult to prescribe precisely. Qualitatively the electrons and nuclei at the site are distorted by some effective electrical field caused by the rest of the crystal, the field being chosen so as to minimize contributions from higher-order effects. The van der Waals terms and terms arising from configuration interaction with, say, Wannier or ion-pair states of the crystal must be taken into account separately by perturbation theory.

A still less extreme crystal field model would be the third one above -- the distorted nuclei model. It would again give rise to van der Waals and configuration interaction contributions since the electronic eigenfunctions of a free molecule, even though its nuclei have been distorted, are not necessarily equivalent to eigenfunctions of any of the zero-order Hamiltonians in the second model. Thus, the distorted-nuclei model gives rise to the same kind of energy contributions as the $\underset{\sim}{D}_{6h}$ model, but the value of each energy contribution differs for the two models. Even the $\underset{\sim}{k}$-dependent energies differ for the three models. One therefore must realize that, just as in other problems, individual terms in a total energy expression have different values depending upon what representation is used, and the terms add up to the true total energy only in the highest order of approximation.

F. Band Energies

The $\underset{\sim}{k}$-dependent energies of the exciton band can be obtained in closed form to first-order in crystal site wavefunctions from the approximate Hamiltonian matrix discussed in Ref. 13. This first-order energy, expressed in a manner similar to the original Davydov form,[4a] is

$$E^{f\alpha}(\underset{\sim}{k}) \equiv \mathcal{E}^{f\alpha}(\underset{\sim}{k}) - \mathcal{E}^{0} = \epsilon + D + L^{f\alpha}(\underset{\sim}{k}). \tag{13a}$$

When higher order effects are taken into account Eq. (13a) becomes

$$E^{f\alpha}(\underset{\sim}{k}) = \epsilon + D + L^{f\alpha}(\underset{\sim}{k}) + W + w \quad (\underset{\sim}{k}). \tag{13b}$$

In these equations $\mathcal{E}^{f\alpha}(\underset{\sim}{k})$ and $\mathcal{E}^{0}$ are, respectively, the excited and ground state energies of the crystal; $\epsilon = \epsilon^{f} - \epsilon^{0}$ where ϵ^{f} and ϵ^{0} are the excited and ground state energies of a molecule at the site whose eigenfunctions χ^{f}_{nq} are specified by some particular site representation; $D = D^{f} - D^{0}$ is a $\underset{\sim}{k}$-independent band shift term; and $L^{f\alpha}(\underset{\sim}{k})$ is the $\underset{\sim}{k}$-dependent energy associated with the $\alpha^{\underline{th}}$ irreducible representation of the interchange group. The quantities ϵ^{f} and D^{f} were defined in Sec. II-D; ϵ^{0} and D^{0} are analogously defined except that ground state site functions ϕ^{0}_{nq} are employed. To first order, the $\underset{\sim}{k}$-dependent energy $L^{f\alpha}(\underset{\sim}{k})$, which is of primary importance in the consideration of the exciton band structure, is a function of the $\underset{\sim}{k}$-dependent matrix elements $L^{f}_{qq'}(\underset{\sim}{k})$ defined in the last section:

$$L^{f\alpha}(\underset{\sim}{k}) = L^{f}(\underset{\sim}{k}) + a^{\alpha}_{II}\, L^{f}_{I\,II}(\underset{\sim}{k}) + a^{\alpha}_{III}\, L^{f}_{I\,III}(\underset{\sim}{k}) + a^{\alpha}_{IV}\, L^{f}_{I\,IV}(\underset{\sim}{k}). \tag{14}$$

We have dropped the subscripts on the diagonal element $L^{f}_{qq}(\underset{\sim}{k})$ since the

approximation from which Eq. (14) is derived rests on the fact that

$$L_{I\,I}^{f}(\underset{\sim}{k}) = L_{II\,II}^{f}(\underset{\sim}{k}) = L_{III\,III}^{f}(\underset{\sim}{k}) = L_{IV\,IV}^{f}(\underset{\sim}{k}), \tag{15}$$

for each $\underset{\sim}{k}$. Equation (15) is not an approximation, of course, for some special values of $\underset{\sim}{k}$ such as $\underset{\sim}{k} = \underset{\sim}{0}$.[4g]

The quantities W and $w(\underset{\sim}{k})$ in Eq. (13b) represent the contributions from higher-order $\underset{\sim}{k}$-independent shift terms and higher-order $\underset{\sim}{k}$-dependent energies, respectively. Again, it is to be emphasized that, while the value of $E^{f\alpha}(\underset{\sim}{k})$ in Eq. (13b) is independent of representation, the values of the individual parts vary with representation. If free-molecule eigenfunctions are used for the site functions χ_{nq}^{f}, then ϵ is the free-molecule excitation energy, the D and L integrals are written in terms of free-molecule functions, and W and $w(\underset{\sim}{k})$ must contain not only the usual configuration interaction and van der Waals terms, but also terms, both $\underset{\sim}{k}$-independent and $\underset{\sim}{k}$-dependent, arising from energy changes caused by <u>nuclear</u> distortions at the crystal site. If the χ_{nq}^{f} represent functions for a free molecule whose nuclei have been distorted, then ϵ, D, and $L^{f\alpha}(\underset{\sim}{k})$ all have different values than if determined from undistorted free-molecule functions; and W and $w(\underset{\sim}{k})$ are also different.

Rather than specifying any particular representation in this paper, for the purpose of fitting the experimental data we shall simply adopt the form of Eqs. (13a) and (13b) with the understanding that the theoretical values of the parameters depend upon the particular representation chosen.

If the higher-order $\underset{\sim}{k}$-dependent terms $w(\underset{\sim}{k})$ are negligible, the simple form of $L^{f\alpha}(\underset{\sim}{k})$ discussed in the preceding sections is preserved. We shall assume this to be the case for vibrational as well as low-lying electronic excitations in crystalline benzene, and shall show in this and subsequent papers that

such an assumption does not conflict with experimental evidence. Even though the higher-order $\underset{\sim}{k}$-dependent terms must be ignored to preserve the simple form of our equations, for the purpose of fitting experimental data all the higher-order $\underset{\sim}{k}$-independent shift terms, such as the van der Waals terms, may be included without difficulty. Neglecting the $w(\underset{\sim}{k})$, ——— a good approximation when perturbing bands are far removed from the Frenkel exciton band under study, we rewrite Eq. (13b) as,

$$E^{f\alpha}(\underset{\sim}{k}) = \bar{\epsilon} + L^{f\alpha}(\underset{\sim}{k}) + \Delta , \tag{16}$$

where

$$\Delta = \epsilon - \bar{\epsilon} + D + W .$$

The quantity $\bar{\epsilon}$ is just the gas phase excitation energy. In some of our future papers it will be convenient to introduce a "site distortion energy" $P = \epsilon - \bar{\epsilon}$. In Eq. (16) the quantities $L^{f\alpha}(\underset{\sim}{k})$ and Δ can be imagined by the experimentalist as the $\underset{\sim}{k}$-dependent energy and site shift term that give the best fit of the observed exciton band energies relative to the free-molecule energy, and by the theorist as quantities to be calculated using first- and higher-order perturbation theory starting with the best available site functions χ^{f}_{nq}. It is possible further to decompose Δ for degenerate states into a shift term and an intrasite resonance shift contribution. This approach will be taken in a future paper from this laboratory concerning crystal site effects for the benzene system.[15] Knowing $E^{f\alpha}(\underset{\sim}{k})$ and $\bar{\epsilon}$, experiments can generally shed light only on the overall values of $L^{f\alpha}(\underset{\sim}{k})$ and Δ, not on the source of these terms.[16]

It is necessary to make a final comment upon the D-term in Δ. The reader should note that the D-term does not contain contributions from site states other than the ground and particular excited state with which one is

dealing, and is representation-dependent. There has been some ambiguity in the literature about this D-term. Some workers, while using a definition of D similar to ours, and free-molecule basis functions, have tried to equate it to the total experimental gas-to-crystal band shift for the transition. This, of course, is a highly erroneous kind of correlation, especially for electronic excitations, because of the possible presence of relatively large second-order shift terms and the difference between D at the site and D calculated with molecular functions. In some cases, but not benzene, there is also the possible presence of large $\underset{\sim}{k} = \underset{\sim}{0}$ shift terms $L^f(\underset{\sim}{0})$, that cause the mean value of the $\underset{\sim}{k} = \underset{\sim}{0}$ Davydov components not to be related to the mean energy of the whole band. Still other workers have tried to equate the entire gas-to-crystal shift to the $\underset{\sim}{k} = \underset{\sim}{0}$ shift terms. The reader should note that the shifts in neat crystals, in isotopic mixed crystals, and in chemical mixed crystals (i.e., benzene in hexane) are often all of similar size and direction. The effect of resonance interactions is nearly lost in the second case and completely lost in the latter case, indicating that resonance interactions must give a relatively minor contribution to the shift. For some molecular crystal transitions, where the exciton interactions are strong, such correlations between experimental and theoretical band shift terms may be more nearly correct than for the benzene transitions discussed here. However, even in these cases, neglect of site distortion energy and in particular second-order contributions to Δ is probably not justified. (See Fig. 3.)

G. Coupling Constants and Davydov Splittings

Some earlier papers[4b, 4f, 7] concerned with the exciton structure of crystalline benzene expressed first-order energies in terms of coupling constants, M_a, M_b, M_c, $M_{I\,II}$, $M_{I\,III}$, and $M_{I\,IV}$, dropping the superscript f, whence,

$$
\begin{aligned}
L^f(\underset{\sim}{0}) &= 2M_a(\underset{\sim}{0}) + 2M_b(\underset{\sim}{0}) + 2M_c(\underset{\sim}{0}) \\
L^f_{I\,II}(\underset{\sim}{0}) &= 4M_{I\,II}(\underset{\sim}{0}) \\
L^f_{I\,III}(\underset{\sim}{0}) &= 4M_{I\,III}(\underset{\sim}{0}) \\
L^f_{I\,IV}(\underset{\sim}{0}) &= 4M_{I\,IV}(\underset{\sim}{0})
\end{aligned}
\tag{17}
$$

there being an identical set of translationally equivalent interactions along each positive and negative crystallographic direction $\underline{a}$, $\underline{b}$, and $\underline{c}$ and a set of four identical interactions between any molecule and its translationally inequivalent neighbors. While Ref. 7 considered the M's in Eq. (17) to be nearest-neighbor interactions, they are really summed quantities over all members of each set in accordance with Eq. (7). Since translationally

equivalent interactions lying skew to the crystallographic axes have been omitted, the energy contribution $L^f(\underset{\sim}{0})$ in Eqs.(17) is approximate even for $\underset{\sim}{k} = \underset{\sim}{0}$. However, for the $^1B_{2u}$ and $^3B_{1u}$ electronic states of benzene, and undoubtedly also for vibrational states of benzene, the approximation is an excellent one because of the smallness of the omitted terms (vide infra).

For the particular case of $\underset{\sim}{k} = \underset{\sim}{0}$, the resulting four energy levels associated with each nondegenerate molecular state are the Davydov components. These are important since they are the only ones that can be reached by interaction with radiation from the $\underset{\sim}{k} = \underset{\sim}{0}$ ground state of the crystal. In terms of the coupling constants, and with respect to a common origin, $\bar{\epsilon} + \Delta + L^f(0)$, the $\underset{\sim}{k} = \underset{\sim}{0}$ energies are:

$$
\begin{aligned}
E(A) &= 4(+M_{I\,II} + M_{I\,III} + M_{I\,IV}) \\
E(B_1) &= 4(+M_{I\,II} - M_{I\,III} - M_{I\,IV}) \\
E(B_2) &= 4(-M_{I\,II} + M_{I\,III} - M_{I\,IV}) \\
E(B_3) &= 4(-M_{I\,II} - M_{I\,III} + M_{I\,IV}),
\end{aligned}
\tag{18}
$$

where it is understood that the $M_{qq'}$'s refer to $\underset{\sim}{k} = \underset{\sim}{0}$. These equations are exact for the Frenkel model. It should be noted that the mean value $\bar{\epsilon} + \Delta + L^f(\underset{\sim}{0})$ of the Davydov components lies at the mean value $\bar{\epsilon} + \Delta$ of the exciton band only in the case where all $\underset{\sim}{k}$-dependent translationally equivalent interactions are negligible. $L^f(\underset{\sim}{0})$ will be referred to as the $\underset{\sim}{k} = \underset{\sim}{0}$ shift (or the translational shift). This point is important in the analysis of isotopic mixed crystal data, since it is $\bar{\epsilon} + \Delta$, not $\bar{\epsilon} + \Delta + L^f(\underset{\sim}{0})$, that determines the position of the guest energy levels in the ideal case (vide infra).

H. Site Group Splitting and the Ideal Mixed Crystal

Direct manifestation of the reduction in symmetry of molecular quantities in the site is the site group splitting. Symmetry arguments show that degenerate states of the molecule often map into nondegenerate irreducible representations of the site group. This is true in benzene where the molecular symmetry is much higher than the site symmetry (see Fig. 2). Degeneracies present in the molecular state can therefore be removed by the site. The splitting has been called site group splitting[3a] and has been primarily studied in the vibrational spectrum of molecular crystals, but is certainly not limited to vibrations alone.

In order to be able to discuss site group splitting without complications due to interchange group splitting it is suggested that site group splitting be defined phenomenologically as the splitting obtained for the guest in an ideal mixed crystal. The ideal mixed crystal is defined as one in which: (a) the guest is infinitely dilute; (b) the only difference between guest and host is one of isotopic substitution; (c) guest and host have the same symmetry and dimensions; (d) quasi-resonance interactions between guest and host and the effects of isotopic substitution on Δ are negligible. Isotopic mixed crystals approximate fairly closely this definition. In addition small correction terms to be discussed later can be applied to bring the isotopic mixed crystal even closer to the concept of the ideal mixed crystal. The phenomenological definition of the ideal mixed crystal brings into agreement, as close as is thought possible, the observed site group splitting in isotopic mixed crystals and the original idea[3a] that site group splitting is the result of the static field ($\underset{\sim}{k}$-independent) interactions at the site. In the ideal mixed crystal the site group splitting of a degenerate gas phase band will therefore be

quantitatively identical to the difference in the Δ terms of the originally degenerate components. Symbolically this can be written as $(\Delta_x - \Delta_y)$, where x and y designate the degenerate components.

In the neat crystal there are additional resonance contributions to the splitting of free-molecule degenerate states. Excitation exchange interactions will couple not only site group components of one kind (say x) among different sites, but may also couple site group components of different kinds (x and y) among the various sites. The last statement is certainly true when both "kinds" belong to the same site group species (benzene!) but also in some cases where the two "kinds" belong to different site group species.[17] In other words, any degenerate or nearly degenerate levels present after the static interactions have been introduced may be further coupled together by the dynamic ($\underset{\sim}{k}$-dependent) interactions in the neat crystal, or by quasiresonance interactions in the mixed crystal (vi infra). This statement holds whether the near degeneracy arises from site group splitting or from accidental degeneracies present in the system. The latter case when applied to vibrational levels resembles Fermi resonance.[18] It is different from typical Fermi resonance in that the effect is an intermolecular one and that anharmonicities of the usual type need not be present to effect the interaction. (See Fig. 3.)

The essence of the last paragraph is that whenever site group splitting and interchange group splitting are expected together, the total effect cannot be handled even conceptually as a simple superposition of two independent effects. For the benzene crystal, the full 8×8 submatrix must be considered leading to ten independent off-diagonal coupling constants, whose values are not determinable from the limited experimental data obtainable. A separation of the two effects would be justified as a first approximation only if: (a) The site group interaction is an order of magnitude larger than the resonance

interactions, or (b) the site group components are of different symmetry (see, however, footnote 17). Except for these two cases, the so-called site group splitting in a neat crystal will contain contributions not only from the phenomenological site group splitting in the ideal mixed crystal but also from resonance interactions usually discussed within the space group.

The ideal mixed crystal is also a useful concept for discussing non-degenerate states. If, for a real mixed crystal, the deviations from the idealizing conditions can be evaluated quantitatively, the mean value $\bar{\epsilon} + \Delta$ of the exciton band can be found from the mixed crystal energy. This technique allows one to evaluate $L^f(\underset{\sim}{0})$ if the mean value $\bar{\epsilon} + \Delta + L^f(\underset{\sim}{0})$ of the Davydov components is independently known. Similarly, if $L^f(\underset{\sim}{0})$ is known to be negligible, the ideal mixed crystal level can be equated to $\bar{\epsilon} + \Delta$. For the case of benzene vibrations where the $L^f(\underset{\sim}{0})$ are expected to be small, this provides a technique for finding the position of the "forbidden" Davydov component. While these concepts were implicitly utilized by Nieman and Robinson[7] for the determination of the Davydov structure of the lowest excited electronic states of the benzene crystal, their usefulness was neglected in the concurrent interpretation of both electronic and vibrational[5e] exciton structure.

III. EXPERIMENTAL METHODS AND RESULTS

The experiments of Nieman and Robinson[7] on the $^1B_{2u}$ electronic exciton band were repeated. These results will be discussed in some detail to illustrate the theory and to derive the exciton coupling constants using the $\underset{\sim}{D}_2$ interchange group. Infrared transitions in neat and isotopic mixed benzene crystals were also obtained and a few of these spectra will be discussed for further illustration.

The deuterated benzene was obtained from Merck, Sharp, and Dohme, Ltd., Canada, and was vacuum distilled before use. The C_6H_6 was obtained from Phillips Petroleum Co. (99.89 mole % pure) and was used without further purification. The neat crystals for the infrared experiments were made by placing liquid benzene between two CsI windows, which were pressed together in a sample holder. The holder was made from brass and was fitted with indium in order to apply firm, uniform pressure to the soft salt windows. A few drops of benzene were placed on the CsI window, and the sample holder was assembled and attached to the bottom of a "cold-finger" helium dewar in a dry nitrogen atmosphere. The dewar was then assembled, and the sample was frozen to liquid nitrogen temperature (77°K) while the dewar was being evacuated. At this temperature one could see through the sample, and even

upon subsequent cooling to 4.2°K the sample remained clear. Sample thickness, estimated from measurements of absolute absorption intensities[19] in the infrared, was about 5-10 μ. For the ultraviolet experiments, a technique similar to that used by Nieman and Robinson[7] was employed.

The concentration of the isotopic mixed samples was about 1% guest in 99% host. This low concentration was used in order that complete isolation of the guest in the host crystalline lattice could be effected even though to detect infrared absorption this meant that larger, less convenient sample thicknesses were necessary. The thicker samples were made with a 0.050 inch indium wire gasket placed between the CsI windows. When compressed, this spacing was approximately 0.75 to 1.0 mm thick. The gasket was not made into a closed circle, allowing an entrance into which the liquid sample could be introduced. However, indium "tails", with which the sample holder could be sealed after it is filled with benzene, were left attached. The well-mixed[20] sample was then placed in the holder, sealed, and solidified as discussed above. After cooling to 77°K the sample was heavily cracked, although it was possible to see through some portions of it. Some of the infrared spectra were taken at 77°K and some at 4.2°K with no apparent differences observed. These data are presented in Table II and in Figs. 4, 5, 6, and 7. The neat crystal infrared spectra are virtually identical with those already reported in the literature.[19]

IV. DISCUSSION OF EXPERIMENTAL RESULTS

As explained in the Theoretical Section, in order to understand fully molecular crystalline interactions, it is necessary to study both neat and isotopic mixed crystals. With the data obtained from mixed crystals it is possible to isolate and to study separately crystalline interactions arising from different "sources." By varying the isotopic substitution, guest energy states

in such samples can be brought into near resonance with host levels. Therefore, it is not only possible to gain knowledge about the static field interactions but also about the dynamic interactions.

A. C_6H_6 Electronic Band - $^1B_{2u}$

The interchange group structure of this state, as obtained from neat and isotopic mixed crystal absorption spectra, is given in Table III and Fig. 8. In neat crystalline C_6H_6, the 0-0 line of the $^1B_{2u}$ - $^1A_{1g}$ transition[21] has been observed both in absorption and emission. Because of the interchange group selection rules for these processes[13] ($\Delta \underset{\sim}{k} = \underset{\sim}{0}$; $B_1 \rightarrow B_2$; $B_1 \rightarrow B_3$; $B_2 \rightarrow B_3$; $A \rightarrow B_1, B_2, B_3$), only the $\underset{\sim}{k} = \underset{\sim}{0}$ components of the B_1, B_2, and B_3 bands can be observed for transitions involving the totally symmetric ($\underset{\sim}{k} = \underset{\sim}{0}$, A_g) ground state of the crystal. Thus the E(A) level, or alternatively the mean value of the Davydov components, must be located by an indirect method to obtain the M values in Eq. (17).

The 0-0 component in emission is found to be coincident within 5 cm^{-1} with the lowest interchange group component observed in absorption. From the selection rules, one can therefore conclude that the lowest interchange component has B symmetry and that its $\underset{\sim}{k} = \underset{\sim}{0}$ level is at or near the bottom of the band If a state of B_u symmetry were not the lowest factor group component, or, if the $\underset{\sim}{k} = \underset{\sim}{0}$ level were not its lowest state, we would not have observed the 0-0 transition in emission, but would have observed only transitions terminating in vibrational exciton bands of the ground electronic state.[13] (In agreement with this expectation is the fact that only a slight increase in temperature is necessary for complete removal of the 0-0 band in emission.[13]) Without making extensive polarization studies, it is impossible further to assign this state to any one of the three possible B levels (B_{1u}, B_{2u}, B_{3u}). The assignment of the lowest level to one of the B_u levels is consistent with the conclusions reached by Nieman and Robinson.[7]

As mentioned above, in order to obtain the M values from the experimental data, either the position of the A level or the mean value of the Davydov components must be known. Following the method of Nieman and Robinson,[7] and providing the ideal mixed crystal limit can be approached in this way, the latter quantity can be evaluated from isotopic mixed crystal data to which small corrections due to quasiresonance shifts and the $\underset{\sim}{k} = \underset{\sim}{0}$ shift term $L^f(0)$ have been applied. First, the supposed ideal mixed crystal value of the transition energy $(\bar{\epsilon} + \Delta)$ is obtained by correcting the observed 0-0 transition of the isotopic mixed crystal C_6H_6 in C_6D_6 for the quasiresonance shift,[7]

$$\delta \approx 4\beta^2/\Delta E \,, \tag{18}$$

where,

$$\beta^2 = M^2_{I\,II} + M^2_{I\,III} + M^2_{I\,IV} + \tfrac{1}{2}(M^2_a + M^2_b + M^2_c). \tag{19}$$

The β of Nieman and Robinson is used, i.e., $\underline{\beta} = 18\ \mathrm{cm}^{-1}$. The $\underset{\sim}{k} = \underset{\sim}{0}$ shift is then determined such that the β calculated from the splitting and shift terms $[L^{f\alpha}(\underset{\sim}{0})]$ agrees with the measured value. Using the $\underset{\sim}{D}_2$ interchange group and accepting with reservations the interchange group assignments of the observed levels obtained from polarized absorption experiments[2c] with reservations as discussed in Ref. 7, we then calculate from Eq. (17),

$$M_{I\,II} = +\ 6.9\ \mathrm{cm}^{-1}$$
$$M_{I\,III} = +\ 12.4\ \mathrm{cm}^{-1}$$
$$M_{I\,IV} = +\ 11.7\ \mathrm{cm}^{-1}.$$

This calculation is outlined in Tables III and IV. The site shift term $\Delta = -224\ \mathrm{cm}^{-1}$ can be found from the ideal mixed crystal 0-0 transition energy ($37,862\ \mathrm{cm}^{-1}$), determined as above, and the gas phase 0-0 transition energy (36, 086 cm Thus we find that the average $\underset{\sim}{k}$-independent crystal binding energy is about 6.0% larger for an excited state molecule than for a ground state molecule in the normal crystal.[22] It should be noted that the calculated M values differ in sign from those of Nieman and Robinson, who give $-6.9\ \mathrm{cm}^{-1}$, $-12.4\ \mathrm{cm}^{-1}$,

and +11.7 cm^{-1}, as they did not use the $\underset{\sim}{D}_2$ interchange group but instead used the method of Fox and Schnepp[4b] in the determination of the symmetry of their wave functions.[23]

More recent data are apparently inconsistent with the interpretation of Nieman and Robinson. Data on the reverse isotopic mixed crystal, C_6D_6 in C_6H_6, and on band-to-band transitions seem to suggest a total exciton bandwidth only about 1/3 that given by the above M values. This discrepancy, thought to be caused by an isotope effect on the electronic Δ term, is presently the object of further investigation. The new results, which indicate that in benzene the ideal mixed crystal cannot be approximated accurately by the technique of isotopic substitution, will be discussed in a separate paper.[24] All translationally equivalent interactions are found to be small, justifying the assumptions made above and in Ref. 13.

B. Ground State Ungerade Vibrations

Ungerade vibrations can be observed in infrared absorption. In the gas phase only a_{2u} and e_{1u} vibrations are dipole-allowed within the $\underset{\sim}{D}_{6h}$ symmetry group of benzene. In the crystal, because of the loss of exact $\underset{\sim}{D}_{6h}$ symmetry, a partial relaxation of the selection rules occurs, and vibrations of original molecular symmetry a_{2u}, b_{1u}, b_{2u}, e_{1u}, and e_{2u} are observed. One degenerate (e_{1u}) and two nondegenerate vibrations (one b_{1u} and one b_{2u}) will be discussed in detail below.

Degenerate Vibrations -- We have defined site group splitting as the splitting that occurs in degenerate vibrations of guest molecules in an ideal mixed crystal. In order to approach the ideal as closely as possible, the real mixed crystal should be an isotopic mixed crystal in which the guest-host quasi-resonance interactions are reduced to a minimum (i.e., for our case, C_6H_6 guest in a C_6D_6 host or vice versa). Such a choice essentially eliminates contributions from resonance interactions to the observed site splitting. Using this mixed crystal, a 3.8 cm^{-1} site group splitting in crystalline benzene for

the e_{1u} vibration ν_{18} is observed. See Fig. 4. Since the interchange splitting for nondegenerate ungerade vibrations is about 10 cm^{-1}, a quantitative treatment, using site group and interchange group concepts of the degenerate vibrations in the neat crystal does not appear possible. The neat crystal spectrum of the $e_{1u}(\nu_{18})$ band is given in Fig. 5.

Nondegenerate Vibrations -- For these vibrations, in which no site group splitting occurs, the mixed crystal data can be used, as in the case of the $^1B_{2u}$ electronic band, to aid in the interpretation of the pure crystal spectrum. Dilute mixed crystal experiments,[15] using solvents of isotopically modified benzene other than C_6H_6 and C_6D_6, indicate that the quasi-resonance corrections are negligible (less than 1 cm^{-1}) and that Δ is small and independent of the isotopic substitution of the host. Recent calculations of the Davydov structure of benzene vibrational bands,[25,26] that are successful in predicting the correct order of magnitude of the overall splittings would predict negligible interactions between the translationally equivalent molecules. Thus, as a first approximation, we assume the mean value of the Davydov components in the pure crystal to be the value of that vibration in the isotopic mixed crystal. With this assumption, the three observed B levels allow a calculation of the complete interchange group structure (see Figs. 9 and 10). Using, with reservations, the polarization results of Zwerdling and Halford[1e] we can find $M_{I\,II}$, $M_{I\,III}$, and $M_{I\,IV}$ for both the $b_{2u}(\nu_{15})$ and $b_{1u}(\nu_{12})$ vibrational bands. The calculated energies, M values and β values [Eq. (19)] are given in Table IV, and the interchange structures are presented in Figs. 9 and 10. It should be noted, as will be reported later,[27] that the factor group structures corresponding to the same normal mode in crystals of C_6H_6 and C_6D_6 are nearly identical. From the calculated β values it is now possible to check the assumption that the quasi-resonance correction to the mixed crystal data, used to obtain the band centers, is indeed small. Applying Eq. (18) one finds that the quasi-resonance correction is less than the

experimental error, as was assumed. A discussion of the interaction terms will be given elsewhere.[15,26,27]

V. SUMMARY

The major points made in this paper are:

1) The concept of the interchange group is introduced and is applied to the molecules in the primitive unit cell. This group provides a convenient and unambiguous way of discussing the relative signs of the exciton coupling constants.

2) The site distortion energy P and band-shift term Δ are introduced, and together with the D-term are discussed relative to the experimental band-shift.

3) It is emphasized that site wave functions χ^{f}_{nq}, and not molecular wave functions, are the ones of greater significance.

4) Static and dynamic interactions are distinguished and are associated, respectively, with $\underset{\sim}{k}$-independent and $\underset{\sim}{k}$-dependent terms of the Davydov energy equation. These interactions are associated with site operations and transport operations, respectively.

5) The ideal mixed crystal is defined and its importance in the determination of site splittings, band shifts, and forbidden Davydov components is emphasized.

6) The exciton structure of molecular degenerate, or nearly degenerate, states cannot be described simply as site group splitting plus interchange group splitting. We have therefore used the term site group splitting to describe the splitting of molecular degenerate states associated with guest molecules in an ideal mixed crystal.

7) Experimental data, interpreted within the framework of the foregoing theoretical ideas, are presented for the $^{1}B_{2u}$ electronic exciton band and for a few vibrational exciton bands in the electronic ground state.

REFERENCES

[1](a) R. S. Halford and O. A. Schaeffer, J. Chem. Phys. 14, 141 (1946); (b) R. Mair and D. F. Hornig, J. Chem. Phys. 17, 1236 (1949); (c) A. Frühling, Ann. de Phys. 12e Série, t. 6, 26 (1951); (d) S. C. Sirkar and A. K. Ray, Ind. J. Phys. 24, 189 (1950); (e) S. Zwerdling and R.S. Halford, J. Chem. Phys. 23, 2221 (1955).

[2](a) V. L. Broude, V. S. Medvedev, and A. F. Prikhotko, J. Exptl. Theoret. Phys. (U. S. S. R.) 21, 665 (1951); (b) V. L. Broude, V. S. Medvedev, and A. F. Prikhotko, Opt. i. Spektr. 2, 317 (1957); (c) V. L. Broude, Usp. Fiz. Nauk 74, 577 (1961) [Engl. Transl. Sov. Phys.--USP 4, 584 (1962)]; (d) V. N. Vatulev, N. I. Sheremet, and M. T. Shpak, Opt. i. Spektr. 16, 315 (1964); (e) A. Zmerli, J. Chim. Phys., 56, 387 (1959).

[3](a) R. S. Halford, J. Chem. Phys. 14, 8 (1946); (b) D. F. Hornig, J. Chem. Phys. 16, 1063 (1948); (c) H. Winston and R. S. Halford, J. Chem. Phys. 17, 607 (1949); (d) H. Winston, J. Chem. Phys. 19, 156 (1951); (e) L. P. Bouckaert, R. Smoluchowski, and E. Wigner, Phys. Rev. 50, 58 (1936).

[4](a) A. S. Davydov, Theory of Molecular Excitons, (McGraw-Hill, N. Y., 1962); (b) D. Fox and O. Schnepp, J. Chem. Phys. 23, 767 (1955); (c) D. P. Craig and P. C. Hobbins, J. Chem. Soc. 1955, 539; (d) D. P. Craig, J. Chem. Soc. 1955, 2302; (e) D. P. Craig and S. H. Walmsley, Mol. Phys. 4, 113 (1961); (f) D. P. Craig and J. R. Walsh, J. Chem. Soc. 1958, 1613; (g) A. S. Davydov, Usp. Fiz. Nauk 82, 393 (1964). [Sov. Phys.-USP 7, 145 (1964).]

[5](a) D. S. McClure, Solid State Phys. 8, 1 (1958); (b) W. Vedder and D. F. Hornig, Adv. Spectry. 2, 189 (1961); (c) O. Schnepp, Ann. Rev. Phys. Chem. 14, 35 (1963); (d) D. P. Craig and S. H. Walmsley in Physics and

Chemistry of Organic Solid State, Vol. I, ed. by Fox, Labes, and Weissberger, (Interscience, N. Y., 1963), p. 586; (e) D. A. Dows, ibid., p. 609.

[6]G. L. Hiebert and D. F. Hornig, J. Chem. Phys. 20, 918 (1952).

[7]G. C. Nieman and G. W. Robinson, J. Chem. Phys. 39, 1298 (1963).

[8]R.Silbey, S. A. Rice, and J. Jortner, J. Chem. Phys. 43, 3336 (1965).

[9]E. G. Cox, Rev. Mod. Phys. 10, 159 (1958); E. G. Cox, D.W.J. Cruickshank, and J.A.S. Smith, Proc. Roy. Soc. (London) A247, 1 (1958); G. E. Bacon, N. A. Curry, and S. A. Wilson, Proc. Roy Soc. (London) A279, 98 (1964).

[10]R. Kopelman, J. Chem. Phys. 00, 0000 (1967).

[11]These relations do not hold for all values of k.

[12](a) E.P. Wigner, Group Theory (Academic Press, New York, 1959), p. 59; (b) G. F. Koster, Solid State Phys. 5, (1957), reprinted by Academic Press, N.Y.; C. Kittel, Quantum Theory of Solids (John Wiley and Sons, Inc., New York, 1963), Chap. 9.

[13]S.D. Colson, R. Kopelman and G.W. Robinson, J. Chem. Phys. 00, 0000 (1967).

[14]Ref. 12(a), p. 118.

[15]E.R. Bernstein, manuscript in preparation.

[16]This point is discussed by T. Thirunamachandran [Thesis (University College, London, 1961)]. He points out that the importance of the octapole-octapole interactions in determining the Davydov splitting can be evaluated by determining the polarizations of the Benzene exciton components.

[17] This will happen when one or more symmetry operations of different, physically equivalent sites are not parallel. This points out the usefulness of

the interchange group, as some interactions "allowed" by the interchange group appear to be forbidden by the factor group. This apparent contradiction arises because similar but non-parallel operations of different sites may all map into the same class of operations of the factor group. It should be remembered that the site group is only isomorphous with a subgroup of the factor group, not identical with it.

[18] R. Kopelman, J. Chem. Phys. 44, 3547 (1966) and references therein.

[19] W. B. Person and C. A. Swenson, J. Chem. Phys. 33, 233 (1960); J. L. Hollenberg and D. A. Dows, J. Chem. Phys. 39, 495 (1963).

[20] Poorly mixed samples of 1% guest in 99% host and a well mixed sample of higher concentration were studied. The absorptions, while not having the complete exciton structure of the neat crystals, were not as sharp as those of the low concentration isotopic mixed crystals and some bands even exhibited residual splittings. This tends to indicate that, in general, mixed crystal studies, designed to eliminate guest-guest interactions, should be carried out at guest concentrations of less than 2%. The concentrated (5-10%) mixed crystal spectra of J. L. Hollenberg and D. A. Dows [J. Chem. Phys. 39, 495 (1963)] appear much like the above-mentioned poorly mixed samples.

[21] As the molecular symmetry is not conserved in the site, the use of D_{6h} designations for the symmetry of crystal states is not really correct. However, we will retain the notation here merely as a convenient labelling device.

[22] The heat of sublimation for benzene is about 3800 cm^{-1}. G. Milazzo, Ann. Chim. Rome 46, 1105 (1956).

[23] Note that the designation of molecules II and IV has also been changed from that of Nieman and Robinson (also Fox and Schnepp[4b] and Craig and Walsh[4f]) to agree with the crystallographic work of Cox, Cruickshank, and Smith.[10] Because of the restrictions due to the interchange group it would be very awkward to accept the designations of the a, b, and c, axes of Cox, et al. without accepting their numbering of molecules. This designation is consistent with the benzene ac projection shown in Fig. 2.

[24] S. D. Colson, manuscript in preparation.

[25] I. Harada and T. Shimanouchi, J. Chem. Phys. 44, 2016 (1966).

[26] E. R. Bernstein, manuscript in preparation.

[27] E. R. Bernstein and G. W. Robinson, manuscript in preparation.

Table I

Symmetry transformations of the $\underset{\sim}{k} = \underset{\sim}{0}$ one-site excitons

	E	C_2^a	C_2^b	C_2^c	i	σ_a	σ_b	σ_c
ϕ_I^g	ϕ_I^g	ϕ_{II}^g	ϕ_{III}^g	ϕ_{IV}^g	ϕ_I^g	ϕ_{II}^g	ϕ_{III}^g	ϕ_{IV}^g
ϕ_{II}^g	ϕ_{II}^g	ϕ_I^g	ϕ_{IV}^g	ϕ_{III}^g	ϕ_{II}^g	ϕ_I^g	ϕ_{IV}^g	ϕ_{III}^g
ϕ_{III}^g	ϕ_{III}^g	ϕ_{IV}^g	ϕ_I^g	ϕ_{II}^g	ϕ_{III}^g	ϕ_{IV}^g	ϕ_I^g	ϕ_{II}^g
ϕ_{IV}^g	ϕ_{IV}^g	ϕ_{III}^g	ϕ_{II}^g	ϕ_I^g	ϕ_{IV}^g	ϕ_{III}^g	ϕ_{II}^g	ϕ_I^g
ϕ_I^u	ϕ_I^u	ϕ_{II}^u	ϕ_{III}^u	ϕ_{IV}^u	$-\phi_I^u$	$-\phi_{II}^u$	$-\phi_{III}^u$	$-\phi_{IV}^u$
ϕ_{II}^u	ϕ_{II}^u	ϕ_I^u	ϕ_{IV}^u	ϕ_{III}^u	$-\phi_{II}^u$	$-\phi_I^u$	$-\phi_{IV}^u$	$-\phi_{III}^u$
ϕ_{III}^u	ϕ_{III}^u	ϕ_{IV}^u	ϕ_I^u	ϕ_{II}^u	$-\phi_{III}^u$	$-\phi_{IV}^u$	$-\phi_I^u$	$-\phi_{II}^u$
ϕ_{IV}^u	ϕ_{IV}^u	ϕ_{III}^u	ϕ_{II}^u	ϕ_I^u	$-\phi_{IV}^u$	$-\phi_{III}^u$	$-\phi_{II}^u$	$-\phi_I^u$

TABLE II. Some u-vibrational levels of C_6H_6 (in cm^{-1})

Symmetry	Gas[a]	C_6H_6 in C_6D_6[b]	Neat Crystal[b]	Polarization and Symmetry[c]	
			1030.0		
			1032.5		
		1034.8	1033.3		
$e_{1u}(\nu_{13})$	1037	1038.6	1034.6		
			1038.9		
			1039.8		
$b_{1u}(\nu_{12})$					
	1010	1011.3	1006.9	c	B_{3u}
			1008.6	b	B_{2u}
			1009.7	a	B_{1u}
			1142.5	c	B_{3u}
$b_{2u}(\nu_{15})$	1146	1146.9	1148.6	a	B_{1u}
			1150.3	b	B_{2u}

[a] S. Brodersen and A. Langseth, Mat. Fys. Skr. Dan. Ved. Selsk 1, 1 (1956).

[b] Our measurements.

[c] S. Zwerdling and R. S. Halford, J. Chem. Phys., 23, 2221 (1955).

TABLE III. Benzene $^1B_{2u} \leftarrow {}^1A_{1g}$ electronic (0-0) transition (in cm^{-1}) according to the ideal mixed crystal model.

Gas phase[a]	C_6H_6 in C_6D_6	Ideal mixed crystal[b]	Algebraic mean of k band in neat crystal	Algebraic mean of Davydov components[c]	Davydov components[d]	Coupling constants[e]
38086.1	37853.3 ± 0.1	37862 ± 2	37862 ± 2	37872 ± 16	A_u = 37,996 ± 48 B_{2u} = 37,847.1 ± 1.0 B_{3u} = 37,841.8 ± 1.0 B_{1u} = 37,803.2 ± 1.0	$M_{I,II}$ = + 6.9 ± 2 $M_{I,III}$ = +12.4 ± 2 $M_{I,IV}$ = +11.7 ± 2

[a] J. H. Callomon, T. M. Dunn, J. M. Mills, Phil. Trans. Roy. Soc. (London) 259A, 499 (1966)

[b] Corrected for quasi resonance Eq. (18) plus 2 cm^{-1} for the interaction with the lowest vibronic level (ref. 7a).

[c] Corrected for $L^f(\underset{\sim}{0})$, the "$\underset{\sim}{k} = \underset{\sim}{0}$ shift". See Eq. (15) and the following two paragraphs of discussion.

[d] Assignment of symmetry (B_{1u}, B_{2u}, or B_{3u}) is based on polarization data of Broude, ref. 2c.

[e] New data suggest that for benzene isotopic mixed crystals do not closely approach the ideal mixed crystal limit. In particular there seems to be an isotope effect on the Δ term of Eq. (17).

TABLE IV. Various contributions to the energy of some exciton states.

State	Gas to mixed crystal shift[a]	Quasi-resonance shift[b]	Static field term (Δ)[c]	$L^f(\underset{\sim}{0})$, the "$\underset{\sim}{k}=\underset{\sim}{0}$ shift"	β	Exciton coupling constants[d] M I, II	I, III	I, IV
$^1B_{2u}$[e]	-232.8 ± 1	+9 ± 2	-224 ± 3	+8 ± 4	+18 ± 2	+6.9 ± 2	+12.4 ± 2	+11.7 ± 2
$b_{1u}(\nu_{12})$	+ 1.3 ± .5	~0.0	+ 1.0 ± 1	~0.0	+1.7 ± .3	+0.89 ± .2	+0.75 ± .2	+0.54 ± .2
$b_{2u}(\nu_{15})$	+ 0.9 ± .5	~0.0	+ 1.0 ± 1	~0.0	+0.5 ± .3	+0.12 ± .2	+0.34 ± .2	-0.64 ± .2

[a] C_6H_6 in C_6D_6 values compared with indirectly derived gas phase values.

[b] Obtained from β of Nieman and Robinson, ref. 7.

[c] Obtained by adding the first and second columns.

[d] Electronic and vibrational polarization assignments taken from V. L. Broude, Usp., 4, 584 (1962), and S. Zwerdling and R. S. Halford, J. Chem. Phys. 23, 2221 (1955).

[e] See footnote c of Table III.

Figure 1

Diagram of crystalline benzene viewed down the b-axis. The R_{ij} are the center-to-center distances at 77 °K between molecules i and j.

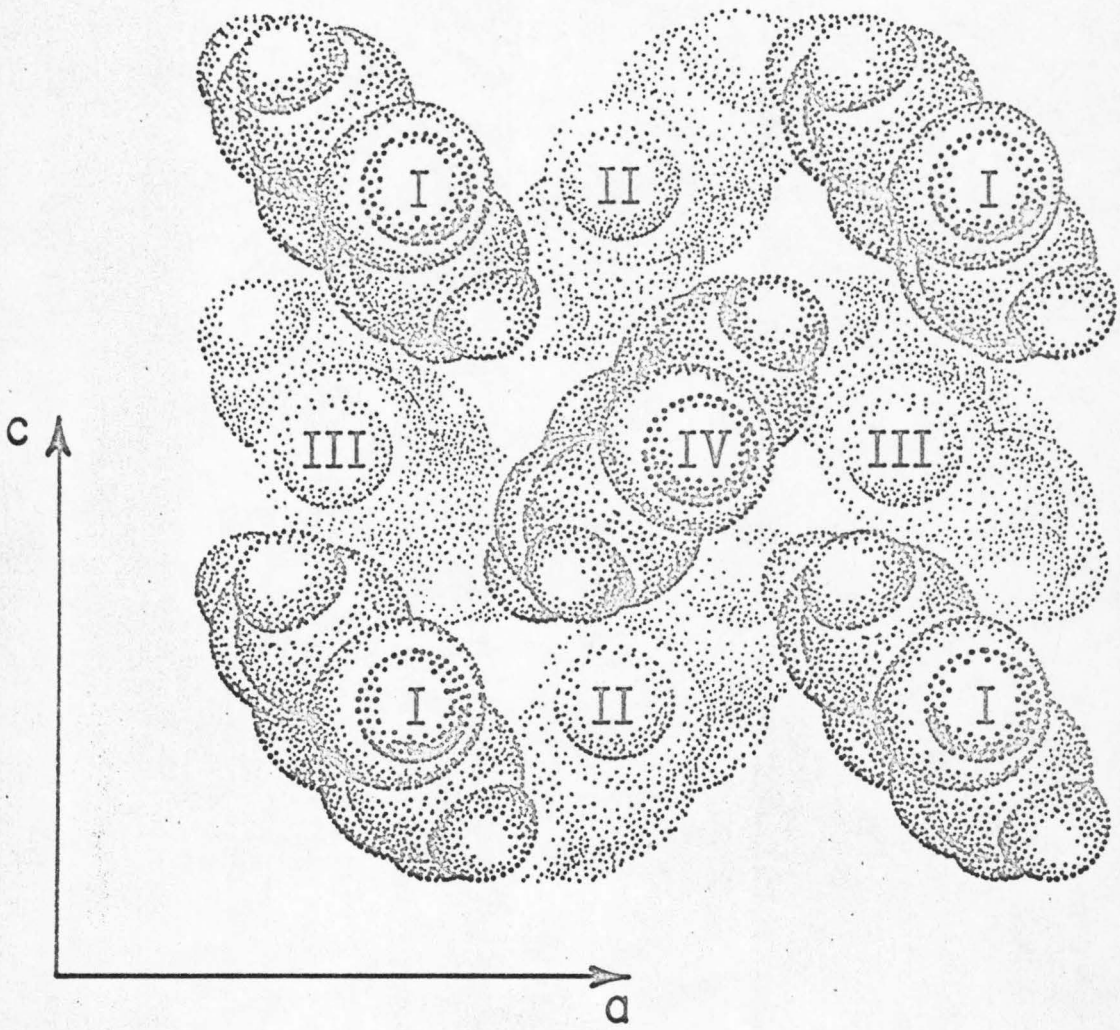

a = 7.37 Å

b = 9.35 Å

c = 6.77 Å

$R_{I\,II}$ = 5.95 Å

$R_{I\,III}$ = 5.76 Å

$R_{I\,IV}$ = 5.00 Å

Figure 2

Correlation among groups pertinent to the benzene crystal.

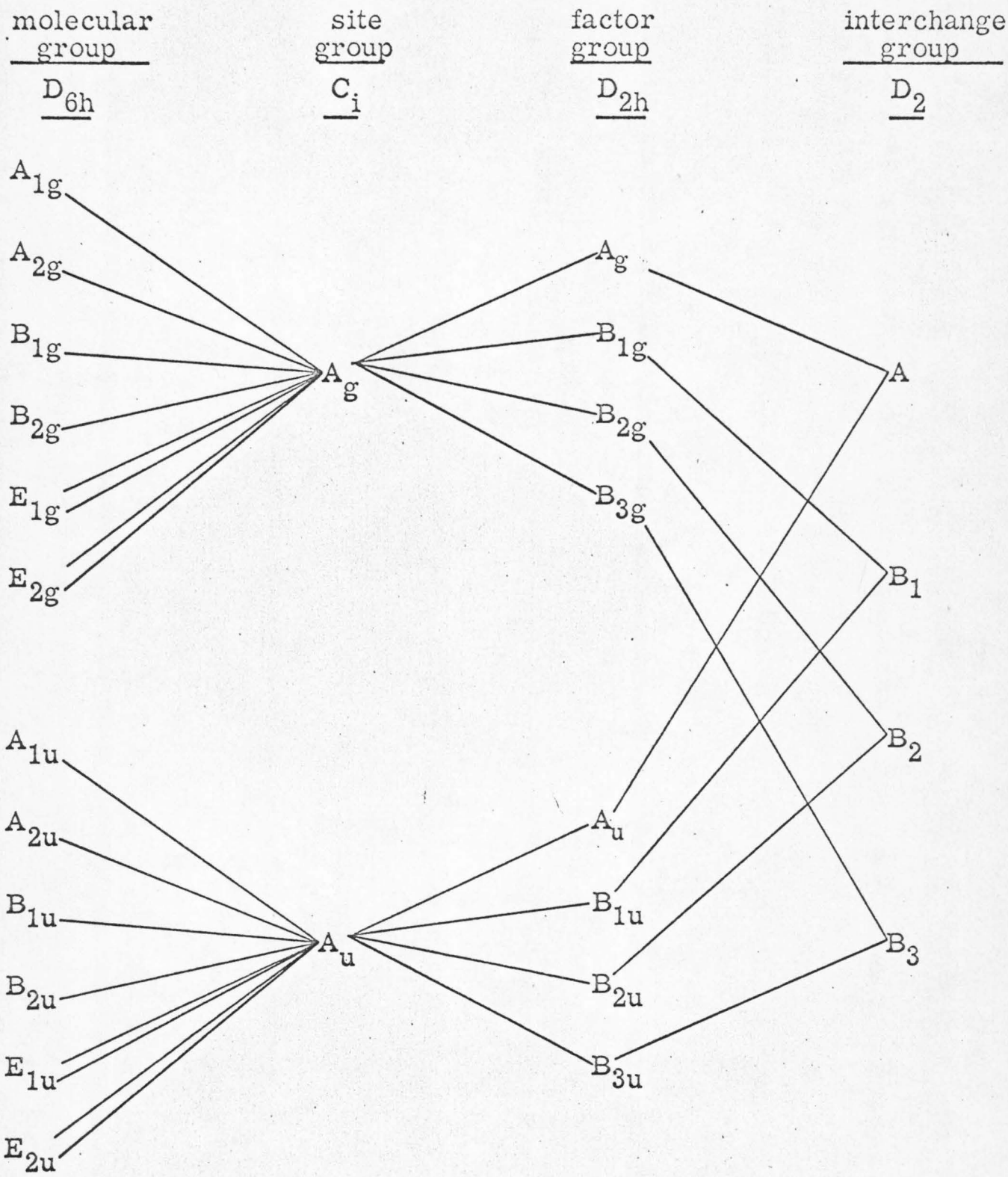
molecular group
D_{6h}
site group
C_i
factor group
D_{2h}
interchange group
D_2
A_{1g}
A_{2g}
B_{1g}
B_{2g}
E_{1g}
E_{2g}
A_g
A_{1u}
A_{2u}
B_{1u}
B_{2u}
E_{1u}
E_{2u}
A_u
A_g
B_{1g}
B_{2g}
B_{3g}
A_u
B_{1u}
B_{2u}
B_{3u}
A
B_1
B_2
B_3

Figure 3

Schematic exciton structure--benzene.

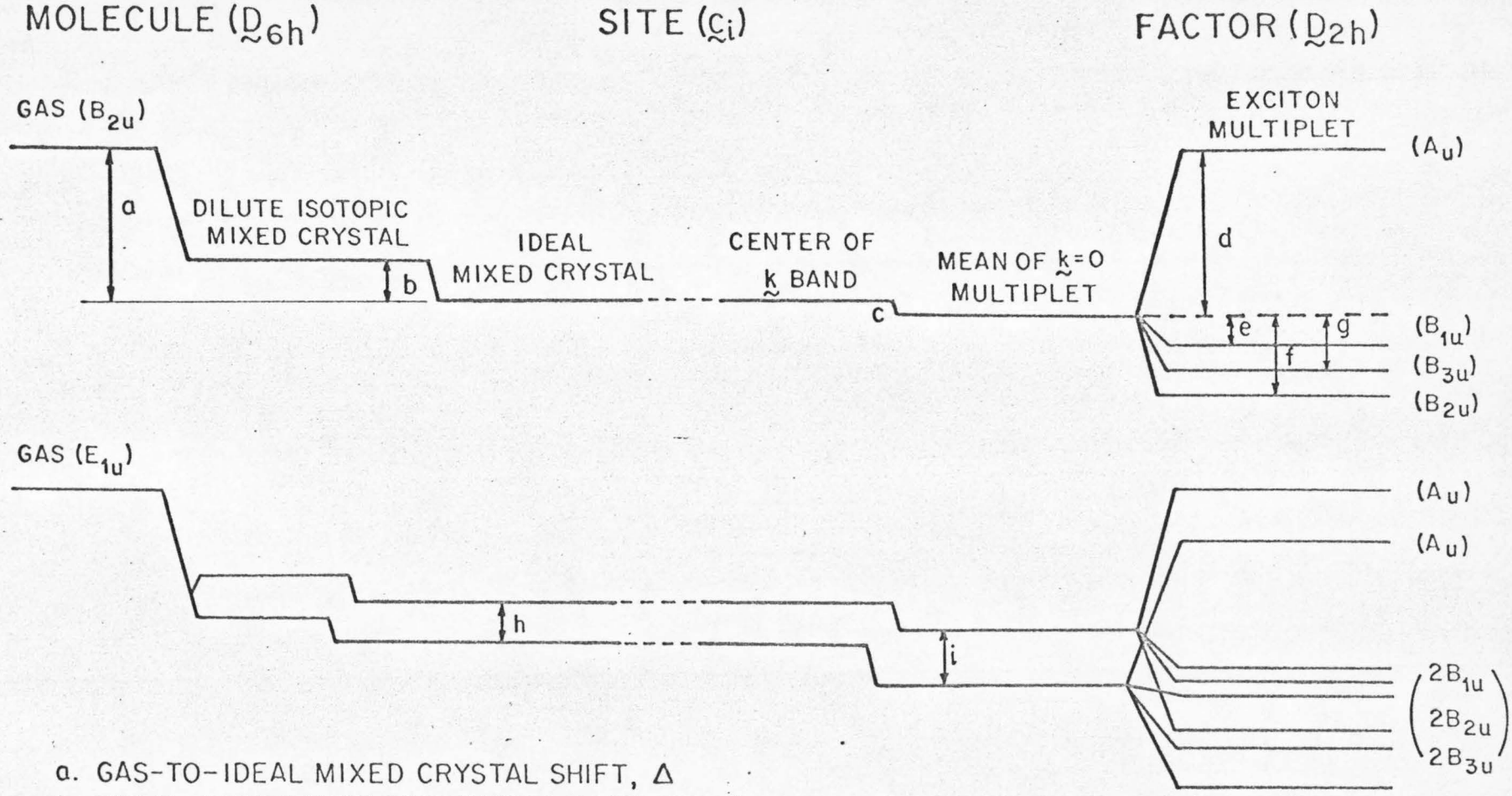

a. GAS-TO-IDEAL MIXED CRYSTAL SHIFT, Δ

b. QUASI-RESONANCE CORRECTION (SEE REF. 7)

c. $\underset{\sim}{k}=0$ SHIFT, $L^f(0)$

d. $4(M_{I,II}+M_{I,III}+M_{I,IV})$

e. $4(M_{I,II}-M_{I,III}-M_{I,IV})$

f. $4(-M_{I,II}+M_{I,III}-M_{I,IV})$

g. $4(-M_{I,II}-M_{I,III}+M_{I,IV})$

} INTERCHANGE SPLITTING

h. $(\Delta^x-\Delta^y)$

i. h PLUS ADDITIONAL NEAT CRYSTAL RESONANCE TERMS

Figure 4

Infrared spectrum of the e_{1u} (ν_{18}) fundamental of 1% C_6H_6 in C_6D_6 at 4.2°K, showing 3.8 cm^{-1} site group splitting.

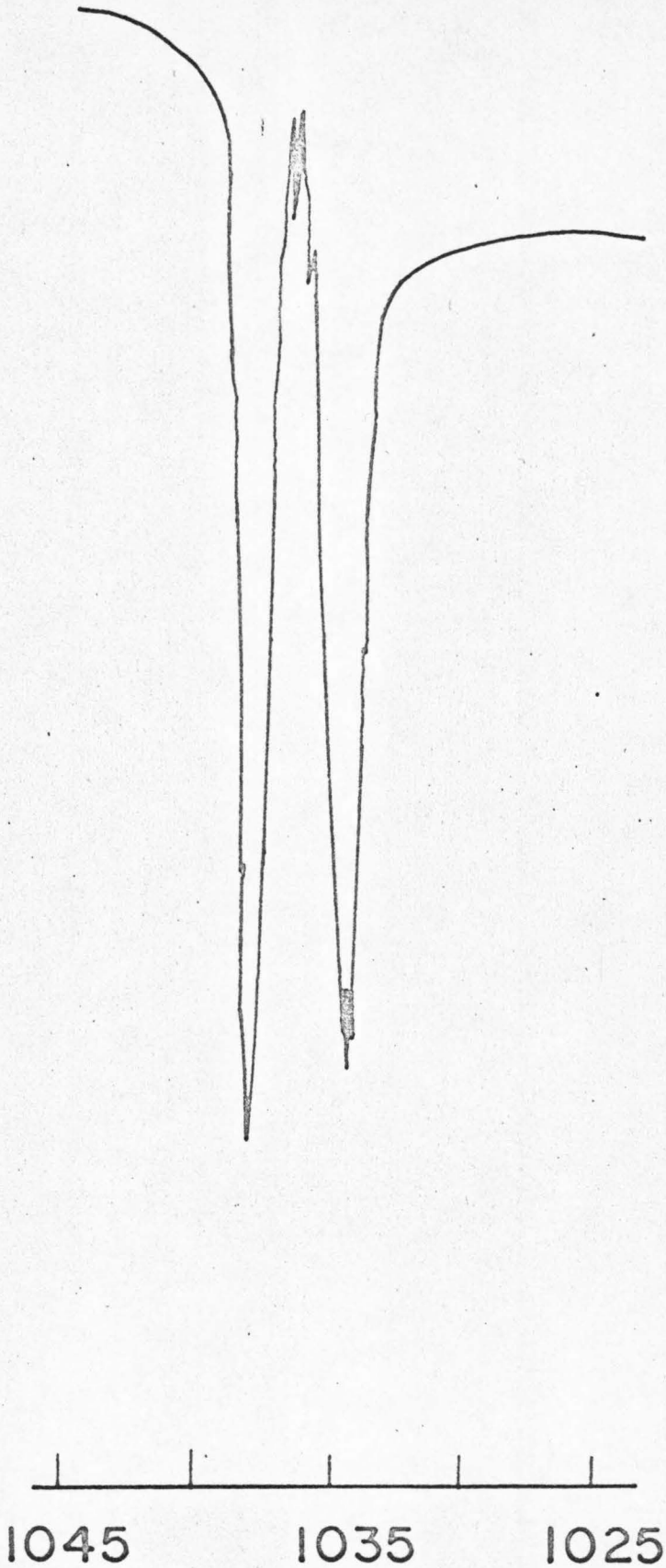
1045
1035
1025

Figure 5

Infrared spectrum of the e_{1u} (ν_{18}) fundamental of neat C_6H_6 at 4.2°K.

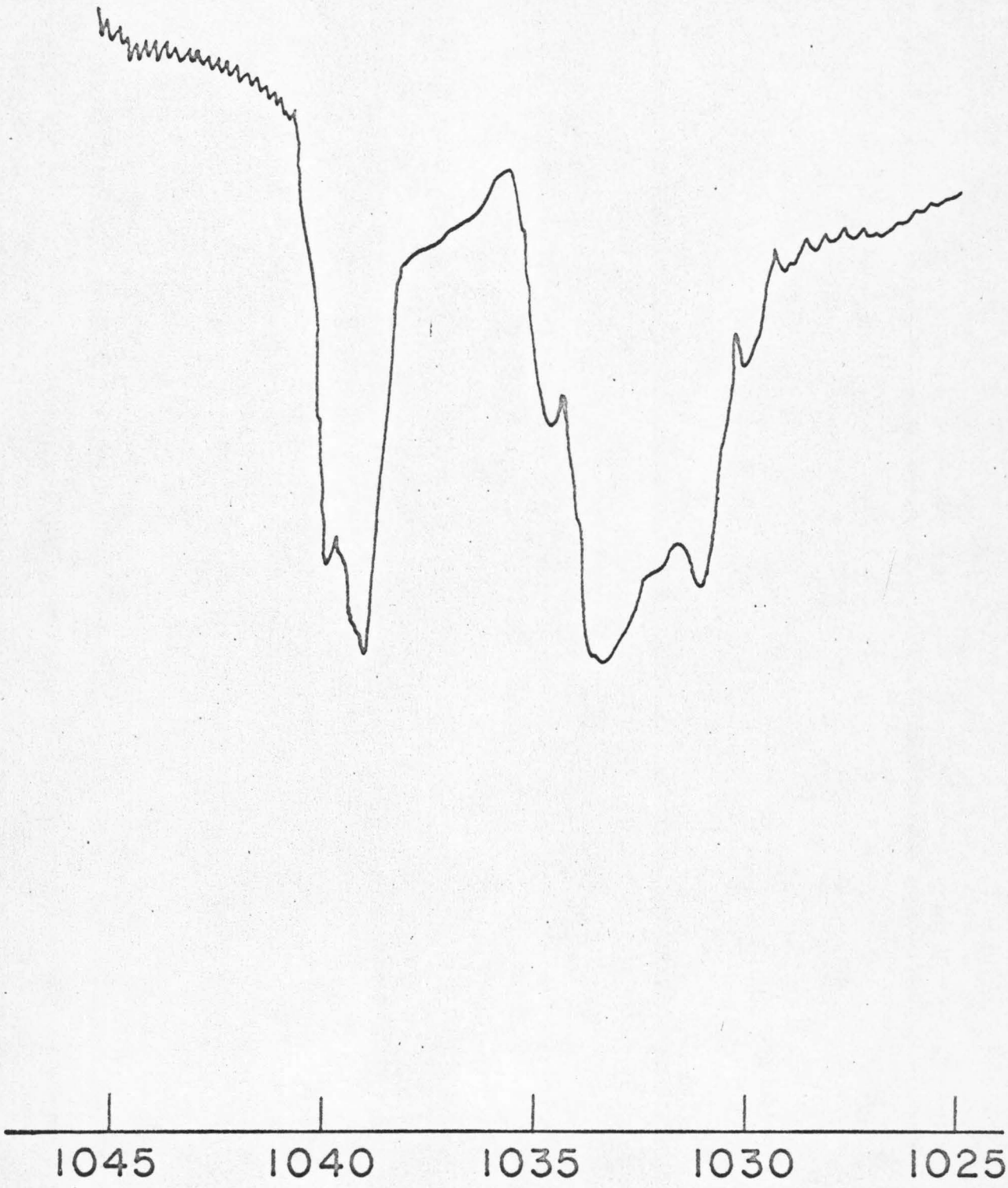
1045
1040
1035
1030
1025

Figure 6

Infrared spectra of the b_{1u} (ν_{12}) fundamental of neat C_6H_6 and 1% C_6H_6 in C_6D_6 at 77°K.

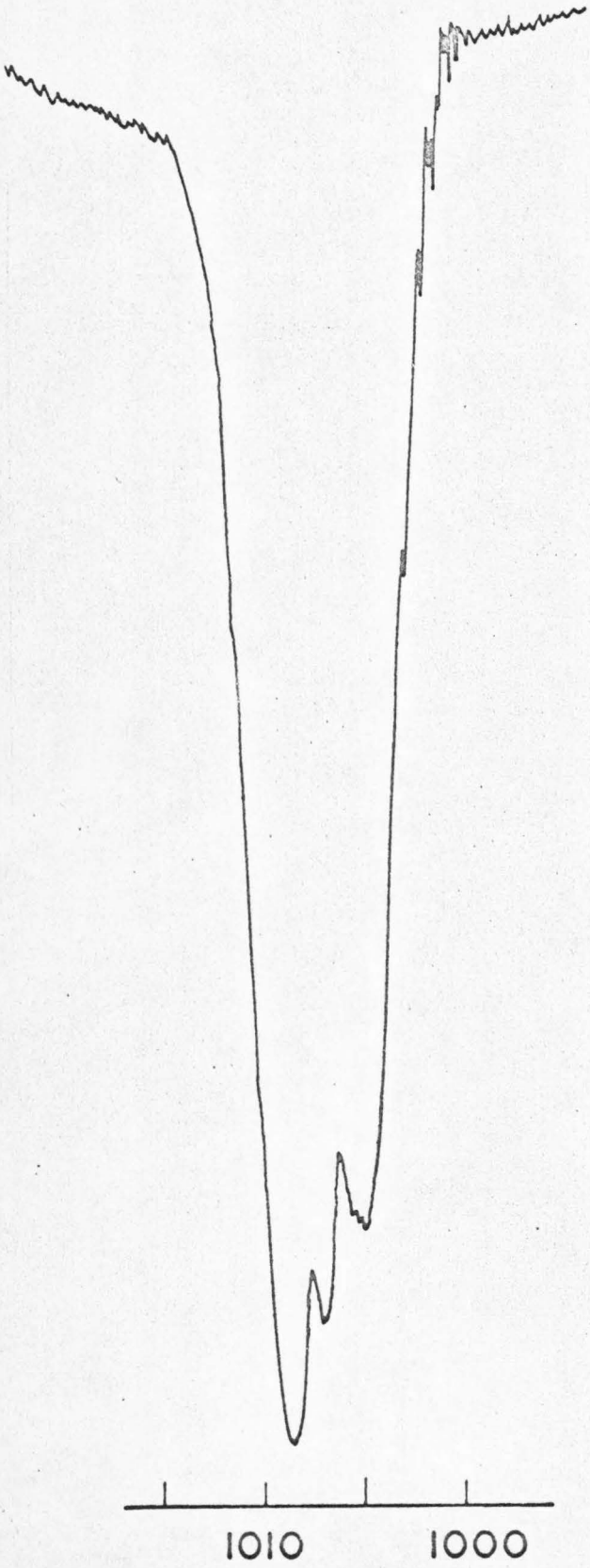
1010
1000


1010
1000

Figure 7

Infrared spectra of the b_{2u} (ν_{15}) fundamental of neat C_6H_6 and 1% C_6H_6 in C_6D_6 at 77°K.

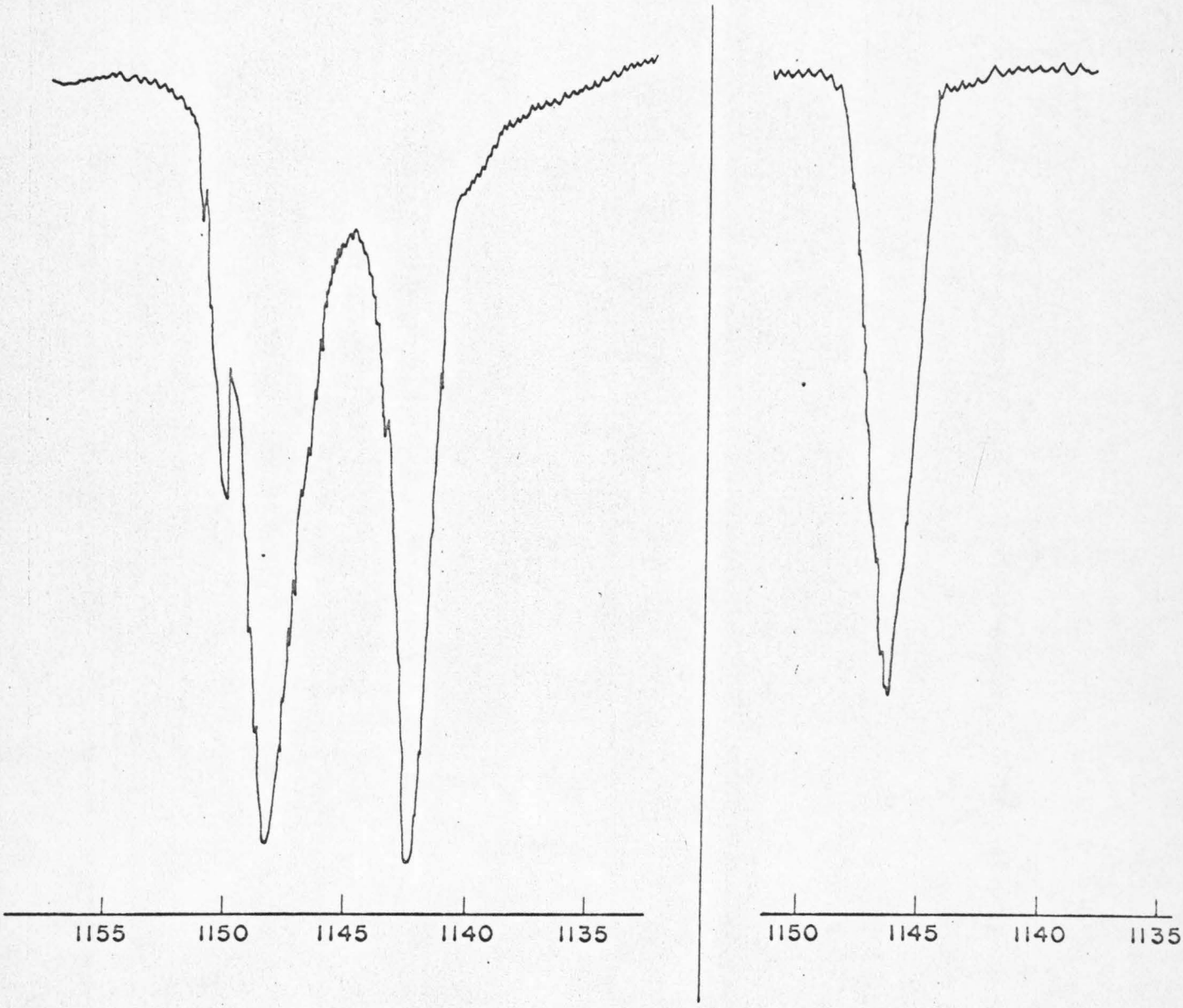
1155
1150
1145
1140
1135
1150
1145
1140
1135

Figure 8

Davydov structure of the $^1B_{2u}$ electronic state of C_6H_6 using data of Nieman and Robinson. The mean lies at 37,872 cm^{-1}. See Table III.

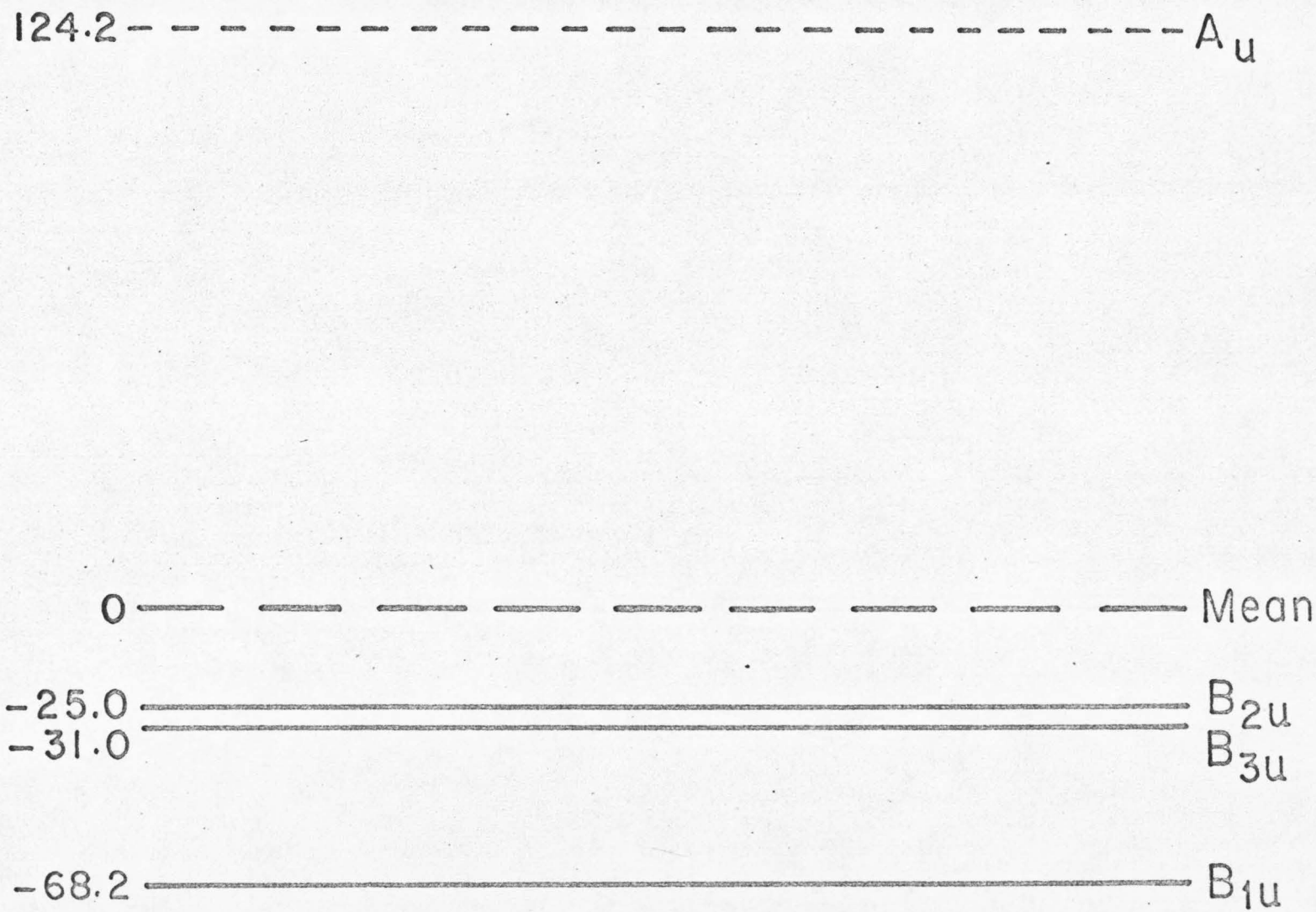
124.2
A_u
0
Mean
-25.0
-31.0
B_{2u}
B_{3u}
-68.2
B_{1u}

Figure 9

Vibrational Davydov structure of the $b_{1u}(\nu_{12})$ band of C_6H_6. The mean lies at 1011.3 cm^{-1}.

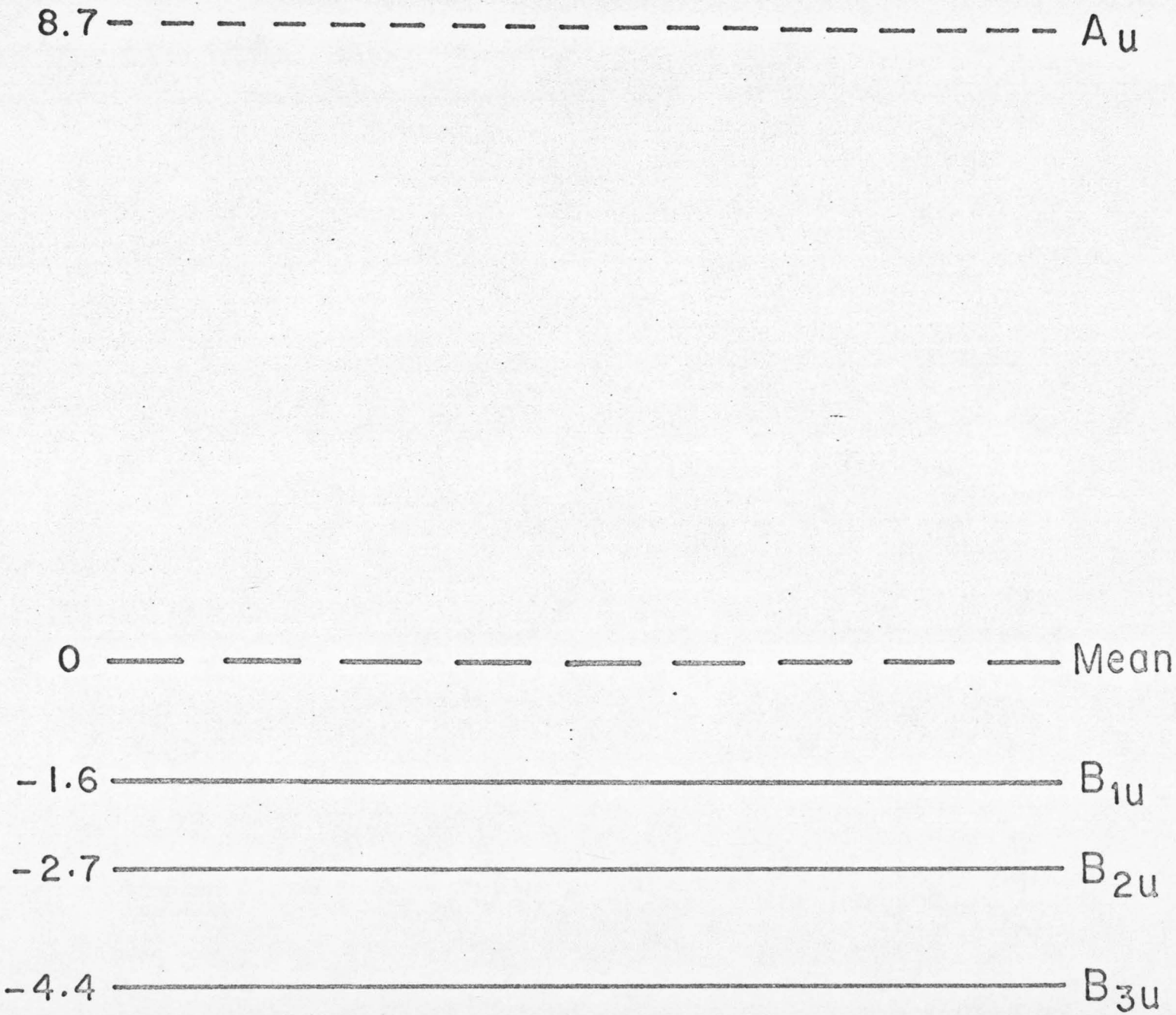
8.7
A_u
0
Mean
-1.6
B_{1u}
-2.7
B_{2u}
-4.4
B_{3u}

Figure 10

Vibrational Davydov structure of the b_{2u} (ν_{15}) band of C_6H_6. The mean lies at 1146.9 cm^{-1}.

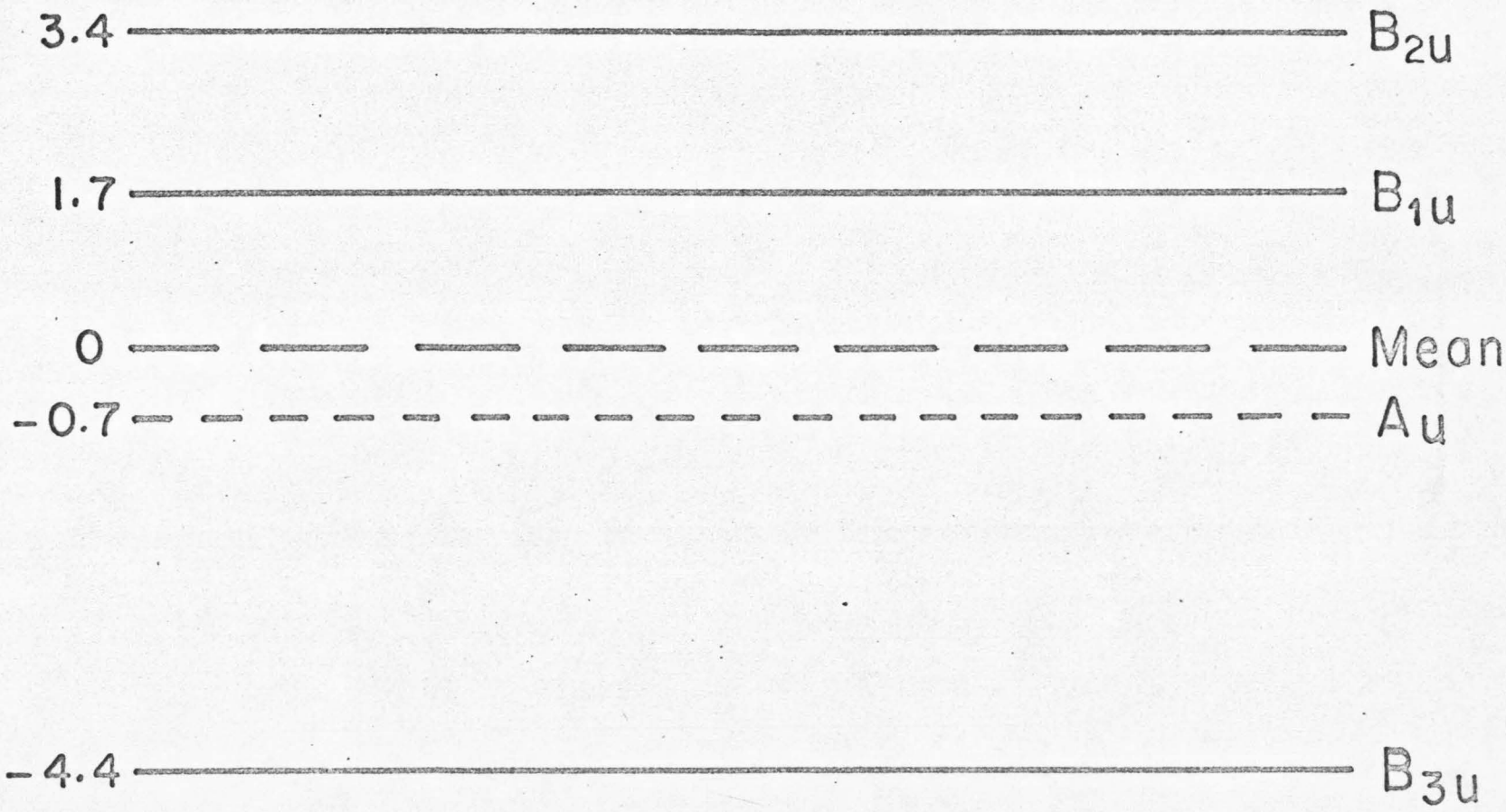
3.4
B2u
1.7
B1u
0
Mean
-0.7
Au
-4.4
B3u

This is not a missing page. It is a result of page misnumbering.

This is not a missing page. It is a result of page misnumbering.

This is not a missing page. It is a result of page misnumbering.

Site Effects in Molecular Crystals--Site Shift, Site Splitting, Orientational Effect and Intermolecular Fermi Resonance for Benzene Crystal Vibrations*†

ELLIOT R. BERNSTEIN‡

Gates and Crellin Laboratories of Chemistry§

California Institute of Technology, Pasadena, California 91109

ABSTRACT

A reduction of the Davydov Theory of energy levels in molecular crystals is developed (to first order in site functions and using the Heitler-London approximation) that is applicable to isotopic mixed crystals. This is then applied to experimental observations on ground state vibrations of various isotopic substituted benzene crystals. Three distinct and characteristic crystal-induced phenomena have been observed experimentally: (1) site group splitting--involving degenerate fundamental vibrations of the molecule that map into non-degenerate site modes; (2) orientational effects--concerning certain benzene isotopic species and their relative positioning in two or more distinct, though physically equivalent, crystal sites; and (3) intermolecular Fermi resonance--near resonance

---

*This work was supported in part by the National Science Foundation.

†Presented at the Spectroscopy Conference in Columbus, Ohio, 1966 (paper number K10).

‡1963-64 Woodrow Wilson Fellow.

§Contribution No. 3300.

interaction between two adjacent site molecules of different isotopic compositions. The first two phenomena are of the same magnitude(3-10 cm^{-1}). We propose a general mechanism to account for this and discuss the differences and similarities between these two effects. The importance of observed site (gas-to-crystal) energy shifts is also discussed in the light of these experimental findings and in the framework of the theory. Finally, intrasite solid-enhanced Fermi resonance is reported and discussed qualitatively.

Applying the Davydov theory, reduced for the case of no resonance interactions (and the neglect of second-order or quasi-resonance effects), we can obtain information concerning the shape of the molecule in the site field, the symmetry of the site field, and the general nature of the intermolecular interactions.

I. INTRODUCTION

Over the past 20 years, two complementary, theoretical approaches have been taken to the problem of Frenkel excitons[1] in molecular crystals. The first one, which could be called the Halford-Hornig approach,[2] is almost purely group theoretical in nature. These authors have discussed such concepts as the relation of the site group and the factor group to the space group, and how, from these groups, selection rules for crystal transitions can be obtained. The second approach, called the Davydov theory,[3] is a technique for obtaining general crystal energy levels. Combining these two theoretical approaches, site, interchange, and factor group interactions have been separated both physically and mathematically in an attempt to clarify their nature.[4] Although the theoretical background for this work has already been outlined in detail in Bernstein, Colson, Kopelman and Robinson (BCKR)[4], we will give a short review of the main ideas of that work for completeness and clarity of presentation.

In this discussion of the energy levels of molecular crystals, it has proven most convenient to begin with the general framework of the Davydov theory,[3] in which a crystal transition from the ground to the f excited state is given by (in the notation of ref. 4),

$$[E^{f\alpha}(\underset{\sim}{k}) - E^{0}] = (\epsilon^{f} - \epsilon^{0}) + D + L^{f\alpha}(\underset{\sim}{k}) \qquad (1)$$

Using a tight binding approximation, additive energies and product wave functions, this is a first-order equation in the energy whose zero-order wave functions are crystal site wave functions χ. The concept of a crystal site wave function, originally introduced by Davydov,[3] though somewhat lost over the intervening years, is of central importance both group theoretically and conceptually. The crystal site wave function can be thought of as representing the molecule as it exists geometrically in the crystal site field. Such

distortions when small, are well represented as a linear combination of molecular states made to transform as the irreducible representations of the crystal site group. The mixing coefficients in such a perturbation scheme could well be the derivatives of the molecular Hamiltonian with respect to the normal coordinates. The zero-order functions are clearly not, as is sometimes assumed, molecular wave functions ψ. If molecular wave functions are used, a first-order equation is not at all meaningful. This point was emphasized by BCKR. The left-hand side of Eq. (1) represents a crystal transition, and $(\epsilon^f - \epsilon^o)$ is the energy difference in the crystal site, D is a first-order energy shift term, and $L^{\alpha f}_{qq}(\underset{\sim}{k})$ incorporates the exciton band splitting terms.[4] The superscript α labels a particular irreducible representation of the interchange group.[4,5] We can write these terms out explicitly when we consider the crystal-site wave functions. This has been done by BCKR and further details of this theoretical development can be found there together with the explicit forms of the wave functions.

Here we are interested in the effect of the crystal site on a given molecule in the absence of resonance terms. Mathematically, the $L^f_{qq'}(\underset{\sim}{k})$ terms disappear in first order if the excited site wave function ϕ^f_{nq} is used instead of the one site exciton wave function $\phi^f_q(\underset{\sim}{k})$. We can accomplish this separation of terms <u>physically</u> (if second-order "quasi-resonance" effects are negligible -- "the ideal mixed crystal"[4]) by using a <1% isotopic mixed crystal. The subscript nq of ϕ^f_{nq} and ϕ^o_{nq} now refers to the crystal position of the impurity molecule. Thus, in an isotopic mixed crystal, the energy levels of the isotopic impurity are given to zero order in crystal site wave functions and first-order in crystal energy, as

$$(E^f - E^o) = (\epsilon^f - \epsilon^o) + D. \qquad (2)$$

It can be shown that for the case of benzene ground-state vibrations second-order effects, such as quasi-resonance[6] are less than one cm^{-1} and can be neglecte We are thus concerned with Eq. (2) in this work. However, this is still not the most convenient form for our purposes; it would be more useful to be able to compare the effect of the crystal site on the molecule with the gas phase transitions. When the effect of the site is only a small perturbation on the molecule (that is, when both gas and crystal transitions have almost the same energy--as is true for benzene), we can write the site function χ as a linear combination of molecular functions ψ. If we substitute these functions into the first term on the right-hand side of Eq. (2), the crystal transition energy $(E^f - E^0)$ can be decomposed into the following three terms:

$$(E^f - E^0) = (\bar{\epsilon}^f - \bar{\epsilon}^0) + P + D. \qquad (3)$$

The bar over the ϵ's implies the molecular energy states [$(\bar{\epsilon}^f - \bar{\epsilon}^0)$ is the gas phase transition energy], and P represents the higher-order terms in the molecular wave functions contributing to the crystal site energy. We shall call P the site distortion energy.[4] It includes ground, as well as excited, state contributions. This is still a strictly <u>first-order equation in site functions</u> but now broken down into three, instead of the usual two, terms. To preserve the usual form of the Davydov presentation, however, we could write Eq. (3) as

$$(E^f - E^0) = (\bar{\epsilon}^f - \bar{\epsilon}^0) + \Delta \qquad (4)$$

where

$$\Delta = P + D.$$

Δ is the first-order site contribution to the observed crystal energy levels and it is through this term that the mechanism for site splittings, site shifts and the orientational effect, aside from the exclusion of higher order effects, can be understood. BCKR point out that, certainly in general and especially for electronic states, higher order terms (W in their rotation) could contribute significantly to the energy shift term Δ. For the ground state vibrations we assume this not to be the case; such interactions should affect all the vibrations roughly the same in that they simply lower the energy of the ground electronic state. We should point out here that we have exactly paralleled the BCKR development in that the site functions χ are assumed to be exactly known. There is, however, a drawback to this general approach to the problem of crystal energy levels. It is no longer completely obvious what terms contribute to the site energy with respect to the gas phase energy, as all of these contributions now become hidden in the exact site wave function, χ. On the other hand a perturbation approach, such as that used to separate $\bar{\epsilon}$ and P, allows all these terms to be presented step-by-step. Thus resonance and near resonance terms in the perturbation can be found and discussed separately in the usual manner. We will thus later discuss this perturbation approach to crystal site functions (see Sec. 3e) and how the D + P terms can be further broken down for the case of degenerate and nearly degenerate crystal site states.

Applying the above theoretical ideas to our experiments, we will investigate the effect of the crystal site on the ground state vibrations of an isotopic guest molecule in the host crystal and in return learn about the site field. Using these site effects, it will be possible to discuss semi-quantitatively the magnitude of "static" interactions in molecular crystals and to

characterize uniquely the symmetry and nature of the site field in the benzene crystal. Specifically we will attempt to correlate Δ in a consistent fashion with the site shift, site splitting and orientational effect. We will document that the effect of host or guest isotopic substitution on these interactions is negligible (that is, the potentials governing these interactions are independent of isotopic substitution), while the major factor for their determination is the amplitude of the atomic displacements caused by the given vibrational mode. Greatly enhanced intrasite Fermi resonance is observed for the individual guest molecules. Intersite Fermi resonance is discussed for host-guest systems in which a strong guest transition is in resonance with an otherwise unobserved host vibration.

II. EXPERIMENTAL

All isotopic substituted benzenes used (C_6H_5D, p, m-$C_6H_4D_2$, sym-$C_6H_3D_3$, m-$C_6H_2D_4$, C_6HD_5, C_6D_6) were purchased from Merck, Sharpe, and Dohme of Canada, Ltd.; the C_6H_6 (Research Grade) from Phillips Petroleum Company. The samples of the isotopic guest in either a C_6H_6 or a C_6D_6 host varied in concentration from 0.50% to 1.0% and were either 0.225 mm or 0.500 mm thick. For very intense bands (for example, the e_{1u} and a_{2u} bands of C_6H_6) a 0.50% guest solution was used in the holder with the 0.225 mm sample space. The holder consists of two copper rings with grooves for 0.050-inch diameter indium wire upon which CsI windows are placed. The indium serves to apply firm, uniform pressure to the soft windows and aids in the thermal contact between the CsI and the copper. When the two halves of the holder are screwed together, the windows are spaced by either a 0.050-inch or 0.026-inch indium wire gasket (not made into a closed circle), which, when compressed, gives, quite reproducibly, the above quoted sample thicknesses. After assembly of the holder, the benzene mixture is injected into the holder through the gap left in the indium spacer. This gap is then sealed

with the remaining tails of the indium spacer. Such a technique usually produces a cell which is vacuum tight (i.e., the holder can be evacuated from the outside without loss of liquid benzene in the cell). The sample holder is then attached to the cold finger of a helium dewar and brought to liquid nitrogen temperatures in about 10 minutes. The sample thus produced is decidedly polycrystalline but not opaque. Samples were studied at both 4.2°K and 77°K with no essential difference observable in the spectra. Most of the data reported here were taken at 77°K for convenience.

All spectra were taken on a Beckman IR-12. The typical resolution in the region of interest (350-1500 cm^{-1}) was about 0.75 cm^{-1} and in some cases as good as 0.50 cm^{-1}. All line widths are believed to be instrument limited in some cases but are generally dependent on the quality of the crystal and on the concentration of the studied isotope. Thick, well prepared, low concentration ($\sim$0.1% guest) crystals gave lines of $<$0.5 cm^{-1} half width. The data thus obtained are reported in Tables I to VI and some representative spectra are displayed in Figs. 1 to 17.

III. DISCUSSION

a. General Ground State Vibrational Structures of the Isotopes

Of the 20 benzene normal modes ($2a_{1g}$, $1a_{2g}$, $2b_{2g}$, $4e_{2g}$, $1e_{1g}$, $1a_{2u}$, $2b_{1u}$, $2b_{2u}$, $2e_{2u}$, $3e_{1u}$) only a_{1g}, e_{1g}, e_{2g} (Raman), and e_{1u}, a_{2u} (infrared) fundamentals have been observed directly in the gas phase due to the D_{6h} group theoretical selection rules for dipole allowed transitions. All other gas phase bands are known from combinations that have total symmetry e_{1u} or a_{2u} for the infrared spectra or a_{1g}, e_{1g} or e_{2g} for the Raman spectra. These selection rules apply exactly only to the isotopic species C_6H_6 and C_6D_6, which possess the full $\underset{\sim}{D}_{6h}$ symmetry; in the isotopes of lower symmetry, sym-$C_6H_3D_3$, p-$C_6H_4D_2$, C_6H_5D, the gas phase activity of vibrations is given

to first order not by the group character table selection rules but by correlation to active modes in C_6H_6 or C_6D_6. Thus, in general, only modes that correlate to or mix with a_{1g}, e_{1g}, e_{2g}, e_{1u}, or a_{2u} will have an appreciable intensity in the gas phase Raman or infrared spectra, implying that in terms of selection rules, the substitution of a deuterium atom for a hydrogen atom in benzene is not a large perturbation.

While the crystal environment changes the gas phase energy only slightly (see Sec. 3c), the selection rules are clearly much different. The molecular symmetry is reduced at least in theory to $\underset{\sim}{C}_i$, and thus all vibrations having $\underset{\sim}{u}$ symmetry are active in the infrared and all vibrations having $\underset{\sim}{g}$ symmetry are observed in the Raman. Of course, this last statement deals with intensity enhancement and is difficult to make quantitative, but, for example, all e_{2u}, b_{1u} and b_{2u} vibrations are observed in the infrared. The gas phase ($\underset{\sim}{D}_{6h}$) allowed vibrations are still the most intense in the Raman and infrared, as would be expected for molecular crystals. It should be emphasized that this breakdown of gas phase selection rules does not necessarily imply large crystal site interactions, even though these intensity changes do appear to be the most dramatic effect of the site on the molecule. It is not clear just how to relate the size of the intermolecular interactions to their intensity enhancement. Such interactions are probably most reliably determined from their effects on the molecular energy levels (site shifts, site splittings and orientational effects).

A remark should also be made concerning the symmetry assignments and numbering of the vibrational transitions of the non-$\underset{\sim}{D}_{6h}$ isotopes. In most cases there is strong mixing between vibrations of the same symmetry. This becomes even further complicated for degenerate vibrations where, due to this mixing, assignment to the $\underset{\sim}{a}$ or $\underset{\sim}{b}$ split component is at best tenuous. The assignments made in this paper, where conflicts or ambiguities exist, are chosen to agree with the emission work of Bernstein, Colson, Tinti and

Robinson.[8] This approach is taken, as in some cases the symmetry assignments can be made unambiguously from vibronic arguments. Throughout this paper we will use the molecular point group to characterize the symmetry of the crystal site vibrational states. While this is a convenience only and it is realized that this designation is of limited value for the work presented here, it is useful and of interest to know to which state of the molecule a crystal site vibration corresponds.

Tables I-VI and Figs. 1-17 give the isotopic mixed crystal spectra for C_6H_6, C_6D_6, sym-$C_6H_3D_3$, p-$C_6H_4D_2$, C_6H_5D and C_6D_5H in the C_6H_6 and/or the C_6D_6 host. Vibrations have been observed for all these isotopic derivatives but since this work deals mainly with the "splittings" and "shifts" of well-known bands, the only data reported is that where the assignments are certain. In fact the data for two of the studied isotopes, m-$C_6H_4D_2$ and m-$C_6H_2D_4$ (Fig. 17), are not even given in tables since complications due to the orientational effects, poor gas phase data, mixing of vibrations and inherent isotopic impurity, make many assignments almost impossible. However, it is believed that the conclusions and discussions in this paper are very well documented with this complete, though not exhaustive, presentation of data.

b. Solid-Enhanced Fermi Resonance

Solid-enhanced Fermi resonance has been discussed in detail by Strizhevsky.[9] The number of possible interacting states is increased in the solid because of splittings and reduced symmetry. While his statements are completely general, his discussion deals with resonance between an accidentally degenerate fundamental and overtone or combination. These resonances are, of course, present in the benzene systems, and are, for the most part, well known,[10,11,12] but do not appear to be stronger in the

solid than in the gase phase (vide infra). Examples are given in Figs. 1 and 2 of the (20) ~ (8 + 19) ~ (1 + 6 + 19) 3000 cm^{-1} region of C_6H_6 and 2250 cm^{-1} (20) ~ (1 + 19) of C_6D_6.

In an isotopic mixed crystal of benzene, there is a chance of further Fermi resonance between fundamentals due to the decrease in symmetry of the molecule; that is, fundamentals that were orthogonal in $\underset{\sim}{D}_{6h}$ symmetry can now mix in the "$\underset{\sim}{C}_i$-distorted" molecule of the crystal. This crystal site-induced molecular distortion can be viewed as an increased anharmonicity of the site potential function with respect to the free molecule force field, allowing the increased Fermi resonance to be treated in the standard way through the anharmonic terms in the (site) potential function. This statement is subject to three qualifications: 1) the site distortion of the molecule must be sufficient to destroy the orthogonality of the fundamentals, i.e., the site-induced anharmonicity is sufficiently large;2) the fundamentals must be "accidentally degenerate" in energy; and 3) we must be able to detect the resonance if it occurs. Conditions 1) and 2) are best satisfied by C_6H_5D and sym-$C_6H_3D_3$, m-$C_6H_4D_2$ and m-$C_6H_2D_4$. These last two isotopes however have so many accidental degeneracies in the crystal that the spectra are very difficult to interpret and thus cannot be given as clear examples of this phenomenon even though it is extensively present. There are usually two methods for detecting the presence of Fermi resonance; anomalous energy shifts, and intensity distortions. The latter is by far the most sensitive but, due to the difficulty of knowing the intensities of fundamentals of isotopic substituted benzene and how these are affected by the crystal, we use the criterion of anomalous energy shift from the gas phase values for an indication of Fermi resonance in the solid. When such resonances and mixings are "forbidden" or small in the molecule, even very weak crystal perturbations can envoke dramatic charges in the spectra. Thus the 925 cm^{-1} region of sym-$C_6H_3D_3$, the

980 cm^{-1} region of C_6H_6D, the 3000 cm^{-1} region of C_6H_6 and the 2250 cm^{-1} region of C_6D_6 all represent examples of this crystal induced intra-site mixing or resonance of gas phase orthogonal fundamentals under the reduced symmetry of the crystal. Looking at Table IV it is obvious the ν_5, ν_{15} and ν_{17} are interacting with one another in sym-$C_6H_3D_3$ as these gas-to-crystal (site) shifts are much larger and of different sign than the site shifts of these vibrations in the other isotopes. Table II shows the same phenomenon for ν_1, ν_{17}, ν_5 and ν_{12} of C_6H_5D. One of the most striking shifts appears for ν_{13}($\sim$ 20 cm^{-1}) of C_6D_6, as given in Fig. 1 and Table VI. In C_6H_6 (Table I and Fig. 2) the mixing between ν_{13}, ν_{20}, ($\nu_{19} + \nu_8$), ($\nu_1 + \nu_6 + \nu_{14}$) and others is so extensive that it becomes impossible to identify the absorptions with specific vibrations. In Fig. 3 we see also that due to intra-site Fermi resonance the spectra of m-$C_6D_4H_2$ is almost impossible to assign uniquely. While this spectra may further be complicated by the presence of other isotopes a possible partial assignment of the absorptions is presented on the figure.

c. The Crystal Structure

Since we will be further interested in the effects of the crystal site on the molecular fundamentals of the benzene isotopes in a more specific fashion than just discussed it is very important to know the site symmetry and the exact shape of the molecule in the crystal site. We first, of course, must look at the available X-ray and neutron diffraction data for the crystal.

The benzene crystal structure, as given by Cox et al.,[13] is space group D_{2h}^{15} with four molecules per unit cell at sites of C_i symmetry. All sites are crystallographically and physically equivalent. Cox et al., however, conclude that the benzene molecule is both hexagonal and planar even though the molecules reside in an environment of no greater than C_i symmetry. The neutron diffraction data of Bacon et al.,[14] extrapolated to

77°K, corroborate these conclusions. The thermally corrected C–C distance is 1.390 Å ± 0.002 Å, and the corrected H–H distance is 1.083 Å ± 0.004 Å where the deviations in bond lengths are assumed to be within the experimental error. The carbon atoms are all out of the "carbon best plane" by ± 0.0015 Å, the hydrogen atoms are out of the "hydrogen best plane" by ± 0.0093 Å, and the maximum deviation of any atom out of the combined equally weighted "best plane" of the molecule is ± 0.0118 Å. As significant as these differences appear to be, because of thermal corrections and other uncertainties, both Cox and Bacon are forced to conclude that they lie within experimental error. Thus from crystallographic data alone the molecular shape, within the experimental error of measurement, reflects the $\underset{\sim}{D}_{6h}$ symmetry of the free molecule.

If we approach the problem from a physical point of view, we see that the site is almost of $\underset{\sim}{C}_{2h}$ symmetry--with a plane passing through atoms 1 and 4, for example. We find further that the deviations from the assumed planarity are most consistent with this <u>effective</u> site symmetry. On the other hand, it would be incorrect to assume that the site has an effective six-fold axis, as the crystal does not have one. We can resort to the spectra of the benzene crystal to understand both the physical state of the molecule in the crystal and the nature of the distorting environment. Figure 18 gives geometrical representations of some possible physical site symmetries ($\underset{\sim}{C}_i$, $\underset{\sim}{C}_{2h}$, $\underset{\sim}{D}_{2h}$).

The most obvious effect that the crystal environment can have on the molecule is to change the energy of the ground state vibrational transitions. These site shifts are discussed in Sec. 3d. In Sec. 3e we will give evidence that the benzene molecule is nonhexagonal in the ground electronic state, while in Secs. 3f and 3g, we will present experimental information concern-

ing the physical nature of the crystal site and the extent to which this affects the molecular energy levels and selection rules.

d. Site Shifts

The importance of the site shifts for the interpretation of exciton theory has already been discussed.[4] To first order in site functions the site shift is given by Δ of Eq. (4). The explicit form for the components of Δ in terms of crystal site function is given by BCKR[4] and using molecular wave functions P can be written as

$$P = \left\{ \langle \sum_q{}' C_q^f \psi_q | H_o | \sum_\ell{}' C_\ell^f \psi_\ell \rangle \quad - \quad \langle \sum_n{}' C_n^o \psi_n | H_o | \sum_m{}' C_m^o \psi_m \rangle \right\}$$

where the prime on the summation sign indicates that $q = f$, $\ell = f$, $n = 0$, $m = 0$ are omitted from the summations, ψ's are molecular wave functions and H_0 is the crystal site Hamiltonian given as $H_0 \chi_\nu = \epsilon_\nu \chi_\nu$. P can be thought of as a configurational mixing of molecular states in the reduced symmetry of the crystal site. The terms in H_0 that cause this mixing are those that represent the distortion of the molecule from its gas phase equilibrium (hexagonal) configuration to that of the molecule in the site. Such terms, for small distortions, might be represented as derivatives of the molecular geometry with respect to the normal coordinates. This contribution to Δ as well as the D term is discussed in BCKR, along with the possible affect of higher order contributions to the site shift. These authors present reasonability arguments to the affect that higher order term W will be the major contribution to the shift, at least for electronic states. It is not at all clear which of the components will be the major contributor to Δ for the ground state vibrations. For simplicity and clarity of presentation a first order theory

will be rigorously and perhaps arbitrarily adhered to, as the experimental data on the ground state vibrations does not appear at present to demand the inclusion of the higher order terms.

In the case of degenerate vibrations, the site shift can be measured from the gas phase value to each of the crystal components and can be either a red or blue shift for each component of the split band. It is also possible to obtain a mean or average site shift for a degenerate vibration, $\bar{\Delta}$ which can be compared to the Δ for a nondegenerate band. Two distinct and consistent cases present themselves: bands, both degenerate and nondegenerate, for which the mean or average gas-to-crystal shift is of the order of 10 cm^{-1}; and bands for which this mean shift is of the order of 0-2 cm^{-1}.

The experimental site shifts can be determined from the tables of data. We will discuss a few pertinent and representative cases for the isotopes as examples of the various types of typical vibrations; a_{2u}, ν_{11} (strong dipole transition, gas phase allowed), e_{2u}, ν_{16} (weak, crystal allowed), e_{1u}, ν_{18} (medium, gas phase allowed), and b_{1u}, ν_{12} and b_{2u}, ν_{15} (weak, both crystal allowed). In particular we are interested in whether or not such shifts are present, if such shifts do exist what trends can be determined from isotope to isotope or vibrational state to vibrational state, and what are the host or guest isotopic effects on these shifts (the so-called isotopic effect on the Δ term). There are, of course, problems with this comparison: vibrational mixing so that the character of a given vibration is changed from isotope to isotope; the chance of increased or further mixing

in the crystal with respect to the gas due to enhanced Fermi resonance in the solid; and the inaccuracy of the gas phase data where, due to the presence of rotational structure and the restriction of selection rules (a_{2u}, e_{1u} are the only directly observed symmetries) the exact frequencies are probably only good to $\pm$ 2-5 cm^{-1}. In this section and throughout this paper we have tried to discuss only those vibrations for which it is believed these complications are minimized.

The easiest comparison to begin with is the out-of-plane $\nu_{11}(a_{2u})$ vibration. The site shifts $\Delta^{\nu_{11}}$ are:

	C_6H_6	C_6H_5D	$pC_6H_4D_2$	$sC_6H_3D_3$	$mC_6H_2D_4$	C_6D_5H	C_6D_6
$\Delta^{\nu_{11}}(C_6H_6)$ =	--	15.4	17.8	14.4	15.0	15.3	15.3 cm^{-1}
$\Delta^{\nu_{11}}(C_6D_6)$ =	23.9	15.4	17.8	14.6	15.0	15.3	-- cm^{-1}

measured in both C_6H_6 and C_6D_5 hosts where applicable. Aside from the large value for C_6H_6 there appears in general to be no isotopic effect on the Δ, either from the solvent or the guest. This certainly appears to be true of the solvent. The large value of Δ for C_6H_6 is well outside combined experimental error; while it could be due to an isotopic effect on the interactions, certainly no trend is obvious from the data. Thus we cannot really draw any conclusions until other vibrations are considered.

For the out-of-plane, $\nu_{16}(e_{2u})$ the mean shifts $\bar{\Delta}$ obtained by averaging the site components are as follows:

	C_6H_6	$C_6H_5D(b_2)$	$sC_6H_3D_3$	C_6D_6
$\bar{\Delta}^{\nu_{16}}(C_6H_6)$ =	--	7.1	13.8	11.9 cm^{-1}
$\bar{\Delta}^{\nu_{16}}(C_6D_6)$ =	10.9	8.6	--	--

but it must be remembered here that for the nontrigonal isotopes, interaction between the two components is greatly enhanced in the solid.

These data indicate to us only that the site shift Δ for these vibrations is nonnegligible and certainly of the order of the other effects to be discussed later, any isotopic effect on the shifts are certainly small ($\sim 1\ cm^{-1}$).

The mean shifts for ν_{18}, a planar e_{1u} vibration in $\underset{\sim}{D}_{6h}$, on the other hand, appear to be $< 2\ cm^{-1}$:

	C_6H_6	C_6H_5D	$pC_6H_4D_2$	$sC_6H_2D_3$	C_6HD_5	C_6D_6
$\bar{\Delta}^{\nu_{18}}(C_6H_6)$ =	--	~1	~1	0.5	~0	-2.0
$\bar{\Delta}^{\nu_{18}}(C_6D_6)$	~1.0	~1	~1	0.5	~0	--

and again no concrete trend presents itself. It must be emphasized, that while $\bar{\Delta} \approx 0$, Δ is not really zero for this vibration as each site component is shifted from the degenerate gas phase value (C_6H_6, $C_6H_3D_3$, and C_6D_6) by about 1-2 cm^{-1} and from the nondegenerate gas phase values ($pC_6H_4D_2$, C_6H_5D, C_6D_5H) by about 1 cm^{-1}. The shift for C_6D_6 is probably affected by the presence of ν_{15} which can interact with it in the crystal.

For our last comparison of the site shifts of the various isotopes we look at the planar $\nu_{15}(b_{2u})$ and $\nu_{12}(b_{1u})$ vibrations. The shifts are:

	C_6H_6	C_6H_5D	$pC_6H_4D_2$	$sC_6H_3D_3$	C_6D_6
$\Delta^{\nu_{15}}(C_6H_6)$ =	--	0.5	~2	-4.0	3.4
$\Delta^{\nu_{15}}(C_6D_6)$ =	0.9	0.6	~1	-4.0	--

	C_6H_6	C_6H_5D	$pC_6H_4D_2$	$sC_6H_3D_3$	C_6D_6
$\Delta^{\nu_{12}}(C_6H_6)$ =	--	--	--	--	1.0
$\Delta^{\nu_{12}}(C_6D_6)$ =	1.3	-3.8	-5	--	--

These shifts are highly erratic and are an excellent indication that the crystalline environment changes these vibrations to a meaningful extent, from isotope to isotope. For these vibrations the large shifts (C_6H_5D ν_{12}, $pC_6H_4D_2$ ν_{12}, $sC_6H_3D_3$ ν_{15}, C_6D_6 ν_{15}) can all be correlated to the presence of other vibrations close by and thus a strong Fermi interaction is quite likely. One must thus be very careful in making general statements concerning these vibrations and their interactions (both static and dynamic) in the crystal.

We have not covered all the available data in the text and the tables should be consulted for a more complete picture. What we have presented are representative, and thus of necessity rather obvious, examples of all the extreme cases that can be traced through most of the isotopes. Others fall in between and become perhaps less easily categorized. To sum up the data on the site shifts the only consistent trend that is apparent is, for a given vibrational species, Δ is a constant independent of the isotopic modification of the guest or host molecule. The two cases that are generally found are $\Delta \sim 1$ cm^{-1} for planar vibrations and $\Delta \sim 10$ cm^{-1} for non-planar vibrations. Exceptions to this trend for a given state occur but can be explained by solid enhanced Fermi resonance between the nearly degenerate gas phase fundamentals. We can thus conclude from our data that there is no significant isotopic (host or guest) effect on the Δ term for the ground vibrational states, and thus the interaction potentials themselves appear to be independent of isotopic substitution.

e. Site Group Splitting

Site group splitting results from the lifting of a molecular degeneracy by the interaction of a molecule with the surrounding low-symmetry crystal site

field. Group theoretically this means that a degenerate irreducible representation of the molecular group maps into at least one nondegenerate irreducible representation in the site group. For benzene, only C_6H_6, C_6D_6, or sym-$C_6H_3D_3$ can therefore show site group splittings. We now define site group splitting phenomenologically as the splitting of degenerate states observed in the "ideal mixed crystal".[15a] Using this definition, Eq. (2) provides the obvious mechanism for site group splitting, δ_{ss}, of a degenerate state:

$$\delta_{ss} = (\Delta^+ - \Delta^-) = (D^+ - D^-) + (P^+ - P^-) \tag{5}$$

where the + and - refer to the higher (χ^+) and lower (χ^-) energy site states of the originally gas phase degenerate state of the isotopic impurity. Before proceeding with the detailed discussion of the site group splitting let us further consider the relative magnitudes of the terms comprising this contribution to the total site splitting, δ_{ss}. The P term can be found in Sec. 3d and the term $(D^+ - D^-)$ of Eq. (5) has the form[4]

$$\sum_{n'q'} \left\{ \langle \chi^+_{nq} \chi^o_{n'q'} | H' | \chi^+_{nq} \chi^o_{n'q'} \rangle - \langle \chi^-_{nq} \chi^o_{n'q'} | H' | \chi^-_{nq} \chi^o_{n'q'} \rangle \right\}$$

in which χ^+_{nq} and χ^-_{nq} are the high and low energy crystal site states, of the guest molecule, respectively. This term represents the difference in interaction of two site charge distributions with their nearest neighbors in the crystal. This difference in principle could be quite large (for example, in the case of electronic dipoles), but for benzene ground state vibrations one would expect it to be small. On the other hand, the P term is composed of integrals of H_o, the crystal site Hamiltonian, over sums of molecular functions (see Sec. 3d). This mixing of states is due to the distortion of the molecule by the crystal site field. Since however the

components of the molecular degenerate state should be very similar in their ability to mix with the other states of the complete molecular set, we might expect that $P^+ \approx P^-$. In a like manner it can be argued that higher order terms may not contribute to δ_{ss}. Then, while P(W) could contribute significantly to the site shift, the major contribution to the site group splitting, δ_{ss}, could come from $(D^+ - D^-)$.[15b] Although the above is somewhat conjectural in nature it is clear that the site splitting is given by Eq. (5) to first order and can be obtained in higher order with the addition of terms such as $(W^+ - W^-)$ to δ_{ss}. (Ref. 4 discusses the presence of such terms in Δ.)

In order to fully understand the nature of site splitting we consider a perturbation approach to the crystal site symmetry states χ^+_{nq} and χ^-_{nq} and therefore D. As we did before to separate the ϵ into $\bar{\epsilon}$ and P we write (for an e_{1u} vibration as an example),

$$\chi^x = \sum_\nu C^x_\nu \psi_\nu \text{ and } \chi^y = \sum_\mu C^y_\mu \psi_\mu$$

where ψ_ν is the molecular eigenfunction of the molecular Hamiltonian, h, and $h\psi_\nu = \bar{\epsilon}_\nu \psi_\nu$. The coefficients are integrals over the crystal site Hamiltonian H_o. Upon substituting these perturbation wave functions into the above expression for D, it is obvious that all the molecular states can contribute to the site splitting of any other given molecular state. This break down of D^f is analogous to the separation of ϵ^f into $\bar{\epsilon}^f$ and P^f. However, there can be various dynamic or resonance intra site coupling interactions which can serve to further mix these levels, adding to the site splitting. The first is a dynamic "Jahn-Teller type" interaction that could couple the levels, χ^x and χ^y, through the low-lying lattice vibrations.

These accoustical phonons could distort the molecule in such a way as to make the degnerate or nearly degenerate states χ^x and χ^y unstable with respect to such motion. A subsequent "tunneling" between these states would then mix the χ^x and χ^y states contributing to the site splitting. For benzene such an occurrence is not likely as the lattice modes do not appear to interact strongly with the vibrations. This is evidenced by the almost complete lack of temperature dependence of the vibrational spectra from 77°K to 1.8°K. We can thus tentatively, and somewhat arbitrarily on both intuitive and experimental grounds, eliminate this contribution to the mixing of χ^x and χ^y. The second dynamic mechanism by which these two states can couple is intra site or site-induced Fermi resonance, arising from a crystal-site-induced "anharmonicity". Using a perturbation language these terms would arise from the difference between h and H_o. There are, of course, limitations on this resonance coupling, one of which is that χ^x and χ^y, constructed to transform as irreducible representations of the site group, must have the same symmetry. That is to say the molecule degenerate component states, x and y, in our example, must map into the same irreducible representation of the site group. This is true of benzene where the site has $\underset{\sim}{C}_i$ symmetry and thus both $e_{1u}(x)$ and $e_{1u}(y)$ map into A_u. If, on the other hand, the benzene crystal had a crystallographic site of $\underset{\sim}{C}_{2h}$ symmetry with the C_2 axis through carbon 1 (the molecular y-axis), then $e_{1u}(x)$ would map into B_u, $e_{1u}(y)$ would map into A_u and no such coupling could take place (the methyl halides represent a real example of such a case[16]). A further limitation on such a coupling between site states belonging to the same irreducible representation is the energy

separation between these states. Assuming this initial separation to be small ($\lesssim 10\ cm^{-1}$) and providing the crystal induced "anharmonicities" in the free molecule "harmonic" potential function are sufficiently large, we can use standard degenerate perturbation theory[7] and couple the χ^x and χ^y states to form the new site states, χ^+ and χ^-. This coupling, as in standard Fermi resonance treatments, is effected by the anharmonic terms present in the new force field due to the crystal site distortion of the molecule. The site induced Fermi resonance is a direct consequence of the crystal reduction of the molecular symmetry and the site symmetry of the first order wave functions χ^x and χ^y. Thus we have seen that dynamic <u>intra</u> site effects can contribute to the site group splitting as well as the static site distortion energy and the <u>inter</u> site term, D.

Since we have, at least for benzene, limited the considerations to an <u>intra</u> site Fermi resonance coupling and the static terms in Δ we will try to discuss the experimental result of this and the next section in such a way as to evaluate, if possible, the relative contribution of each to the site group splitting. Two distinct cases of vibrations, as classified by their Δ shifts from the gas phase values, seem to present themselves: vibrations of the e_{1u}-type, with a mean Δ of $\sim 0\ cm^{-1}$, and of the e_{2u}-type with a mean of Δ of $\sim 10\ cm^{-1}$. It should be emphasized that Δ^+ and Δ^- can be either positive or negative (see Sec. 3f, also), thus making a mean Δ of $\sim 0\ cm^{-1}$ capable of giving a site group splitting of about $5\ cm^{-1}$, which is not inconsistent with the observed benzene site splitting.

It is interesting to look at the site group splitting as a function of solvent and solute for the various isotopes with degenerate vibrations. For comparison the reader is referred to Sec. 3d where the site shifts are listed for these vibrations. Again it is emphasized that the vibrations

discussed in the text are representative of the general case, and are chosen as exemplary because they remain relatively unmixed from isotope to isotope and are experimentally well determined. The tables should be consulted for the remainder of the data.

We first look at the (planar) e_{1u} vibration ν_{18} for which the mean Δ is $\sim 0.0\ cm^{-1}$ in all the isotopes. The site group splitting as a function of the host, $\delta_{SS}^{\nu_{18}}$(host), for ν_{18} is, in cm^{-1}:

	C_6H_6	$C_6H_3D_3$	C_6D_6
$\delta_{SS}^{\nu_{18}}(C_6H_6)$	-	2.8	(4.1)
$\delta_{SS}^{\nu_{18}}(C_6D_6)$	3.8	3.3	-

A few comments are in order: First, the C_6D_6 number is not certain due to a possible Fermi resonance between ν_{18} and ν_{15} (See Fig. 4b). Second, it might be possible to comment on δ_{SS} for sym-$C_6H_3D_3$ in C_6H_6 as opposed to C_6D_6. Unfortunately, due to the presence of a C_6D_6 transition this comparison is not very conclusive. However, the difference in site group splitting for the two bands is in the expected direction. Due to molecular zero point considerations, the C_6D_6 crystal should be more closely packed and thus squeeze or distort the sym-$C_6H_3D_3$ molecules to a greater extent than the C_6H_6 crystal. Since the molecular centers are now closer together, the C–H and C–C interactions energies are increased; further, an H atom on the guest interacts more strongly with the host molecules than does a D atom. This can be thought of as a "cage effect" -- the smaller the cage the greater the interaction and thus the larger the splitting can be. Such small changes in the site splitting are not obvious indications of isotopic

effects on the interaction potentials, as the potentials remain unchanged while the intersite atomic separations are altered. The above arguments would predict that $\delta_{SS}^{\nu_{18}}(C_6H_6) < \delta_{SS}^{\nu_{18}}(C_6D_6)$ for the sym-$C_6H_3D_3$, as is found experimentally.

The $e_{2u}\nu_{16}$ and ν_{17} vibrations (non planar) can also be compared in the same manner in the various isotopes and different solvents. The site splittings are (in cm^{-1}):

	C_6H_6	sym-$C_6H_3D_3$	C_6D_6
$\delta_{SS}^{\nu_{16}}(C_6H_6)$	-	8.5	10.8
$\delta_{SS}^{\nu_{16}}(C_6D_6)$	8.2	-	-

The C_6D_6 factor group structure obscures the observation of the sym-$C_6H_3D_3$ ν_{16} transition.

	C_6H_6	sym-$C_6H_3D_3$	C_6D_6
$\delta_{SS}^{\nu_{17}}(C_6H_6)$	-	3.7	6.5
$\delta_{SS}^{\nu_{17}}(C_6D_6)$	5.6	2.8	-

Again the interesting case of the sym-$C_6H_3D_3$ splitting is complicated by the distortion of the band shape and the shifting of the absolute energy (see Table IV). Thus because the shift appears in the opposite direction from that of ν_{18} we cannot really make a quantitative statement concerning the effect of the host crystal on site splitting. One point of great importance can be seen in these data. The e_{2u} band $\delta_{SS}^{\nu_{16},\nu_{17}}$ (= 7.0 cm^{-1}) is on the average a factor of 2 greater than $\delta_{SS}^{\nu_{18}}$ (= 3.5 cm^{-1}). This implies that the larger the Δ the larger the δ_{SS}, and that planar vibrations are less affected by the site than non-

planar ones. The data show no obviously large isotopic effects from either the host or guest molecules on the site splitting. This was also found to be the case for the site shift.

The fact that we can observe site group splitting for the degenerate molecular fundamentals of isotopic benzenes (Tables I, IV, VI and Figs. 4 and 5) gives us information concerning the shape of the molecule in the site (or the distortion of the molecule by the site). It is clear that the benzene molecule has lost its three-fold axis, and, in fact, the observed site group splitting can serve as a quantitative measure of the degree of nontrigonality of the benzene in the crystal site. Although it appears that we can say nothing concerning the ground state configuration from Eq. (5) (as it is the same for both states χ_i^+ and χ_i^-), certainly through zero-point arguments[17] the ground state can, at least in principle, be considered to be nontrigonal. All that we can conclude at present is that there is about a 1% difference in energy between two molecule degenerate directions.

Let us now consider the "shape" or symmetry of the site field. We know from the above discussion only that the site has lower than $\underset{\sim}{D}_{3h}$ symmetry. As discussed before, there are only two physically reasonable possibilities for the site symmetry, $\underset{\sim}{C}_{2h}$ and $\underset{\sim}{C}_i$, neither of which is eliminated by this restriction. As shown in Table VIII, neither can selection rules distinguish between these two symmetries which are both consistent with the site group splitting.

f. Orientational Effect

In the last section we considered the effect of the crystal site environment on degenerate states of isotopic modifications of benzene with $\underset{\sim}{D}_{3h}$ or higher symmetry. In this section we consider the effect of the site on non

degenerate molecular states of these and all the other isotopes. For a general formulation of the orientational effect we must turn to group theory. Table IX, extracted from Kopelman's discussion,[18] gives the pertinent information and groups. His technique is rigorously parallel to the interchange approach to crystal wave functions and their symmetry.[4] This highly formalistic approach is in general very useful but is unfortunately not very transparent. Our approach will be of a more physical nature which it is hoped will aid in understanding the origin of the orientational effect.

It is clear that for the placement of H(D) atoms on the hexagonal carbon framework there exists many possibilities for the various isotopes: 1 for C_6H_6 and C_6D_6; 2 for sym-$C_6H_3D_3$; 3 for $pC_6H_4D_2$($pC_6H_2D_4$); 6 for $mC_6H_4D_2$ ($C_6H_2D_4$), C_6H_5D(C_6HD_5), o-$C_6H_4D_2$($C_6H_2D_4$), C_6H_5D(C_6HD_5) and 1, 2, 3$C_6H_3D_3$; and 12 for 1, 2, 4$C_6H_3D_3$. Thus a given isotope of benzene fixed in space except with respect to the 6-fold rotation axis of the carbon hexagon will have the above distinct orientations in free space (site of $\underset{\sim}{C}_1$ symmetry). With a site symmetry greater than $\underset{\sim}{C}_1$, some of the orientations of the molecule in the site become equivalent by symmetry, thus reducing its total number of possible physically distinct orientations. Since the benzene isotopic guest molecules in a host crystal are free to orient randomly with respect to $2\pi M/6$ (M = 1, 6) rotation about the molecular six-fold axes,[18b] we are presented with the above "free space" example in these mixed isotopic molecular crystals. The number of distinct orientations of a molecule in the crystal site, and thus the number of possibly different energies that can be observed in the crystal spectrum of a given gas phase transition, is governed by the site symmetry. We shall now discuss the group theoretical correlations specifically for the benzene crystal, beginning

with the isotopes of highest symmetry.[19] C_6H_6 and C_6D_6 will, of course, show no orientational effect, with respect to covering rotations about the molecular six-fold axis. They will sit in the site field of lower than $\underset{\sim}{D}_{6h}$ symmetry, but since all the (six) molecular positions are equivalent, all orientations of these molecules possess the same energy in the site. Thus, there are no means by which to distinguish between different positionings (orientations) of the molecule in the site and no extra lines show up in the spectra. Consider now sym-$C_6H_3D_3$: although this case is not so obvious, no orientational effects can occur (for $\underset{\sim}{C}_i$ or $\underset{\sim}{C}_{2h}$ site symmetry) as we are concerned with orientation <u>modulo</u> site operations. This can be understood physically by observing that no matter how the molecule is positioned in the site (with respect to the molecular "six-fold axis"), along each <u>distinct</u> site direction, that is, site directions not related by the symmetry of the site group, the molecule contains one hydrogen and one deuterium atom. Since these different site directions are all equivalent in the sym-$C_6H_3D_3$ <u>molecule</u>, again we have no energy difference. It should be pointed out that these two are the only symmetries ($\underset{\sim}{D}_{3h}$ and $\underset{\sim}{D}_{6h}$) for which site group splitting occurs, and it is experimentally verified that, only the degenerate fundamentals belonging to these molecules (C_6H_6, C_6D_6, and sym-$C_6H_3D_3$) are observed to split in the crystal. The isotopic molecules of $\underset{\sim}{D}_{2h}$ symmetry and lower will show an orientational effect. Consider 1,4-$C_6H_4D_2$: one symmetry-related site position sees only D atoms while the other positions, not related to the first by site symmetry (one for $\underset{\sim}{C}_{2h}$ site symmetry and two for $\underset{\sim}{C}_i$ site symmetry) (see Fig. 18), see H atoms. Since these positions in the site field are physically different, energy differences ("splittings") are seen in the spectra on nondegenerate

fundamental bands. It is straightforward to find the number of orientations for isotopic benzenes of lower symmetry in this manner, and these results can be checked against Table IX.

To give a clear concise picture of the orientational effect, and what can be learned from it, let us compare and contrast it to the better known effect of site group splitting. First, the orientational effect, like the site group splitting, is not due to an isotopic effect on the interaction potentials. The low symmetry site distorts the molecular (hexagonal) geometrical framework in a given fashion, independent of the position of the H and D atoms. Thus H(D) atoms can take up random position with respect to these distortions, giving rise to different transition energies for differently oriented molecules (with respect to the site field). Second, unlike site group splitting which is a single guest-molecule phenomenon, orientational effects need at least two guest molecules differently oriented in distinct (but physically equivalent) sites to appear in the spectra. Third, the isotopic molecular species in which site group splitting occurs (those with $\underset{\sim}{D}_{3h}$ symmetry or greater--see Table IX) do not show orientational effects. Fourth, it is thus clear that again unlike site group splitting, the primary information obtained from orientational effects concerns the symmetry and magnitude of the static site field and not the molecular symmetry.

The orientational effects predicted group theoretically can be formalized physically as were the site splittings in the last section. Since, for the orientational effect we need at least two equivalent sites with isotopically substituted molecules (of $\underset{\sim}{D}_{2h}$ symmetry or lower) in different, physically distinct orientations in each site, the energy difference, δ_{OE}, between transitions in these two sites is given by (to first order only),

$$\begin{aligned} \delta^{f}_{OE} &= (\Delta_1 - \Delta_2) \\ &= (D_1 - D_2) + (P_1 - P_2) \end{aligned} \qquad (7)$$

where the subscripts 1 and 2 refer to two isotopic molecules in different sites. The generalization to more than two possible orientations should be obvious. A few remarks are in order concerning Eq. (7). First, at least in principle, P_1 and P_2 do not cancel. Further, each P represents ground and excited state site polarization terms, neither of which probably cancel exactly. Second, unlike the case of site group splitting, the ground state terms in D_1 and D_2 do not cancel as we now deal with distinct molecules in different orientations in two sites. Third, the orientational effect is not really a "splitting" in the same sense as site group splitting, as no fundamental intrasite degeneracy has been removed, only an intersite degeneracy. Fourth, since no intrasite degeneracy exists for these isotopes, the Fermi resonance or dynamic "Jahn-Teller contributions" to the Δ cannot be envoked since a real physical separation of the "degenerate" states exists. As in the case of site splitting, higher order terms could be incorporated into δ_{OE} as $(W_1 - W_2)$.

The orientational effect has been observed on transitions of C_6H_5D,[8] C_6D_5H, m-$C_6H_4D_2$,[8] m-$C_6H_2D_4$, and p-$C_6H_4D_2$.[8] (See Figs. 3, 5, and 6 through 16 and the Tables.) There are three general observations to be made about these data. First, the splittings for a given vibrational type are about 1/2 of the site group splittings indicating the absence of both the Fermi resonance and Jahn-Teller interactions in the Δ term and that the ground state contributions to δ_{OE} are small. Second, all planar vibrations are "split" into a doublet only, with an intensity ratio of 2:1 (indicating a $\underset{\sim}{C}_{2h}$ site symmetry) while nonplanar vibrations tend to "split" into a triplet (indication of a $\underset{\sim}{C}_i$ site). From this we concluded that the site contains an "approximate symmetry plane" which is "conserved" by in-plane vibrations but "destroyed" by out-of-plane vibrations. The out-of-plane vibrations experience the full site symmetry, $\underset{\sim}{C}_i$. Thus, the molecule is neither hexagonal nor planar in the crystal. Third, the effect appears somewhat greater in

the C_6D_6 host than in the C_6H_6 host and also for C_6H_5D than for C_6HD_5 for the sam vibration. We attribute this to a "cage effect" mentioned in the last section. Due to the zero-point energy the C–D distance is shorter than the C–H distance, allowing C_6D_6 molecular centers to get closer together than the C_6H_6 molecular centers. Therefore, an "orientational splitting" should be greater for a molecule in C_6D_6 than in C_6H_6, and considering molecules of the same symmetry, greater for the guest with the greater number of hydrogen atoms, for a given vibration.

Keeping in mind that there are no "dynamic" contributions to the orientational effect, the distinction made above between "planar" and "non-planar" vibrations, and that Δ can be both positive and negative, we can again compare individual vibrations in different isotopic species and solvents.

The planar vibration ν_{18}, which we saw had a small site shift, can be seen to have a small orientation effect and only two components are observed. These are (in cm^{-1}):

	C_6H_5D	p-$C_6H_4D_2$	C_6HD_5
$\delta_{OE}^{\nu_{18}b}(C_6H_6)$	[4.7]	3.7	1.5
$\delta_{OE}^{\nu_{18}b}(C_6D_6)$	2.1	-	2.2
$\delta_{OE}^{\nu_{18}a}(C_6H_6)$	-	-	-
$\delta_{OE}^{\nu_{18}a}(C_6D_6)$	2.8	3.1	-

Figure 8 has the spectra of the ν_{18b} band of C_6H_5D in C_6H_6 and C_6D_6. The intensity change between the two components and the line shape distortion are probably due to the third, unresolved orientational line. This may also account for the anomolously large orientation effect in C_6H_6. A further possible cause of these apparent solvent effects could be a change in crystal site induced resonance between ν_{18b} and ν_{10a} with the different solvents.

On the other hand, the two out-of-plane ν_{16} components have, on the average, a large orientational effect.

	C_6H_5D	$p\text{-}C_6H_4D_2$	(in cm^{-1})
$\delta_{OE}^{\nu_{16a}}(C_6H_6)$	-	-	
$\delta_{OE}^{\nu_{16a}}(C_6D_6)$	-	4.7	
$\delta_{OE}^{\nu_{16b}}(C_6H_6)$	4.3	-	
$\delta_{OE}^{\nu_{16b}}(C_6D_6)$	4.6	-	

This out-of-plane vibration (see Fig. 7) has a larger effect than the in-plane modes a its $\bar{\Delta}$ of 10 cm^{-1} is one of the largest. Thus there appears to be good correlation between a large Δ and large site splitting and orientational effect.

Even though there is a lack of complete data on many isotopes, Fermi resonances in some bands, and low intensity in others, we are forced to conclude that any change in δ_{OE} due to isotopic substitution in the host or the guest is of the order of 1 cm^{-1} or less. Further, for these two vibrations the trend again appears to be that out-of-plane vibrations show the largest δ_{OE}. However, in general such a conclusion cannot unambiguously be reached from the tables of data. We should point out that for C_6H_5D and $p\text{-}C_6H_4D_2$ the orientational effect generally appears to be independent of the mode type. On the other hand the C_6D_5H ν_5 and ν_{10} seem to be consistent with the planar vs. nonplanar break down. Unfortunately these vibrations cannot be observed in the other isotopes. The less sharp distinction here than for site splittings is believed to be a function of the greater mixing of the vibrations of these low symmetry isotopes in both the crystal site and the molecule. This tends to make the planar, nonplanar classification of vibration somewhat less meaningful.

Comparing δ_{OE} and δ_{SS} for a given vibration it is clear that δ_{SS} is greater than δ_{OE} by a very rough factor of 1.5. This indicates the presence of the extra dynamic interactions in the case where the degenerate states reside on one molecule and that the ground state contributions to δ_{OE} are small. Thus the Fermi resonance interaction could contribute as much as 25% to the observed site group splitting.

A further demonstration that these interaction potentials are relatively independent of host or guest isotopic composition and simply a function of the crystal environmental structure is given by the C_6H_5D impurity spectra (ν_{11}, ν_{18}) in m-$C_6H_4D_2$ (Fig. 19). These transitions should be compared with those of C_6H_5D in C_6H_6 and C_6D_6 in Fig. 8, 12 and 15. The sharp lines are due to good crystal quality and the very low concentration of the C_6H_5D. While the absolute energies are not exactly those of the other solvents (See Fig. 19) the δ_{OE}'s are in very good agreement ($\delta_{OE}^{\nu_{18}a}$ (m-$C_6H_4D_2$) = 2.9, $\delta_{OE}^{\nu_{18}b}$ (m-$C_6H_4D_2$) = 3.2 and $\delta_{OE}^{\nu_{11}}$ (m-$C_6H_4D_2$) = 2.4 cm^{-1}).

The most important conclusion to be drawn from the orientational effect lies in the observation that for ν_4 and ν_{10} of C_6D_5H and ν_{17} of p-$C_6H_4D_2$ three orientational lines have been observed. Thus the site symmetry is $\underset{\sim}{C}_i$ and not $\underset{\sim}{C}_{2h}$ as the observation of both two and three lines for the vibrations eliminates the plane of the site field being the molecular plane. It should be noted that these vibrations for which three lines have been observed are the nonplanar ones.

Before leaving this topic it should be pointed out that only the C_6H_5D and p-$C_6H_4D_2$ ν_{11}(a_{2u} C–H out-of-plane) are observed to show any orientation effect--at best quite small--while none is observed for C_6D_5H or m-$C_6H_4D_2$ (see Figs. 11-17). This is quite surprising in light of the previous discussion but is unmistakeably true. The only possible explanation is that the a_{2u}

mode is a symmetric combination of the out-of-plane CH perpendicular bending and thus not much affected by site orientation. Calculations bear this out and further comments concerning this will be made in a forthcoming work.[20]

g. Intermolecular Fermi Resonance

We have thus far focused our attention on the guest molecule alone. We now consider the effects of the presence of isotopic guest molecules on the host, in a crystal of, for example, 1% C_6H_6 in 99% C_6D_6. Both guest and host molecules have inversion symmetry and the guest molecule sits in a site of inversion symmetry, at least in the limit of "infinite dilution." However, approximately 10% of the C_6D_6 (there are 12 nearest-neighbor molecules in the benzene crystal) will not have inversion site symmetry. One might expect therefore to be able to observe g vibrations of C_6D_6 in infrared absorption spectra (a breakdown of $u \leftrightarrow g$ selection rules) in such isotopic mixed crystals, much for the some reason that one observes b_{1u}, b_{2u}, e_{2u} gas phase forbidden transitions in the guest molecules. However such a perturbation on the host would be very much smaller than the site perturbation on the guest. Therefore there must be a new physical mechanism for the intensity enhancement of the C_6D_6 g vibrational transitions if they are to appear in the infrared absorption spectra. It is clear that this is a general phenomenon, not simply limited to the above example--any guest molecule will destroy the host site symmetry and thus change selection rules. The question is, does such a general mechanism, for an intensity enhancement of the forbidden host transition, exist? It is proposed that intermolecular Fermi resonance,[21] caused by a site induced or inter site anharmonicity, is such a mechanism and direct, conclusive evidence is presented for its occurrence in isotopic benzene crystals.

While this may be quite a common occurrence, even in the isotopic benzene crystal systems, we present only a few instances which are completely clear cut, free from interference from isotopic impurities and other transitions. We monitor the $\nu_6 - e_{2g}$ host transition (of C_6H_6 or C_6D_6) with various isotopic impurities present. The very intense guest transition ν_{11} (a_{2u} in C_6H_6) is in this region (697 in C_6H_6 to 513 cm^{-1} in C_6D_6) and we consider this the transition perturbing the host molecule. The e_{2g} transition is <u>not</u> observed in the C_6H_6 host when C_6D_6 (513 cm^{-1}), C_6D_5H (527 cm^{-1}), m-$C_6H_2D_4$ (538 cm^{-1}), sym-$C_6H_3D_3$ (543 cm^{-1}) are present as a guest molecule. However with p-$C_6H_4D_2$ (612 cm^{-1}) and C_6H_5D (621 cm^{-1}) in the C_6H_6 host, a new doublet is observed (see Fig. 12). This is attributed to the $\nu_6 e_{2g}$ degenerate (site group split) C_6H_6 transition observed at 606.3 and 609.4 cm^{-1} in phosphorescence of a C_6H_6 isotopic mixed crystal.[8] Thus only when the energy difference between host and guest transition is small is there an observable effect of the site symmetry loss in the host. This spectra is shown in Fig. 12. A possible further instance of this mechanism occurring in isotopic benzenes mixed crystals can be found in the intensity of the C_6H_5D peak (ν_{11}), (See Fig. 12) which is difficult to explain unless intermolecular Fermi resonance is envoked. C_6H_5D is a natural impurity in the C_6H_6 host, but certainly not as great as the 1% p-$C_6H_4D_2$ which was added for the experiment.

Thus intermolecular Fermi resonance between p-$C_6H_4D_2$ (ν_{11}) or C_6H_6 (ν_{11}) and C_6H_5D (ν_{11}) is a good possibility. In this instance the levels need not be as close together as in the previous case, as both transitions are intense and dipole-allowed in the molecule. Although in both cases only small energy shifts ($\lesssim 1.0$ cm^{-1}) are observed, the intensity enhancement is the most important factor in the Fermi resonance in solids.[9] Other examples of this with the same set of vibrations are presented in Figs. 12-16. Another

case of this type of intersite Fermi resonance that seems to have played a role in the benzene spectra is that of C_6D_5H impurity in C_6D_6. Hollenberg and Dows[22] assigned the a_{2u} of C_6D_5H as a part of the C_6D_6 a_{2u} exciton band. The a_{2u} of C_6D_5H at 527 cm^{-1} is very intense (of the order of other bands of the C_6D_6 spectra) and we propose this to be due to intermolecular intensity borrowing through the Fermi resonance mechanism. Note that the effect should be very pronounced here as the a_{2u} bands of both molecules are intense, gas phase allowed and very close in energy.

It is very difficult to say anything quantitative concerning crystal intermolecular Fermi resonance due to the lack of an accurate crystal site wave function. Clearly this is a crystal effect alone, and a subtle one at that. Although we cannot use the Davydov formalism as outlined here to discuss this phenomenon as the one site exciton function is used and the assumption of no intersite overlap is made, one can obviously treat this phenomenon in higher order as is ordinary Fermi resonance.[21]

IV. CONCLUSION

From the three observed phenomena, site group splitting, orientational effects, and intermolecular Fermi resonance, it is possible to make the following statements concerning the benzene crystal:

a) The molecule in the crystal has neither a six-fold axis nor is it planar.

b) The physical site symmetry is C_i and not C_{2h}. The possibility of a C_{2h} site symmetry with the horizontal plane being the plane of the molecule is eliminated by the observation that both two and three components are observed for various vibrations. This does show, however, that the site has an approximate plane of symmetry, perpendicular to the molecular plane,

which is "preserved" by the planar and destroyed by the nonplanar vibrations. Only out-of-plane vibrations exhibit the three orientational lines which is consistent with and strongly supports the above conclusion.

c) The out-of-plane vibrations, from the data on site shifts, splittings and the orientational effect, are found to be more sensitive to the nature of the site potential field and the site symmetry. The out-of-plane vibrations are expected to be sensitive to the inter-molecular potential as the atomic displacements of these fundamentals are larger (by almost a factor of five on the average) than for the in-plane modes. Thus these greater amplitude atomic displacements account for the fact that the large crystal effects are always found associated with the out-of-plane modes (b_{2g}, e_{1g}, a_{2u}, e_{2u} in $\underset{\sim}{D}_{6h}$ symmetry).

d) To within the experimental error (± 0.5 cm^{-1}) no isotopic effects on the interaction potentials can be observed.

e) Since both site splitting and orientational effect seem to be independent of mode classification (C–C, C–H, H–H), we can tentatively conclude (pending calculations)[20] that C–H as well as H–H intermolecular interactions are of importance for these splittings.

f) Generalizing from the specific data given in the text in such a way as to obtain average site group splittings and orientational effects for given vibrations it appears that for the benzene vibrations considered, $\delta^{\nu}_{SS} \approx 1.5\,\delta^{\nu}_{OE}$. Since the orientational effect δ^{ν}_{OE} is an <u>inter</u>-site phenomenon, that is the two or three site states are spacially separated, and the site group splitting δ^{ν}_{SS} is an <u>intra</u>-site phenomenon, both states on the same site, dynamic effects can contribute only to the site group splitting, not the orientational effect. On the other hand, the ground state contributions to the orientational effect do not cancel as they do for the site splitting. It is therefore difficult

to quantitatively compare the two effects but it is clear that since there are terms in common, the resonance contributions to δ_{SS} are larger than the ground state contributions to δ_{OE}.

ACKNOWLEDGMENT

The author wishes to express his gratitude to Professor G. W. Robinson for helpful discussions and suggestions concerning this work.

REFERENCES

[1]J. Frenkel, Phys. Rev. 37, 17, 1276 (1931).

[2]R. S. Halford and O. H. Schafer, J. Chem. Phys. 14, 141 (1946); R. S. Halford, J. Chem. Phys. 14, 8 (1946); H. Winston and R. S. Halford, J. Chem. Phys. 17, 607 (1949); D. F. Hornig, J. Chem. Phys. 16, 1063 (1948).

[3]A. S. Davydov, Theory of Molecular Excitons (McGraw-Hill Book Co., Inc., New York, New York, 1962) and Usp. Fiz. Nauk. 82, 396 (1964).

[4]For a more complete and detailed account of the form and implications of this development see E. R. Bernstein, S. D. Colson, R. Kopelman, and G. W. Robinson, "Vibrational and Electronic Exciton Structure in Molecular Crystals-Benzene," J. Chem. Phys., submitted for publication.

[5]See Ref. 4 for the full-group theoretical breakdown of the molecular exciton problem and also R. Kopelman, "Interchange Symmetry for Molecules and Crystals," J. Chem. Phys., submitted for publication.

[6]Ref. 4 and G. C. Nieman and G. W. Robinson, J. Chem. Phys. 39, 1298 (1963).

[7]G. Herzberg, Molecular Structure and Molecular Spectra II Infrared and Raman Spectra (Van Nostrand, 1964), p. 215 ff.

[8]E. R. Bernstein, S. D. Colson, D. S. Tinti, and G. W. Robinson, "Fine Structure Observed in Electronic Absorption and Emission Spectra in Isotopic Mixed Benzene Crystals under High Resolution," J. Chem. Phys., to be published.

[9]V. L. Strizhevsky, Opt. i Spektroskopiya 8, 86 (1960).

[10]E. B. Wilson, Phys. Rev. 46, 146 (1934).

[11]G. Herzberg, Infrared and Raman Spectra of Polyatomic Molecules (D. Van Nostrand, New York, 1950), p. 362.

[12]S. Brodersen and A. Langseth, Mat. Fys. Skr. Dan. Ved. Selsk 1, 1 (1956).

[13]E. G. Cox, Rev. Mod. Phys. 10, 159 (1958); E. G. Cox, D.W.J. Cruickshank and J.A.S. Smith, Proc. Roy. Soc. (London) A247, 1 (1958).

[14]G. E. Bacon, N. A. Currey, and S. A. Wilson, Proc. Roy. Soc. (London) A289, 98 (1964).

[15a]This concept (see Ref. 4) implies Eq. (2) is rigorously correct not just to first order in site functions. This is a good approximation for ground state vibrations of benzene. In the excited electronic states it is possible to apply the second-order correction term (quasi resonance -- Ref. 4 and Ref. 6) and still use the concept of the "ideal mixed crystal".

[15b]This statement and the conclusions that can be drawn from it are verified in detail by calculation of the site splitting and orientation effect, E. R. Bernstein manuscript in preparation.

[16]R. Kopelman, J. Chem. Phys. 44, 3547 (1966).

[17]There are 10 degenerate fundamentals whose average site group splitting is $\sim 4\ cm^{-1}$, which gives a zero point contribution of $\sim 10\ cm^{-1}$. This is greater than kT at 4.2°K.

[18a]R. Kopelman, "Interchange Symmetry for Molecules and Crystal," J. Chem. Phys., submitted for publication.

[18b]E. R. Andrew and R. G. Eacles, Proc. Roy. Soc. (London) A218, 537 (1953).

[19]In the following discussion, when we refer to an isotopic species we always mean the system of that species as a guest in one of the symmetrical hosts (C_6H_6 and C_6D_6).

[20]E. R. Bernstein, manuscript in preparation.

[21]Formally this is no different from the more usual intramolecular Fermi resonance, and the mathematical approach is the same as that given in Ref. 5. The only change is in the wave functions which are now site functions belonging to the two neighboring molecules.

[22]J. C. Hollenberg and D. A. Dows, J. Chem. Phys. 37, 1300 (1962).

TABLE I.

1.0% C_6H_6 in 99.0% C_6D_6 (u vibrations only)

Vibration Number and Type	Symmetry in D_{6h}	Gas Phase[a] cm^{-1}	Energy in cm^{-1}	Comment	Site Splitting cm^{-1} (δ_{SS})
(C-C) nonplanar ν_{16}	e_{2u}	398.1	404.8 413.0	W, Equal I	8.2
(C-H) nonplanar ν_{11}	a_{2u}	673	694.1 696.9	W ^{13}C Sharp	
(C-H) nonplanar ν_{17}	e_{2u}	967	978.3 983.9	Both lines are blue shaded Equal I	5.6
(C-C) planar ν_{12}	b_{1u}	1010	1011.3	Sharp	
(C-H) planar ν_{18}	e_{1u}	1037	1034.8 1038.6	Sharp, Equal I	3.8
(C-H) planar ν_{15}	b_{2u}	1146	1146.9	Sharp	
(C-H) planar ν_{14}	b_{2u}	1309	1308.0 1312.6	^{13}C	
(C-C) planar ν_{19}	e_{1u}	1482	1460-78	B and flat	
(C-H) planar ν_{20}	b_{1u}	3043	3012.5[b]		
ν_{13}	e_{1u}	3057	3033.9		?
$\nu_{19} + \nu_8$	e_{1u}	3083	3038.9		
$\nu_1 + \nu_6 + \nu_{19}$	e_{1u}	3100	3046.2		
plus			3060.3		
other			3072.5		
combinations			3078.5		
			3082.5		
			3087.5		
			3094.1		

[a] Prodersen and Langseth, Mat. Fys. Skr. Dan. Ved. Selsk. 1, 1 (1956) and Calloman, Dunn, and Mills, Phil. Trans. Roy. Soc. (London) 259, 499 (1966).

[b] Some of these lines have been assigned erroneously as factor group components of C_6H_6 ν_{20} e_{1u} band and ν_{13} b_{1u} band by Hollenberg and Dows, J. Chem. Phys. 37, 1300 (1962).

KEY:
VW = very weak
W = weak
B = broad
I = more intense component of a double
FR = Fermi resonance
S = shoulder

TABLE II.
1.0% C_6H_5D in 99.0% C_6H_6 and C_6D_6

Vibration Number and Type		Symmetry in D_{6h}	Symmetry in C_{2v}	Gas Phase[a] cm^{-1}	Energy C_6H_6 cm^{-1}	Energy C_6D_6 cm^{-1}	Comment	Orientational Effect cm^{-1} (δ_{OE})
(C-C) nonplanar	ν_{16}	e_{2u}	b_2	381	385.9 390.2	387.8 392.4	W I,B	~4.5
			a_2	403		c.410	VW, B	
(C-H) nonplanar	ν_{11}	a_{2u}	b_2	607	621.4 623.5	621.4 623.6	I, B (621.0 S) induces ν_6 (e_{2g}) in C_6H_6 606.0, 608.8	2.2
(C-C) nonplanar	ν_4	b_{2g}	b_2	698		703.9		
(C-H) planar	ν_{18}	e_{1u}	b_1	857	854.1 858.8	856.9 859.0		~3.4
(C-H) nonplanar	ν_{17}	e_{2u}	b_2	924	935.9	936.4		
(C-C) planar	ν_1	a_{1g}	a_1	983		980.0	B, W	
(C-H) nonplanar	ν_{17}	e_{2u}	a_2	967		986.2	B, W	
(C-H) nonplanar	ν_5	b_{2g}	b_2	984	997.7	996.9	Blue shaded and B,W	
(C-C) planar	ν_{12}	b_{1u}	a_1	1007		1003.2	Red shaded	
(C-H) planar	ν_{18}	e_{1u}	a_1	1034		1032.7 1035.5	B	2.8
(C-H) planar	ν_{15}	b_{2u}	b_1	1077	1078.1	1078.3	Red shaded	
(C-H) planar	ν_9	e_{2g}	b_1	1158	1157.5	1157.4		
(C-H) planar	ν_9	e_{2g}	a_1	1174		1175-1193	($\nu_{11}+\nu_{10}$) in C_6D_6 near by	
(C-C) planar	ν_{19}	e_{1u}	a_1	1446		1435.7 1444.8	($\nu_{17}+\nu_{10}$) in C_6D_6 near by	
(C-C) planar	ν_8	e_{2g}	b_1	1576		1576.2 1580.0	S ($\nu_6+\nu_1$)	
			a_1	1593		1592.5	W, B	

[a]Brodersen and Langseth, Mat. Fys. Skr. Dan. Ved. Selsk. 1, 7 (1959).

KEY: VW = very weak
W = weak
B = broad
I = more intense component of a double
FR = Fermi resonance
S = shoulder

TABLE III.

1% p $C_6H_4D_2$ in 99% C_6H_6 and C_6D_6

Vibration Number and Type	Symmetry D_{6h}	Symmetry D_{2h}	Gas Phase[a] cm^{-1}	Energy cm^{-1} C_6H_6	Energy cm^{-1} C_6D_6		Orientational Effect cm^{-1} (δ_{OE})
(C-C) nonplanar ν_{16}	e_{2u}	b_{1u}		367.6 372.3			~ 4.7
(C-H) nonplanar ν_{11}	a_{2u}	b_{1u}	596	613.7 613.9	613.7	Possible splitting, shaded symmetrically in D_6, induces ν_6 (e_{2g}) 605.5, 607.7 in H_6, 579.5, 580.4 in D_6	< 1.0
(C-H) planar ν_{18}	e_{1u}	b_{3u}	817	817.6 821.3		Sharp I	3.7
(C-H) nonplanar ν_{17}	e_{2u}	b_{1u}	871	882.9 885.8	882.3 885.3 885.9		3.0
(C-H) nonplanar ν_{17}	e_{2u}	a_u	967		977.8 979.8	I	2.0
(C-C) planar ν_{12}	b_{1u}	b_{2u}	997		990.6 993.7	I	3.1
(C-H) planar ν_{18}	e_{1u}	b_{2u}	1032		1031.0 1034.1	I	3.1
(C-H) planar ν_{15}	b_{2u}	b_{3u}	1104		1104.3 1106.4	B, ~equal I	~ 2.0
(C-H) planar ν_{14}	b_{2u}	b_{3u}	1291	1297.6	1294.5 1295.3	Blue shaded, VW	< 1.0

[a] Brodersen and Langseth, Mat. Fys. Skr. Dan. Ved. Selsk, 1, 7 (1959).

KEY: VW = very weak
W = weak
B = broad
I = more intense component of a double
FR = Fermi resonance
S = shoulder

TABLE IV.

1.0% Sym (1, 3, 5) $C_6H_3D_3$ in 99.0% C_6H_6 and C_6D_6

Vibration Number and Type	Symmetry		Gas Phase[a] cm^{-1}	H_6 Energy cm^{-1}	D_6 Energy cm^{-1}	Comment	Site Splitting cm^{-1} (δ_{SS})
(C-C) nonplanar ν_{16}	e_{2u}	e"	368	377.5 385.0			8.5
(C-H) nonplanar ν_{11}	a_{2u}	a_2''	531	538.8 539.2 545.3	538.9 539.3 545.6	^{13}C (or m-$C_6H_2D_4$ ν_{11}) induces ν_6 (e_{2g}) (580.0, 582.5) in D_6	
(C-C) nonplanar ν_4	b_{2g}	a_2''	697		703.8		
(C-H) planar ν_{18}	e_{1u}	e'	833	831.6 834.4	831.7 835.0	ν_{15} and ν_{18} C_6D_6 near by and C_6D_5H ν_{18}	~3.0
(C-H) planar ν_{15}	b_{2u}	a_2'	912	908.1	908.0		
(C-H) nonplanar ν_5	b_{2g}	a_2''	917	927.4	928.5		
(C-H) nonplanar ν_{17}	e_{2u}	e"	924	935.7 939.4	936.0 938.8	D_6 combination near, and C_6D_5H in C_6D_6	3.7
(C-H) planar ν_9	e_{2g}	e'	1101		1102.5 1104.9	B I	~3

[a] Brodersen and Langseth, Mat. Fys. Skr. Dan. Ved. Selsk. 1, 1 (1956).

KEY: VW = very weak
W = weak
B = broad
I = more intense component of a double
FR = Fermi resonance
S = shoulder

TABLE V.

C_6D_5H in C_6H_6 and C_6D_6

Vibration Number and Type	Symmetry in D_{6h}	Symmetry in C_{2v}	Gas Phase[a] cm^{-1}	Energy in C_6D_6 cm^{-1}	Energy in C_6H_6 cm^{-1}	Comment	Orientational Effect cm^{-1} (δ_{OE})
(C-H) nonplanar ν_{11}	a_{2u}	b_2	512	527.3	527.3		
(C-H) nonplanar ν_{10}	e_{1g}	b_2	706	715.9 717.8 720.6			~ 5
(C-H) planar ν_{18}	e_{1u}	b_1	838	837.6 839.8	837.4 838.9		~ 2
(C-H) nonplanar ν_5	b_{2g}	b_2	922	930.7 935.6 938.6	930.4 934.5 938.1		~ 7
				1278.2		Combination	

[a] Brodersen and Langseth, Mat. Fys. Skr. Dan. Ved. Selsk. 1, 7 (1959).

TABLE VI.

1.0% C_6D_6 in 99.0% C_6H_6

Vibration Number and Type	Symmetry in D_{6h}	Gas Phase[a] cm^{-1}	Energy cm^{-1}	Comment	Site Splitting cm^{-1} (δ_{SS})
(C-C) nonplanar ν_{16}	e_{2u}	347.8	354.8 364.6	W W	9.8
(C-H) nonplanar ν_{11}	a_{2u}	496	511.3 527.4[b]	 D_5H	
(C-H) nonplanar ν_{17}	e_{2u}	787	791.3 797.8	I	6.5
(C-H) planar ν_{18}	e_{1u}	814	810.5 814.6	Sharp I } FR ?	4.1
(C-H) planar ν_{15}	b_{2u}	824	820.6		
(C-C) planar ν_{12}	b_{1u}	970	971.0		
(C-H) planar ν_{14}	b_{2u}	1282	1285.1	($\nu_{16} + \nu_{10}$) near by	
(C-C) planar ν_{19}	e_{1u}	 1333	1321.3 1326.0 1329.2	^{13}C D_5H (?) II	 < 1.0
(C-H) planar ν_{13}	b_{1u}	2285	2268.1	} FR	
(C-H) planar ν_{20}	e_{1u}	2288	2278.0 2282.5		4.5
$\nu_1 + \nu_{19}$ plus other combinations					

[a] Brodersen and Langseth, Mat. Fys. Skr. Dan. Ved. Selsk. 1, 1 (1956) and Calloman, Dunn, and Mills, Phil. Trans. Roy Soc. (London) 259, 499 (1966).

[b] This band has been erroneously assigned as an interchange group component of the C_6D_6 a_{2u} band by Hollenberg and Dows, J. Chem. Phys. 37, 1300 (1962).

KEY:
VW = very weak
W = weak
B = broad
I = more intense component of a double
FR = Fermi resonance
S = shoulder

TABLE VII. Correlation tables for the benzene isotopes (y-axis through C_1, x-axis between C_5 and C_6, z-axis perpendicular to molecular plane; y-axis preserved).

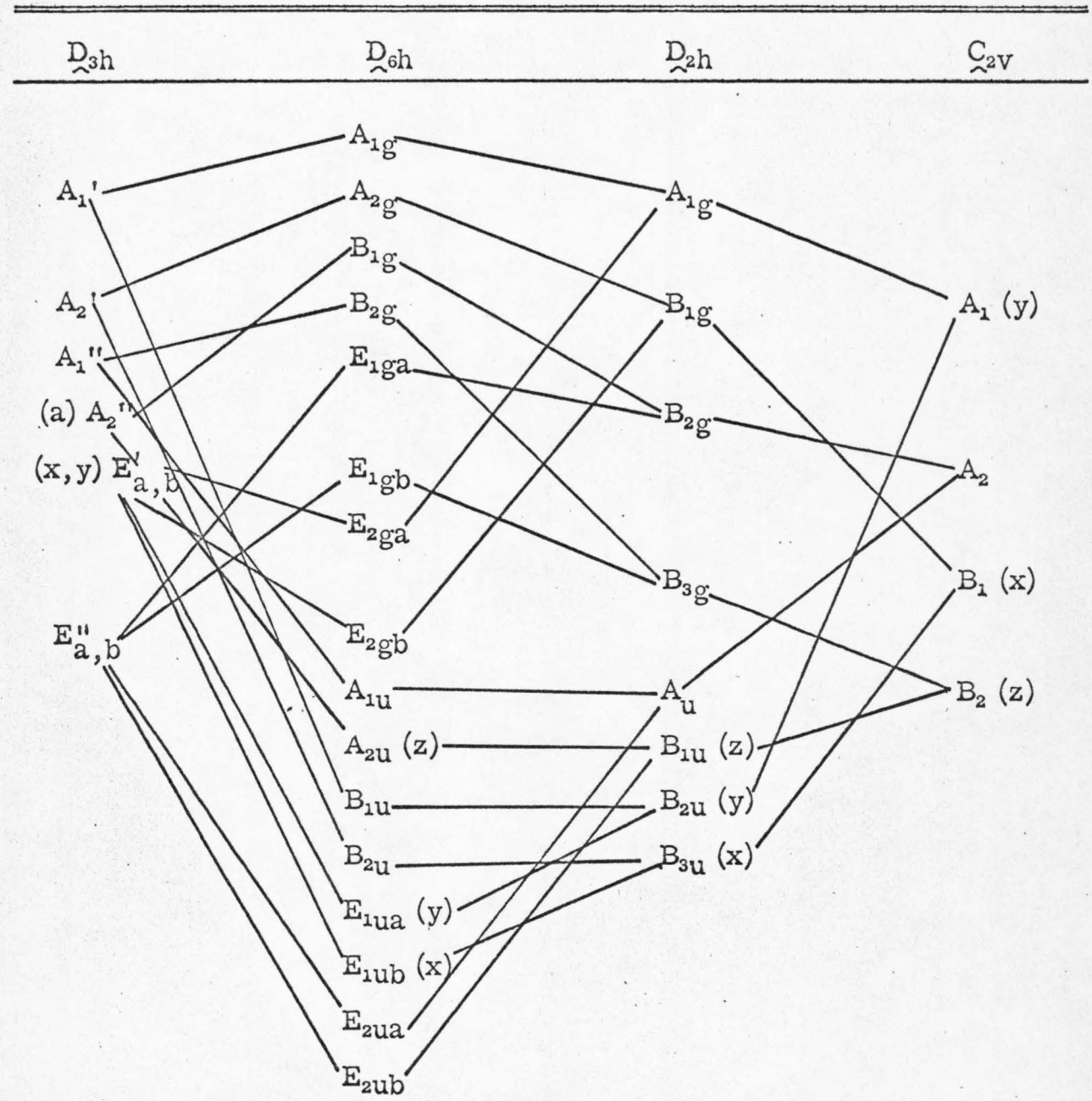

TABLE VIII. Correlation diagram for $\underset{\sim}{D}_{6h}$, $\underset{\sim}{C}_{2h}$, and $\underset{\sim}{C}_i$ (x-axis C_2 preserved).

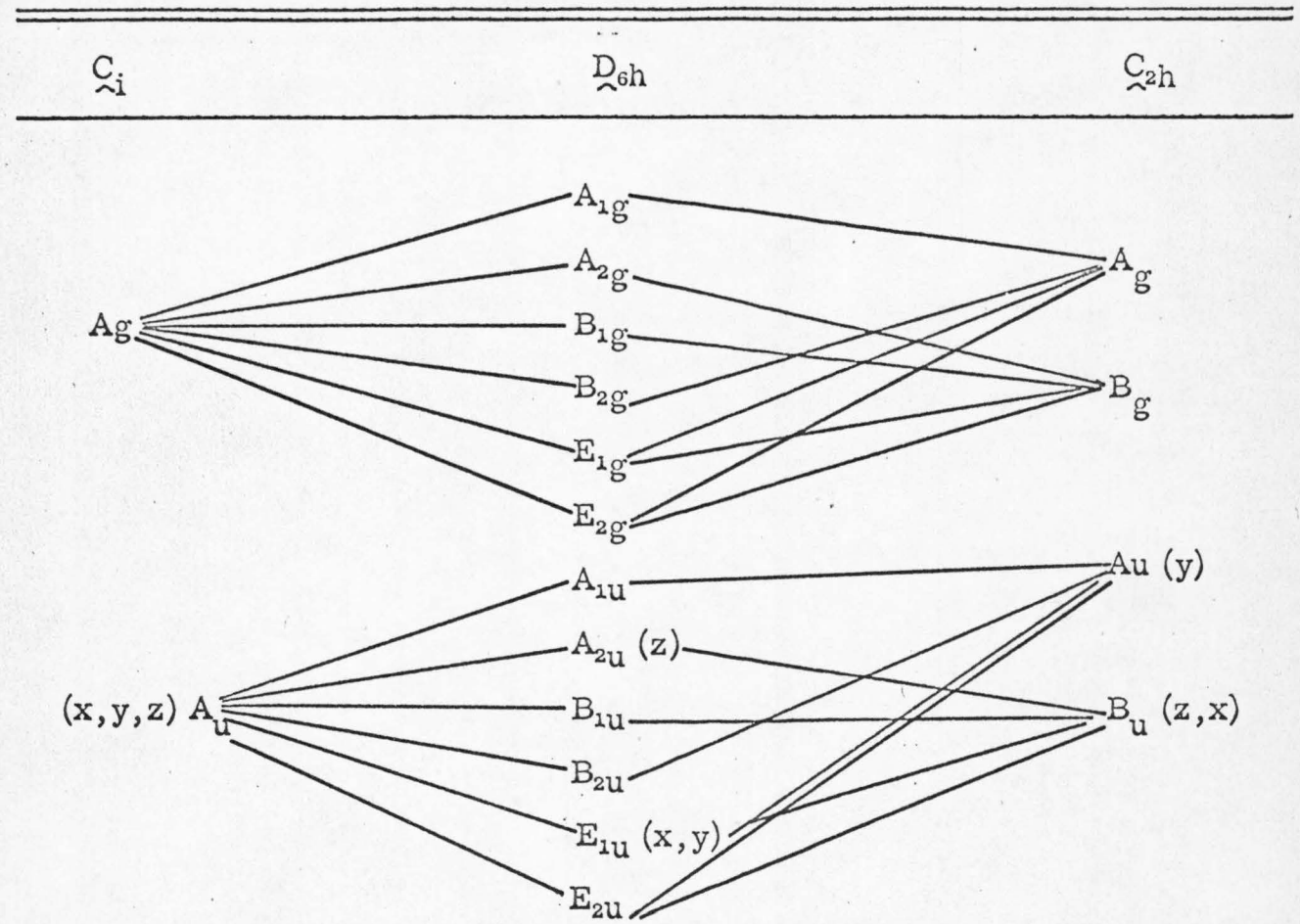

TABLE IX. Orientation effect for benzene ($n_c = 1$).

Substituted Molecule	Group of Unsub. Mole.	Group of Sub. Mole.	Interchange Operations + $\underset{\sim}{A}$	Interchange Group	Number of Distinct Orientations, n_o, for Site			
					S =			
	$\underset{\sim}{G}$	$\underset{\sim}{A}$	$\underset{\sim}{B}$	$\underset{\sim}{N}$, n_b	C_1	C_i	C_{2h}	D_{2h}
C_6H_6 C_6D_6	D_{6h}	D_{6h}	D_{6h}	C_1, 1	1	1	1	1
1,3,5 $C_6H_3D_3$	D_{6h}	D_{3h}	D_{6h}	C_2, 2	2	1	1	1
1,4 $C_6H_4D_2$	D_{6h}	D_{2h}	D_{6h}	C_3, 3	3	3	3,2	2
1,3 $C_6H_4D_2$ 1,2 $C_6H_4D_2$ C_6H_5D 1,2,3 $C_6D_3H_3$	D_{6h}	C_{2v}	D_{6h}	C_6, 6	6	3	3,2	2
1,2,4 $C_6H_3D_3$	D_{6h}	C_s	D_{6h}	D_{6h}, 12	12	6	6,3	3

[1] $\underset{\sim}{G}$ = unsubstituted molecular group.

[2] $\underset{\sim}{A}$ = elements preserved in isotopically substituted molecule.

[3] $\underset{\sim}{B}$ = elements not in $\underset{\sim}{A}$ (not preserved) but equal to the product of an operation in $\underset{\sim}{A}$ with a proper operation of G--these are interchange operations and move the molecule. These operations, together with the elements of $\underset{\sim}{A}$, form a group $\underset{\sim}{P}$.

[4] Elements not in $\underset{\sim}{B}$. Called transform elements. Give optical isomers ($n_c \leq 2$).

[5] $\underset{\sim}{A}\,\underset{\sim}{B} = \underset{\sim}{N}$, where $\underset{\sim}{N}$ is the interchange group with n_b elements. n_b gives the number of orientations of the substituted molecule with respect to the unsubstituted molecule.

[6] Let space have symmetry $\underset{\sim}{S}$.

[7] Then, n_o, the number of physically distinct orientations is found by striking out from the n_b cosets any coset that differs from another by an operation of $\underset{\sim}{S}$. (Clearly $\underset{\sim}{S} \cap \underset{\sim}{A}$ does not strike out any cosets.)

Fig. 1. 1% C_6D_6 in C_6H_6 in the region of gas phase Fermi resonance between ν_{20} and $(\nu_1 + \nu_{19})$. In the crystal ν_{13} as well as other combination-tones can also interact and mix. This is evidenced by the complex structure of the band.

C_6D_6 in C_6H_6

(ν_{13}, ν_{20}, etc.)

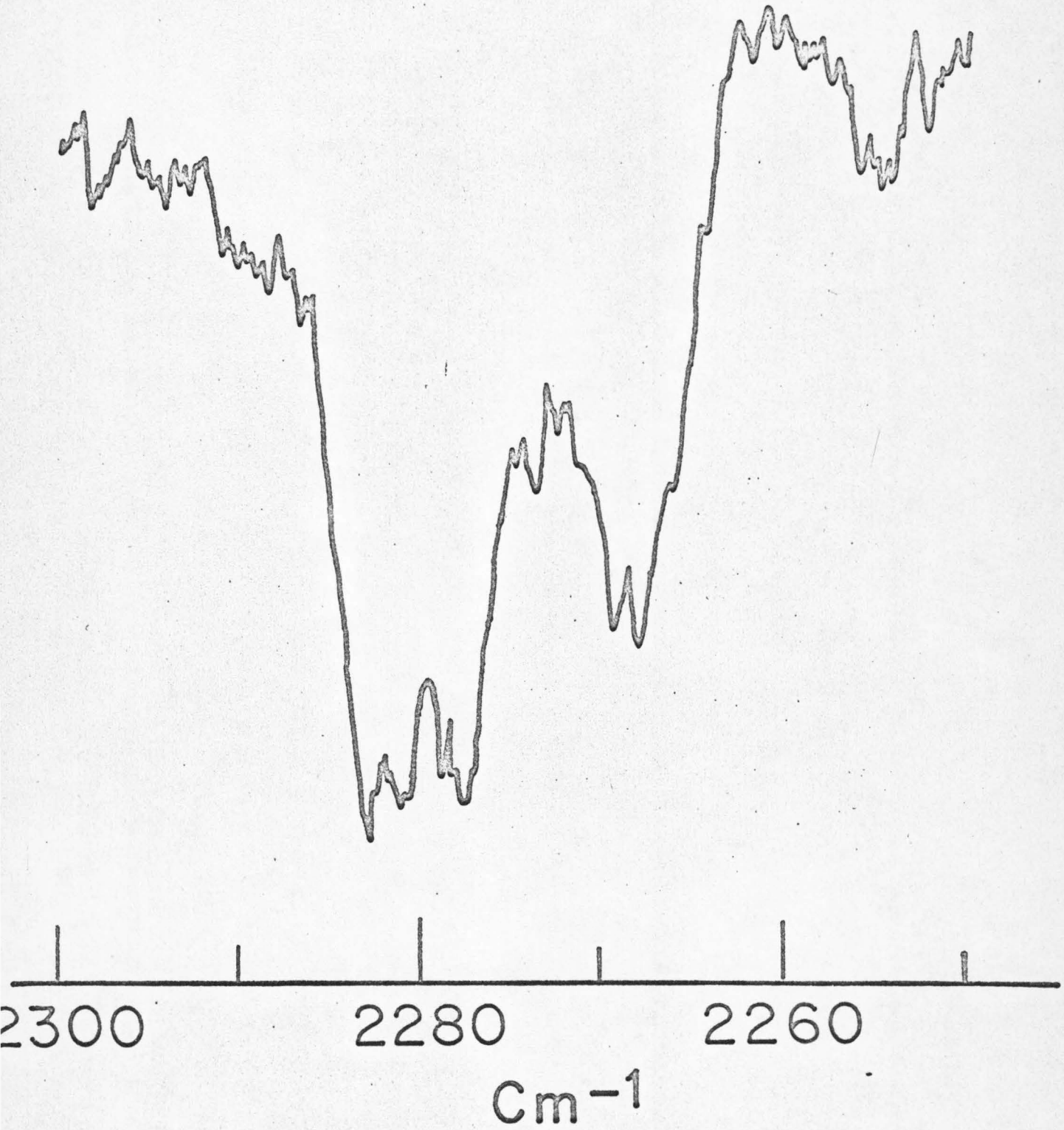

Fig. 2. The hydrogen stretching region of a 1% C_6H_6 in C_6D_6 crystal at 4.2°K. The complex structure of this region indicates an increase in the interaction of many combination-tones and two, ν_{13} and ν_{20}, fundamentals due to the reduction of molecular symmetry by the crystal site.

C_6H_6 in C_6D_6

($\nu_{13}, \nu_{20}, \nu_{19}$ and ν_8, etc)

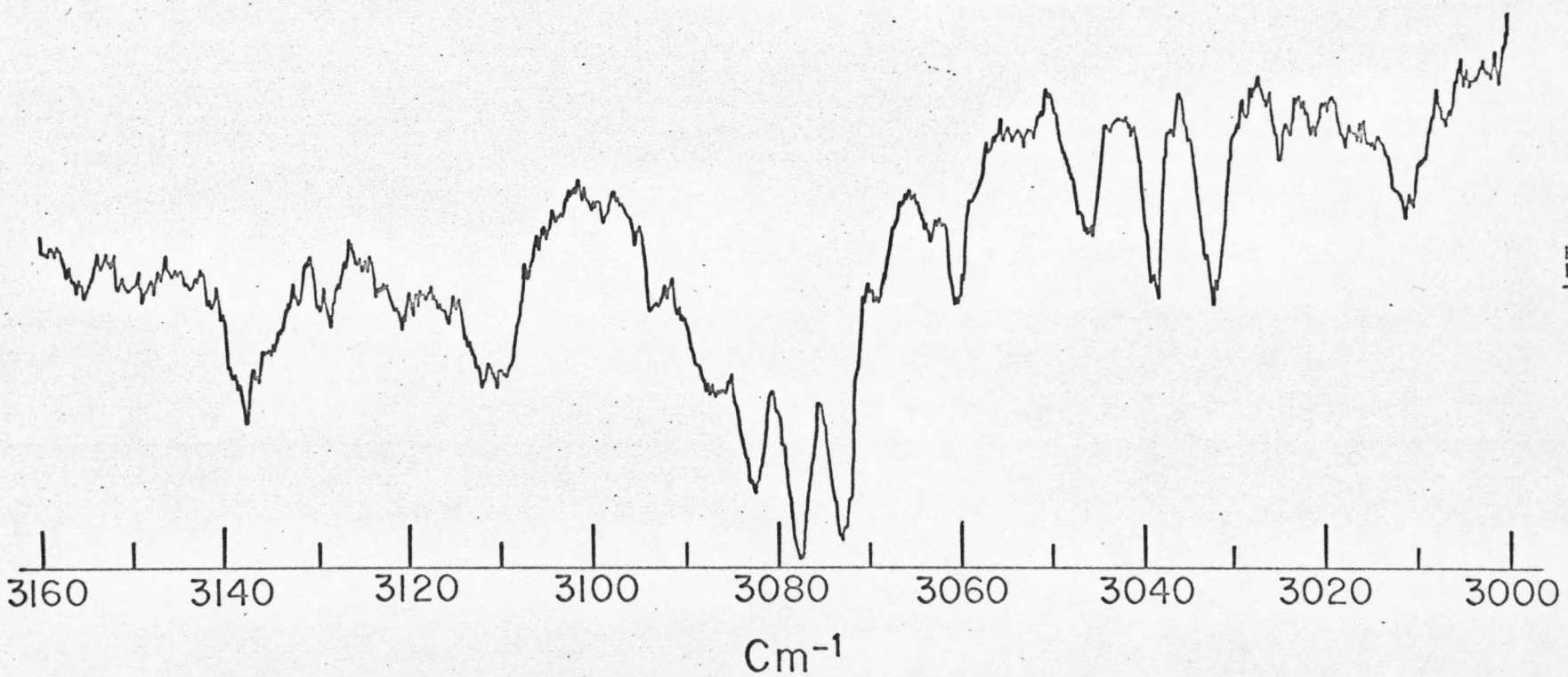

Fig. 3. A portion of the m-$C_6D_4H_2$ in C_6H_6 crystal spectra to indicate the increased interaction between fundamentals in the solid. Note orientation effects on most peaks which further complicates the assignment of these transitions. Possible assignments for some of the observed lines are indicated on the figure, major impurities are p-$C_6H_2D_4$ (990, 875 cm^{-1}) and C_6D_5H (935 cm^{-1}).

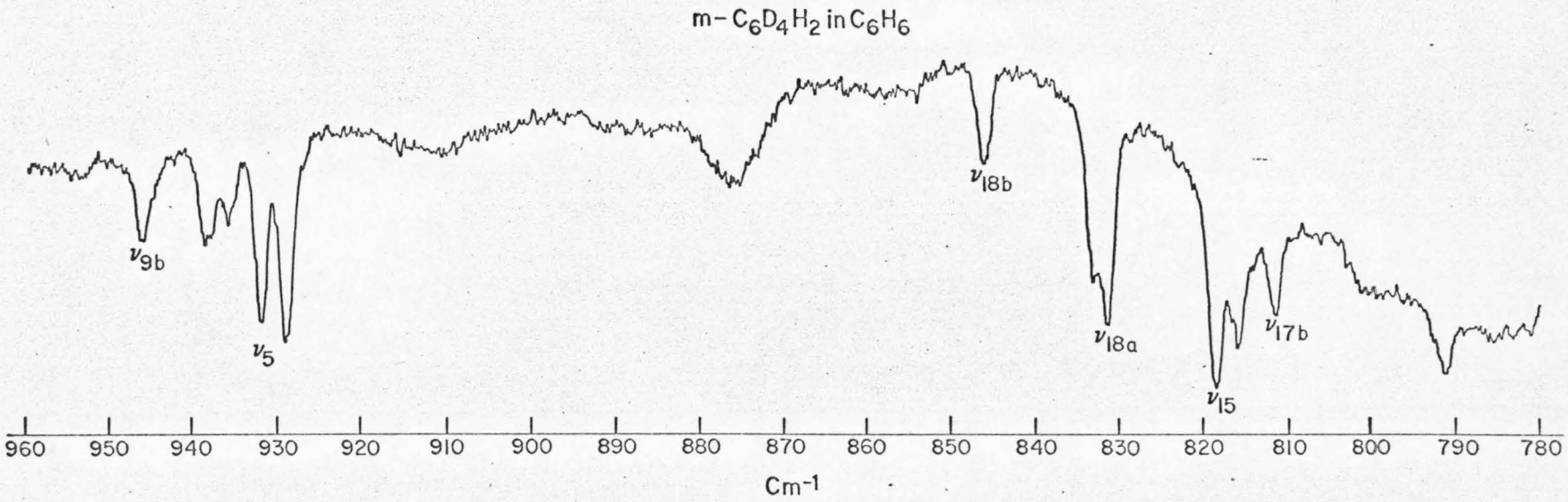
m-$C_6D_4H_2$ in C_6H_6
ν_{9b}
ν_5
ν_{18b}
ν_{18a}
ν_{15}
ν_{17b}
960 950 940 930 920 910 900 890 880 870 860 850 840 830 820 810 800 790 780
Cm^{-1}

Fig. 4a. 0.75% C_6H_6 in C_6D_6 to show site group splitting on the ν_{18} (e_{1u}) degenerate fundamental. $\underset{\frown}{D}^{\nu_{18}} \approx 0.0\ cm^{-1}$. This vibration is discussed in the text (Sec. 3d, 3e, and 3f).

C_6H_6 in C_6D_6

E_{1u}

Note 3.8 cm^{-1} site-group splitting

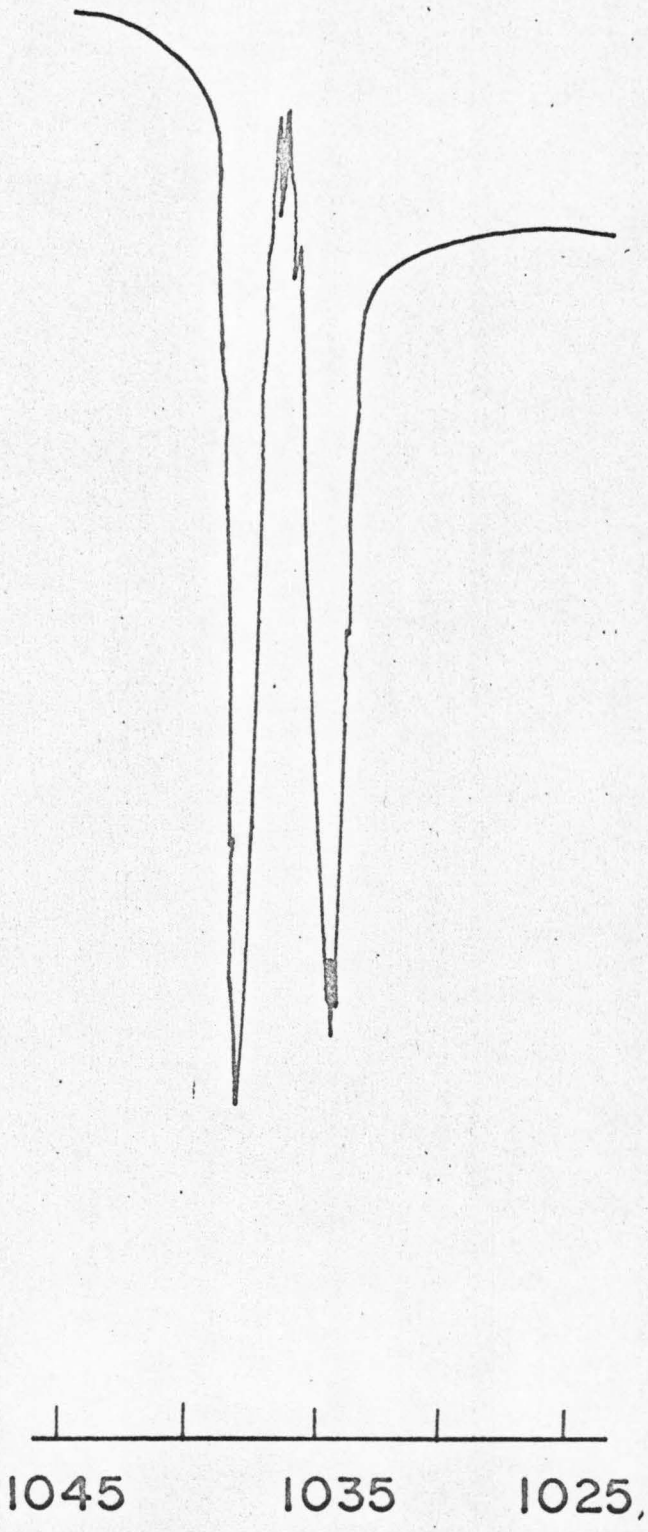

Fig. 4b. 0.30% of C_6D_6 in C_6H_6 showing ν_{18} and ν_{15}.

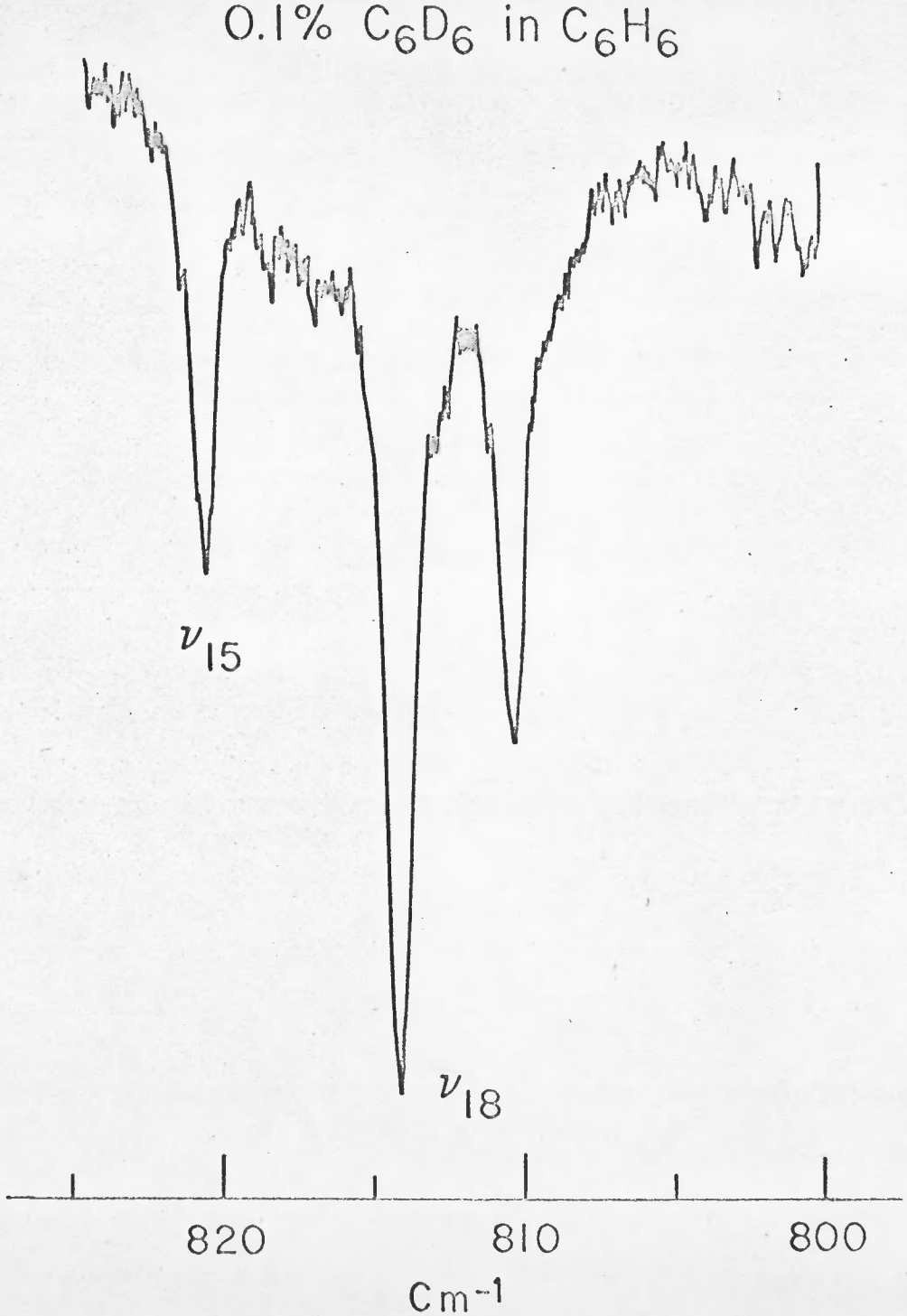
0.1% C_6D_6 in C_6H_6
ν_{15}
ν_{18}
820
810
800
Cm^{-1}

Fig. 5. 0.75% p-$C_6H_4D_2$ and 0.75% sym-$C_6H_3D_3$ in C_6H_6; this shows the apparent similarity between site group splitting and the orientational effect. The two transitions of p-$C_6H_4D_2$ (ν_{18}-b_{3u} and ν_{17}-b_{1u}) show the orientational effect (also see Fig. 6) while the e' (ν_{18}) is site group split (see Fig. 4 as a comparison with C_6H_6 ν_{18} site group splitting).

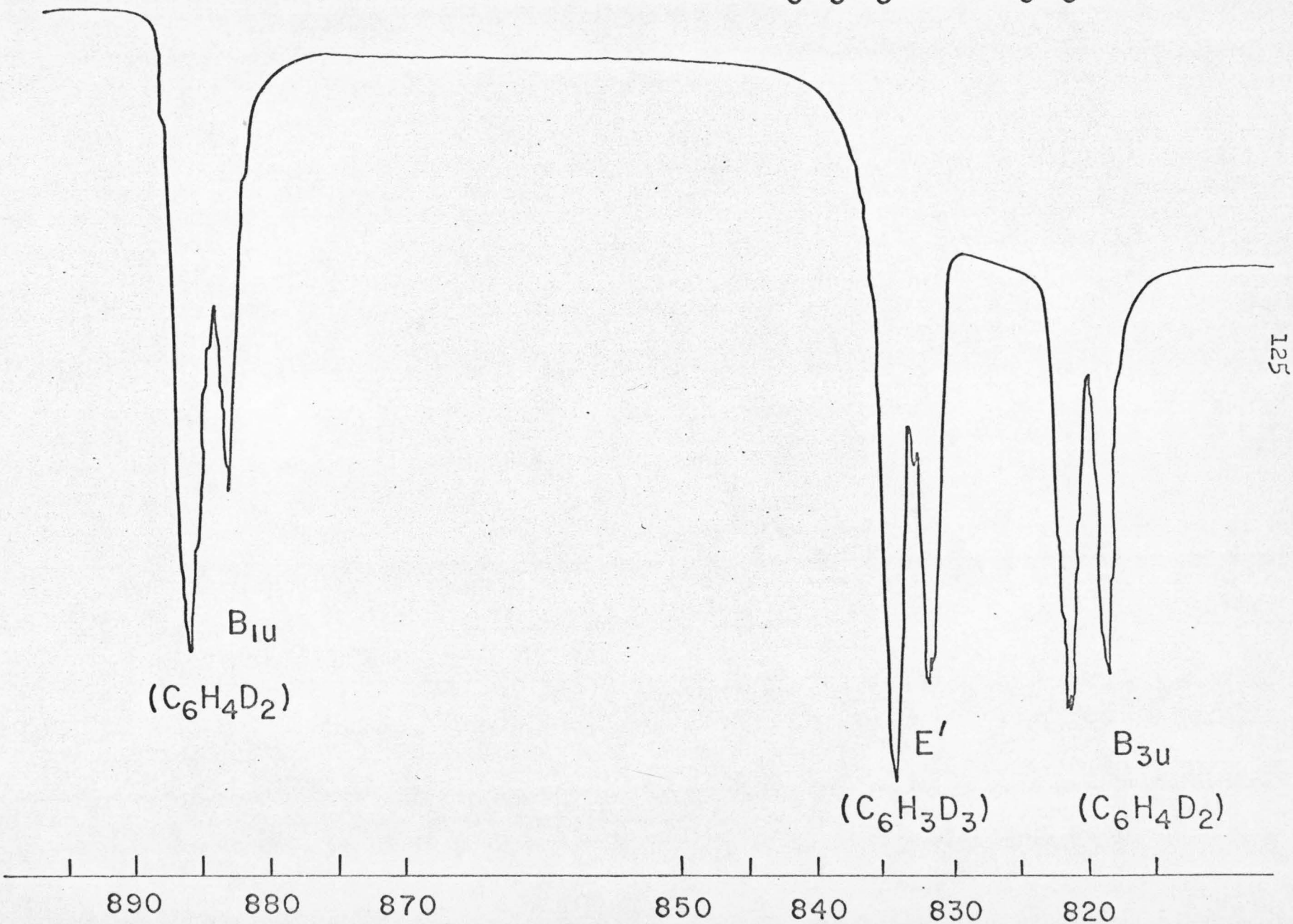
P-$C_6H_4D_2$ (B_{1u} and B_{3u}) sym.-$C_6H_3D_3$ (E') in C_6H_6
B_{1u}
($C_6H_4D_2$)
E'
($C_6H_3D_3$)
B_{3u}
($C_6H_4D_2$)
890
880
870
850
840
830
820

Fig. 6. High resolution trace of ν_{17} of Fig. 6.

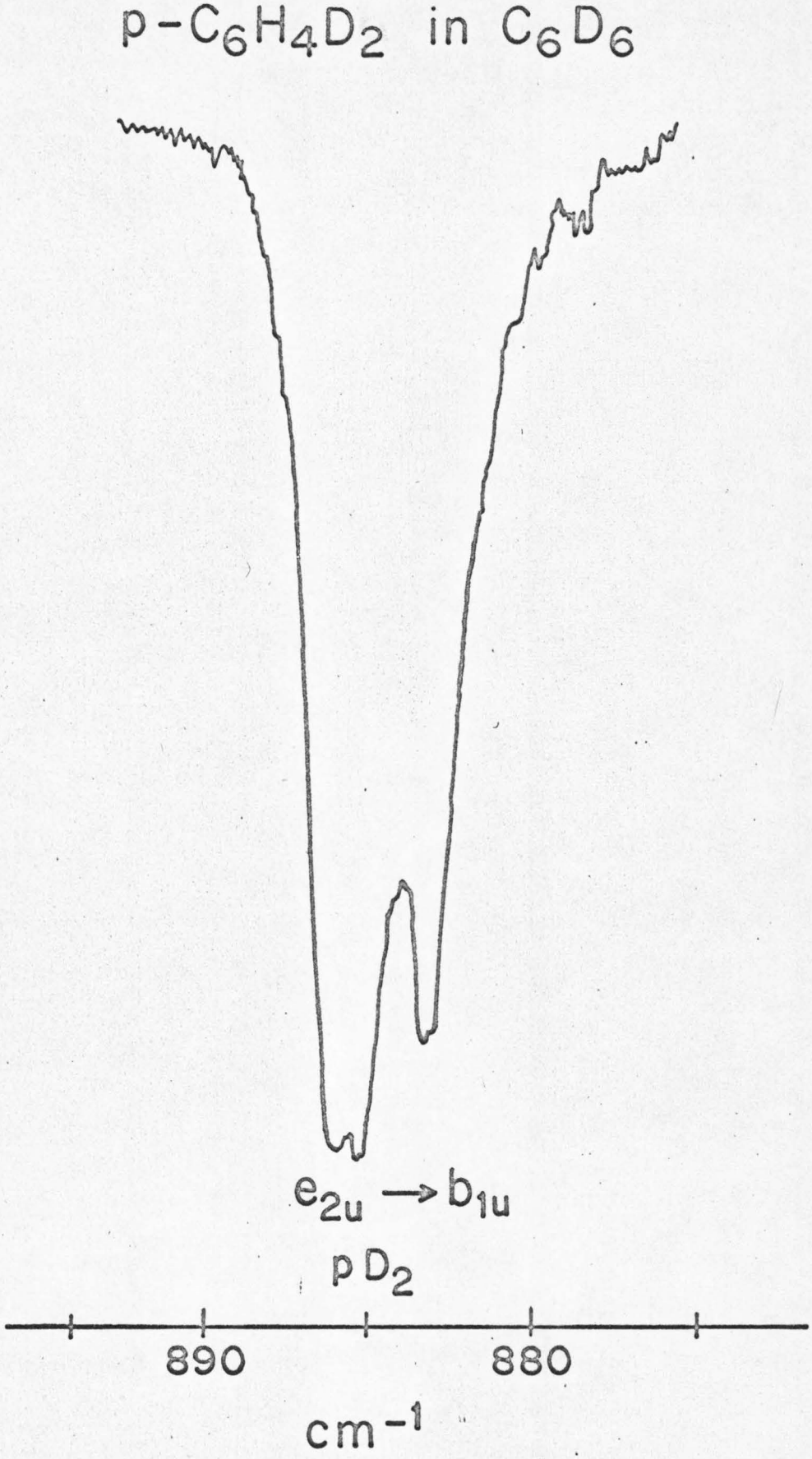
p-C6H4D2 in C6D6
e2u → b1u
pD2
890
880
cm-1

Fig. 7. Orientational effect on ν_{16} (b_{1u}) out-of-plane mode of p-$C_6H_4D_2$ in a 2% sample.

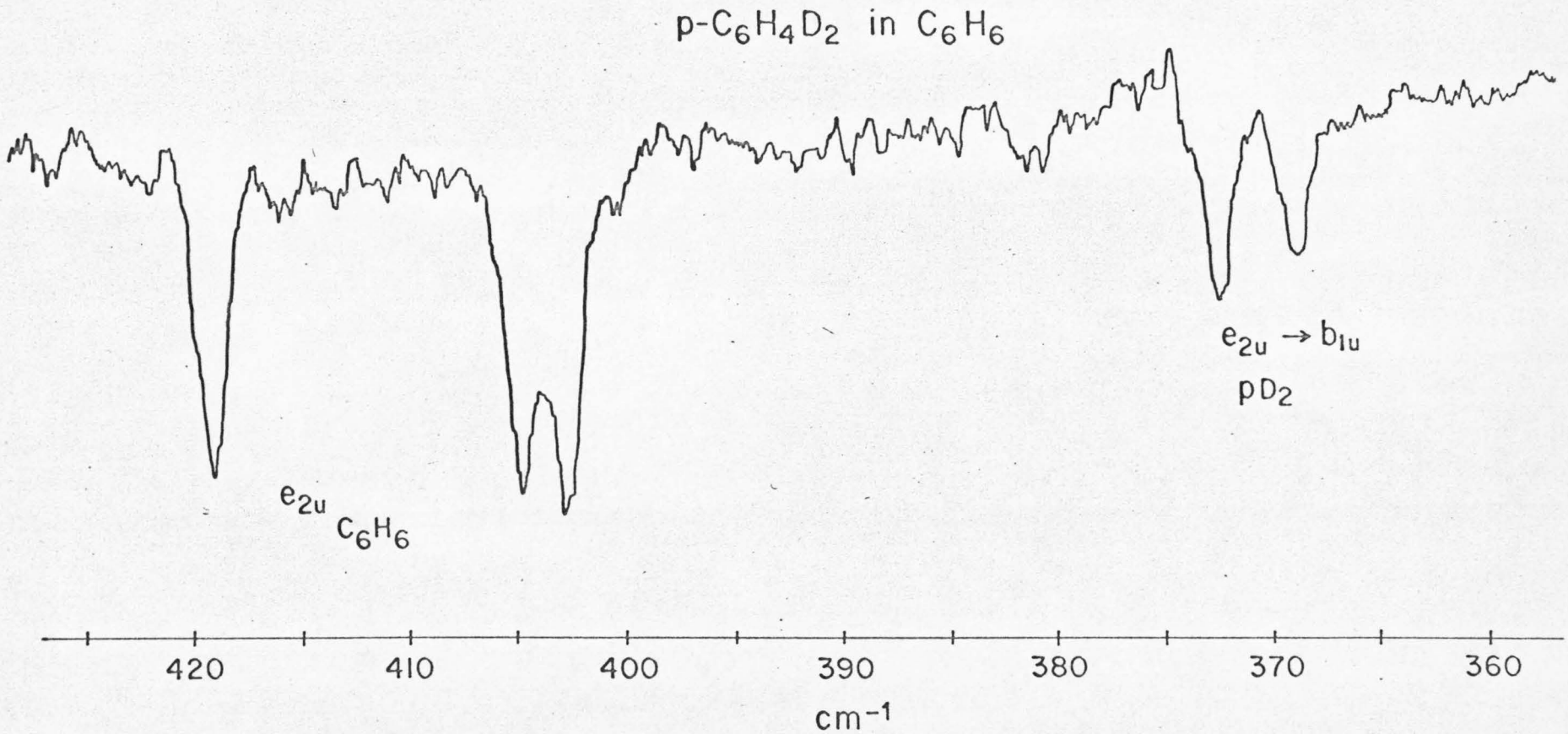
p-C6H4D2 in C6H6
e2u
C6H6
e2u → b1u
pD2
420
410
400
390
380
370
360
cm-1

Fig. 8. 1% C_6H_5D guest in both C_6H_6 and C_6D_6. Note the intensity and energy changes from the two solvents. This is most likely caused by a third unresolved line. ν_{18} (b_1) is observed in both cases.

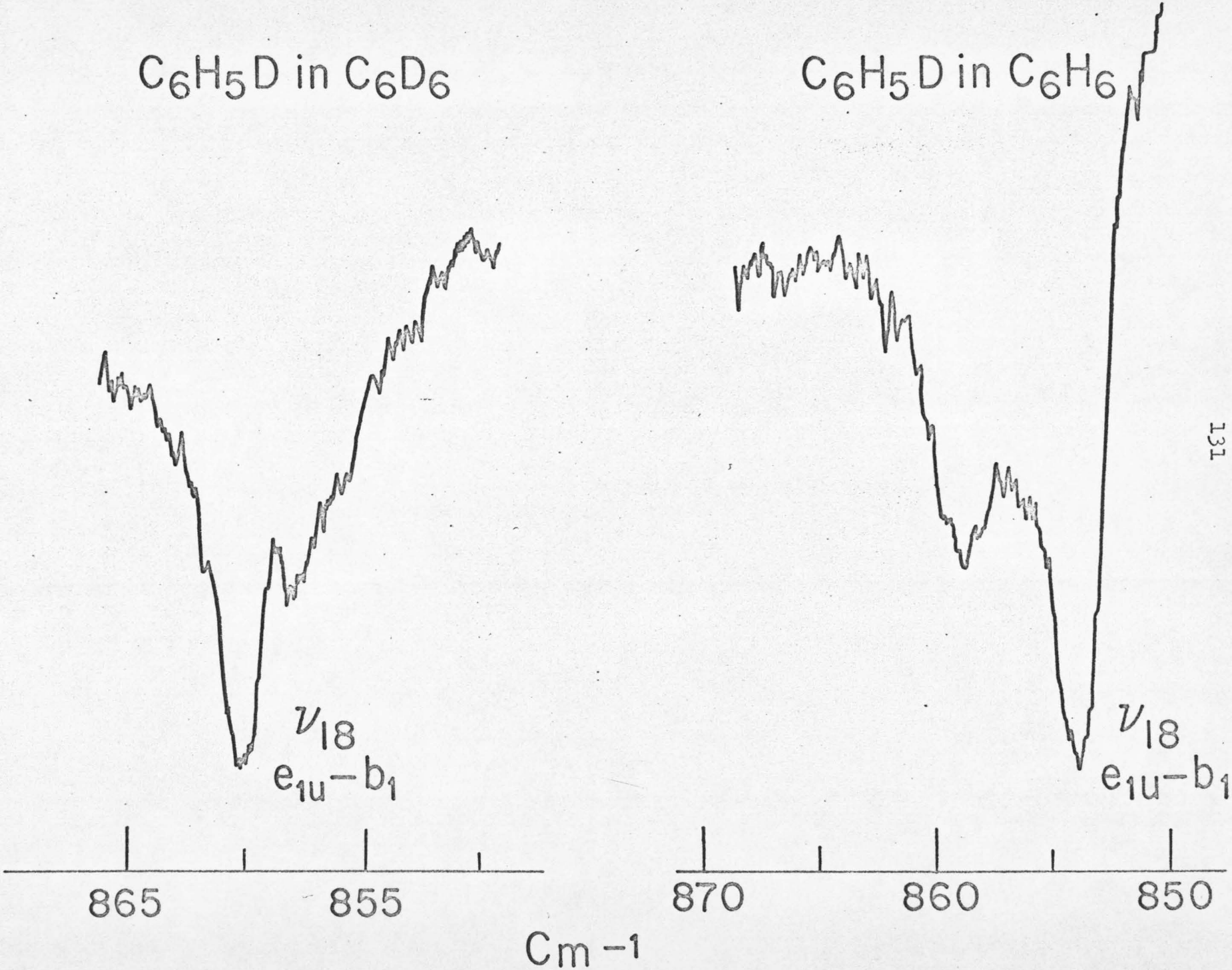
C_6H_5D in C_6D_6
C_6H_5D in C_6H_6
ν_{18}
$e_{1u}-b_1$
ν_{18}
$e_{1u}-b_1$
865
855
870
860
850
Cm −1

Fig. 9. ~2% C_6D_5H impurity (natural) in C_6D_6. This figure illustrates the difference between the "out-of-plane" and "in-plane" orientational effect for the benzene isotopes. ν_5 (b_2) and ν_{10} (b_2) are out-of-plane vibrations and show three orientational components in the spectra (indicating a C_i site--see Sec. 3f), while ν_{18} (b_1) as an "in-plane" vibration shows only two components with a 2:1 intensity ratio (indicating a C_{2h} site).

C_6D_5H in C_6D_6

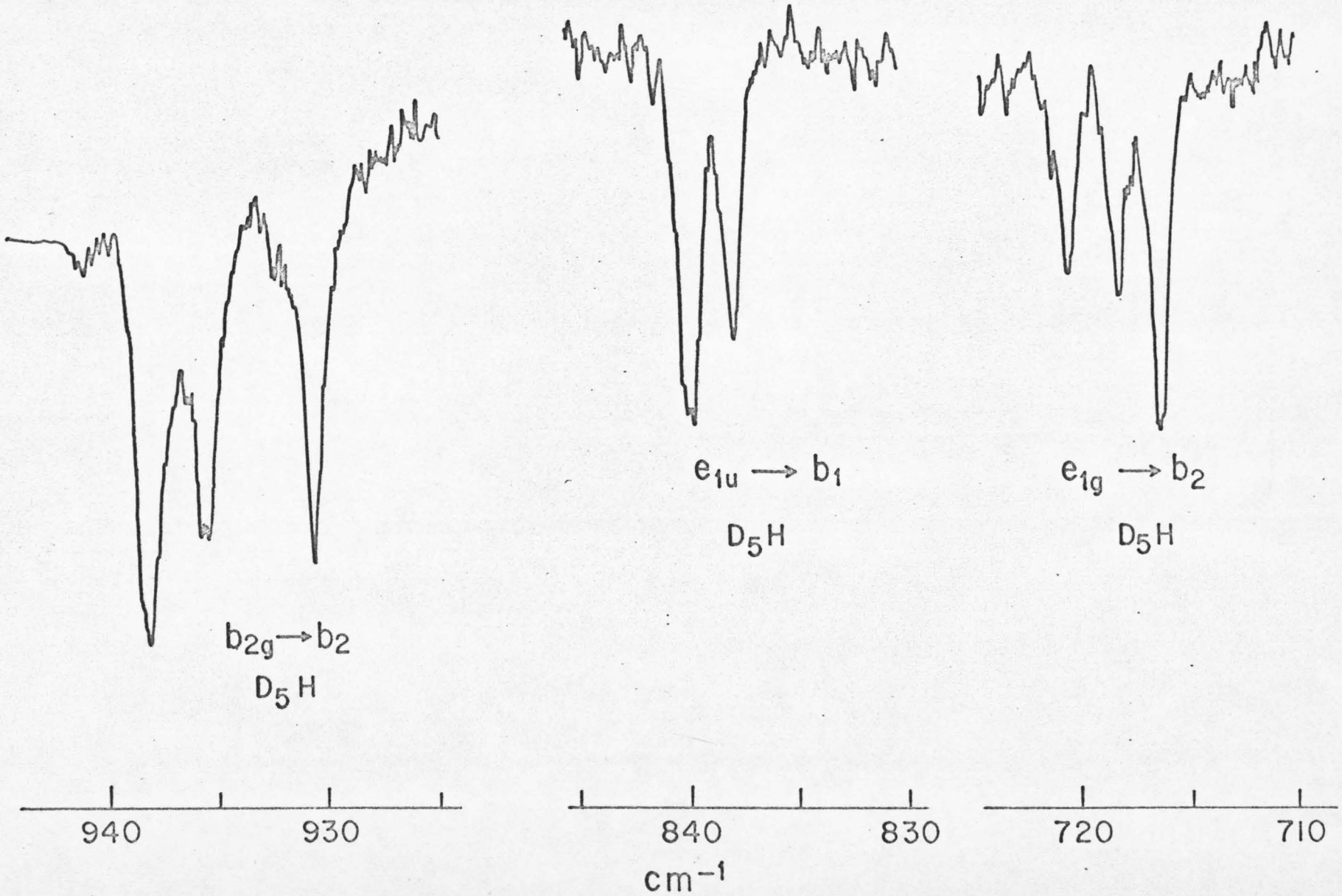

Fig. 10. 2% C_6HD_5 in C_6H_6 showing two of the transitions in Fig. 9. The shoulder on the low-energy side of ν_{18} is not believed to be real. If it is, it represents the only case of an in-plane vibration experiencing the full site symmetry ($\underset{\sim}{C}_i$) and thus effectively destroying the approximate "$\underset{\sim}{C}_{2h}$ plane" of the site.

C_6D_5H in C_6H_6

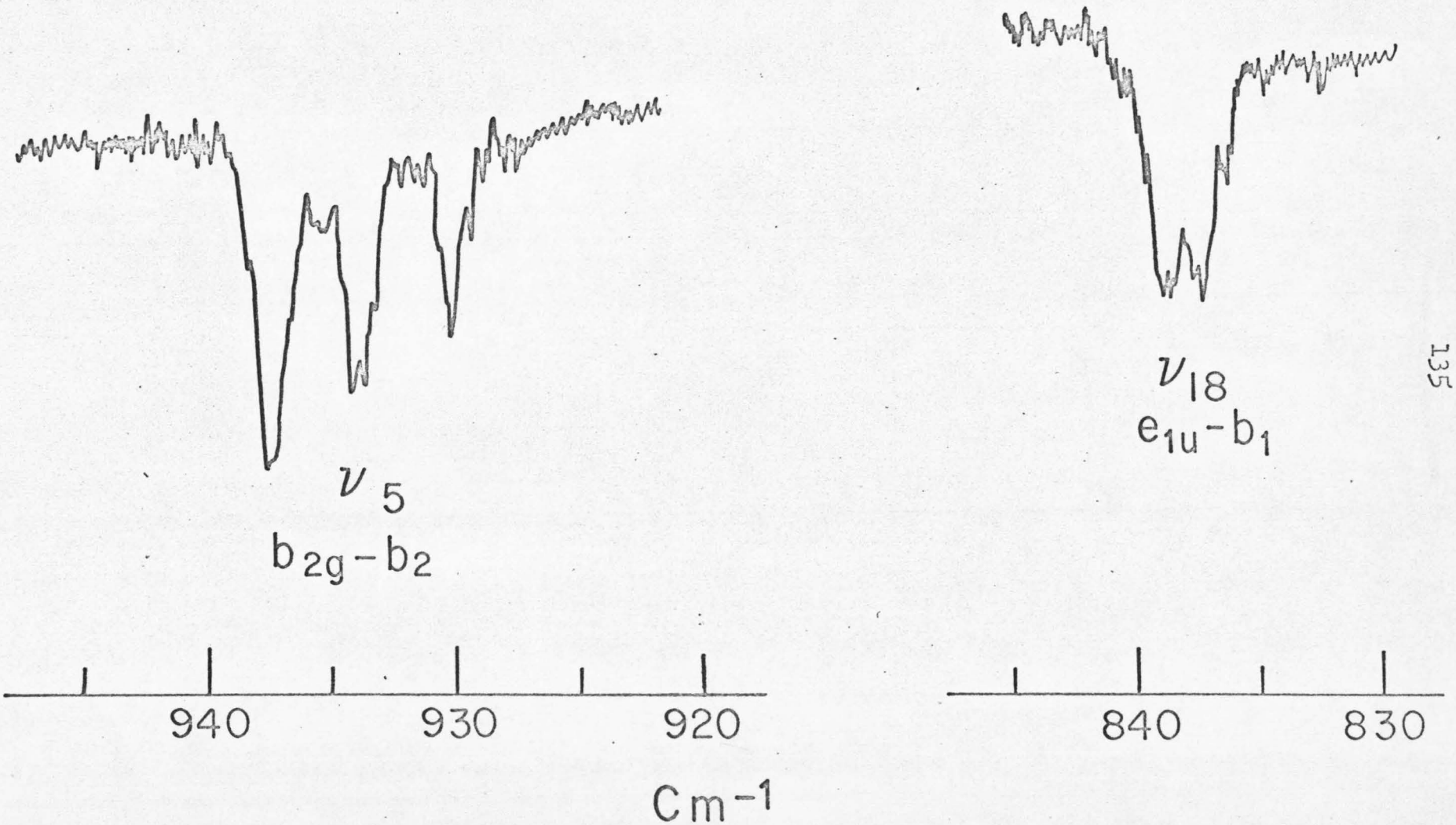

Fig. 11. The ν_{11} band of the three isotopes (of $\underset{\sim}{D}_{3h}$ or higher symmetry) not expected to show orientational effects. Line widths are of the order of 0.75 cm^{-1} and probably instrument limited. It is possible but unlikely that the line assigned to $^{13}CC_5H_3D_3$ is really the ν_{11} of m-$C_6H_4D_2$ [a low (<1%) level impurity in sym-$C_6H_3D_3$].

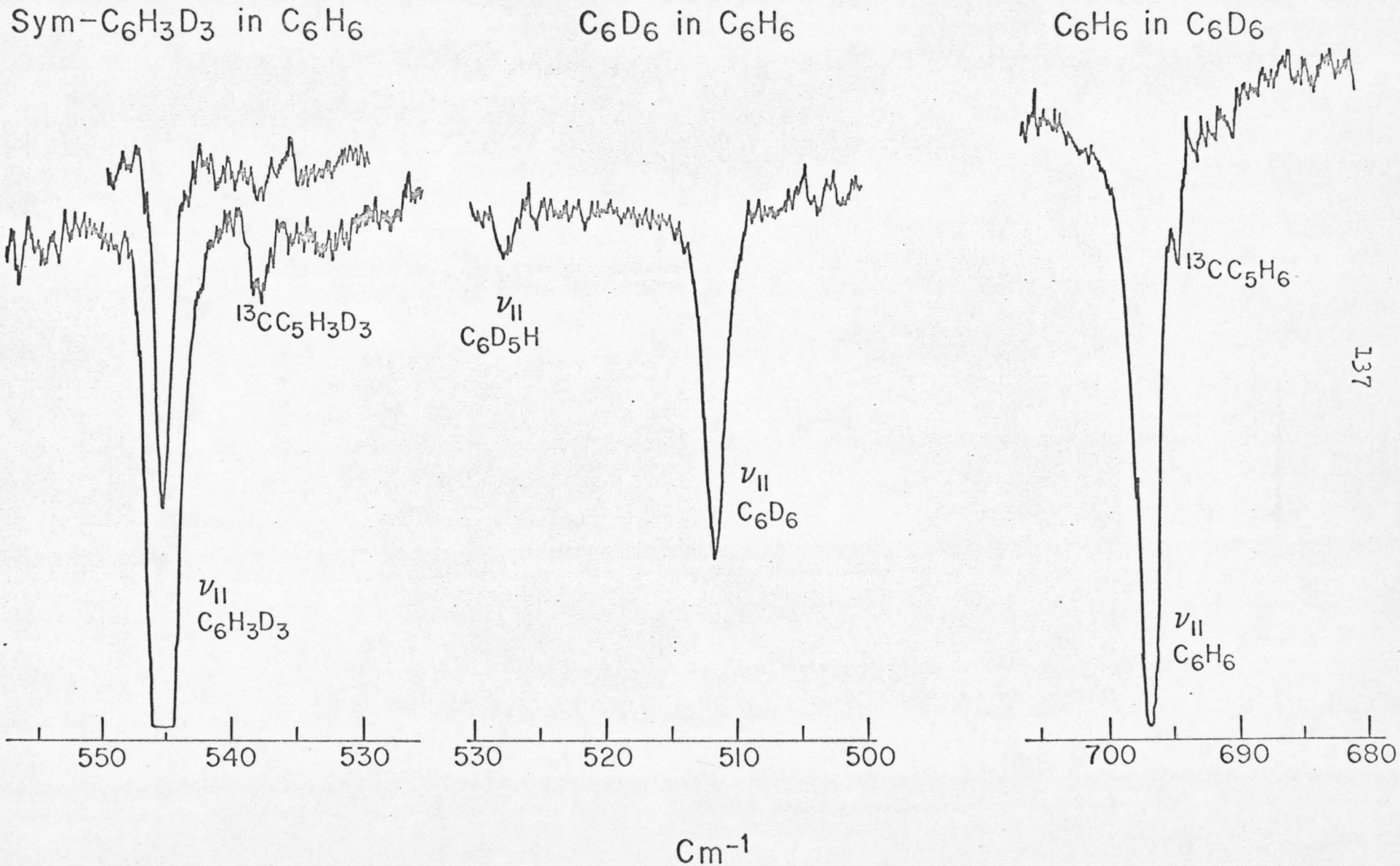
Sym-$C_6H_3D_3$ in C_6H_6
$^{13}CC_5H_3D_3$
ν_{11}
$C_6H_3D_3$
550
540
530
C_6D_6 in C_6H_6
ν_{11}
C_6D_5H
ν_{11}
C_6D_6
530
520
510
500
C_6H_6 in C_6D_6
$^{13}CC_5H_6$
ν_{11}
C_6H_6
700
690
680
Cm^{-1}

This is not a missing page. It is a result of page misnumbering.

Fig. 12. Intermolecular Fermi resonance (see Sec. 3g). The ν_6 C_6H_6 transition has been induced by the ν_{11} p-$C_6H_4D_2$. Note also the orientational effect of ν_{11} C_6H_5D and p-$C_6H_4D_2$. It is possible that the C_6H_5D intensity comes about through the same mechanism.

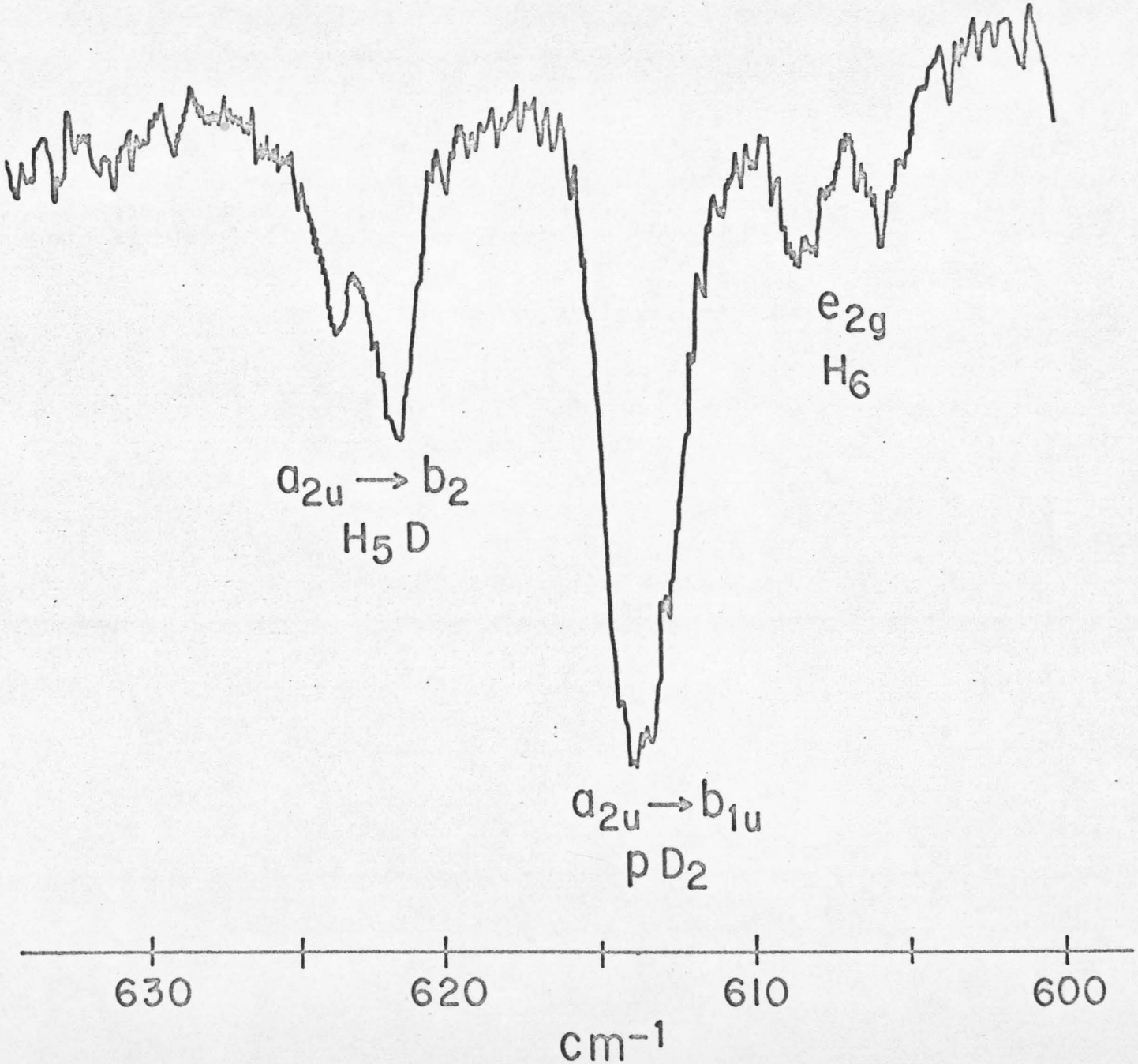
p-C6H4D2, C6H5D in C6H6
a2u → b2
H5D
a2u → b1u
pD2
e2g
H6
630
620
610
600
cm-1

Fig. 13. A further example of ν_6 C_6H_6 being induced by the isotopic guest impurity. See text, Sec. 3g.

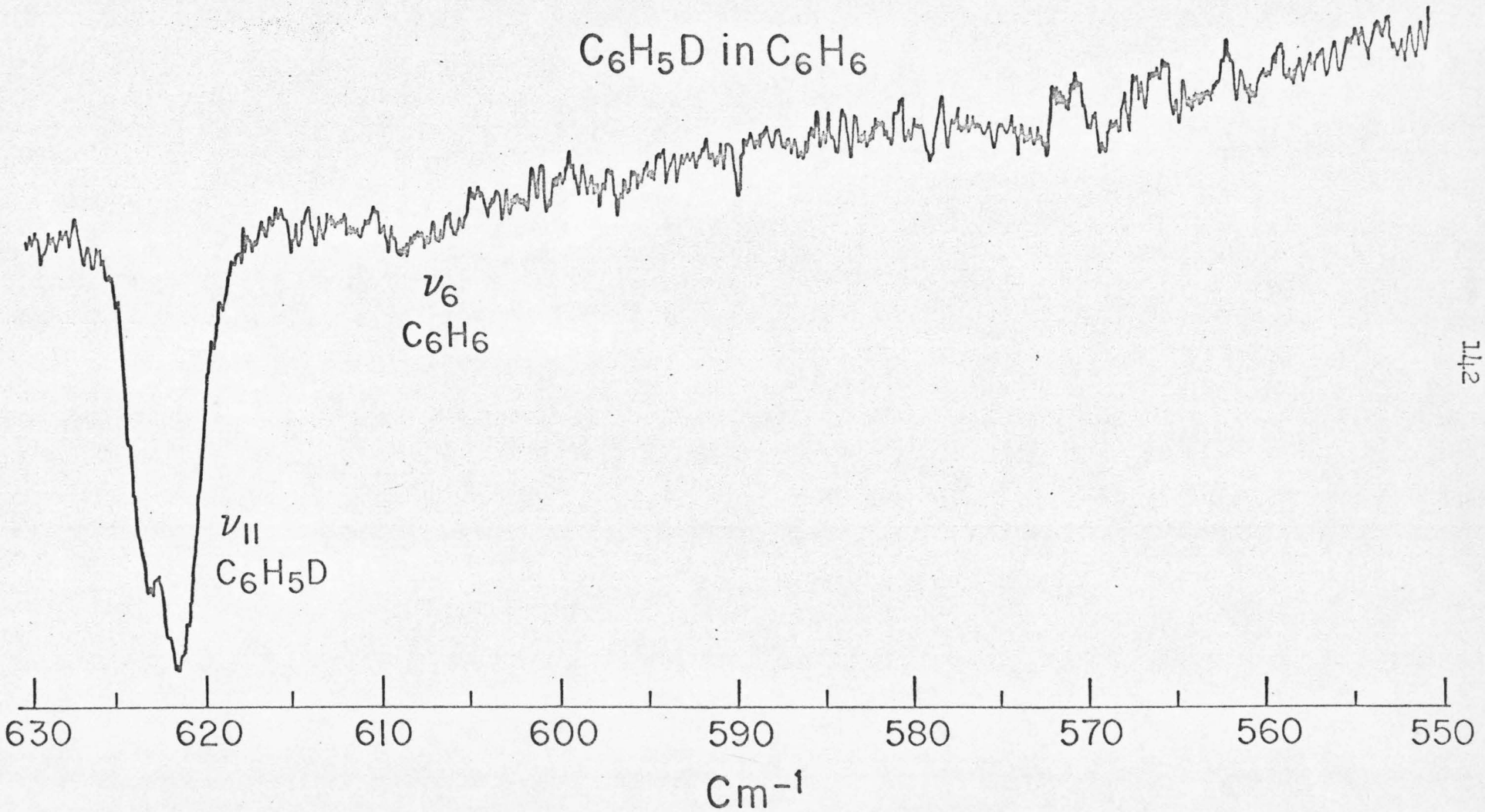
C_6H_5D in C_6H_6
ν_6
C_6H_6
ν_{11}
C_6H_5D
630
620
610
600
590
580
570
560
550
Cm^{-1}

Fig. 14. ν_{11} p-$C_6H_4D_2$ induces, weakly due to the increase energy separation, the ν_6 vibration (e_{2g}) of C_6D_6.

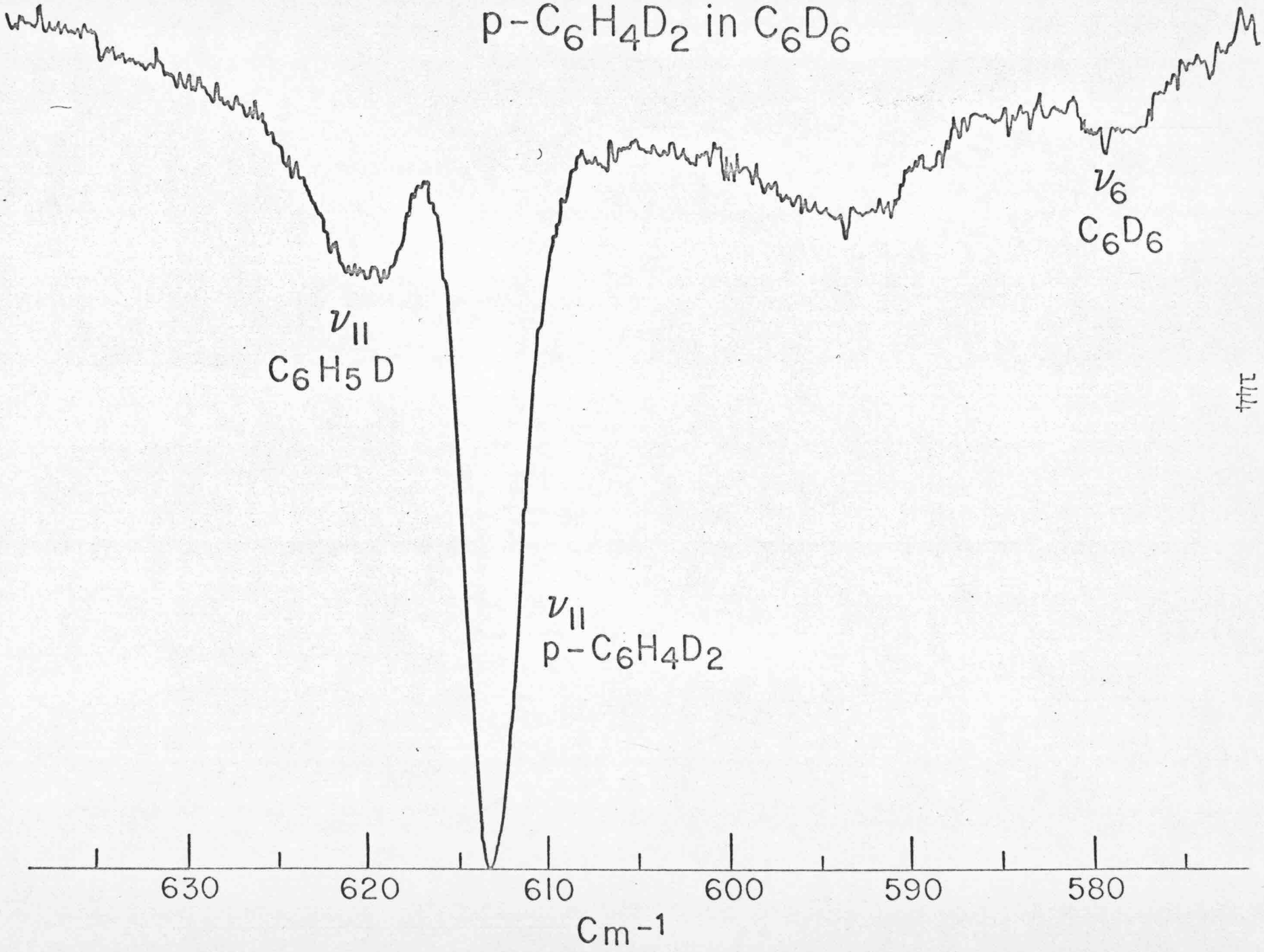
p-C6H4D2 in C6D6
ν11
C6H5D
ν11
p-C6H4D2
ν6
C6D6
630
620
610
600
590
580
Cm-1

Fig. 15. ν_{11} of C_6H_5D does <u>not</u> induce the ν_6 C_6D_6 transition due to the increased energy separation (see Fig. 14).

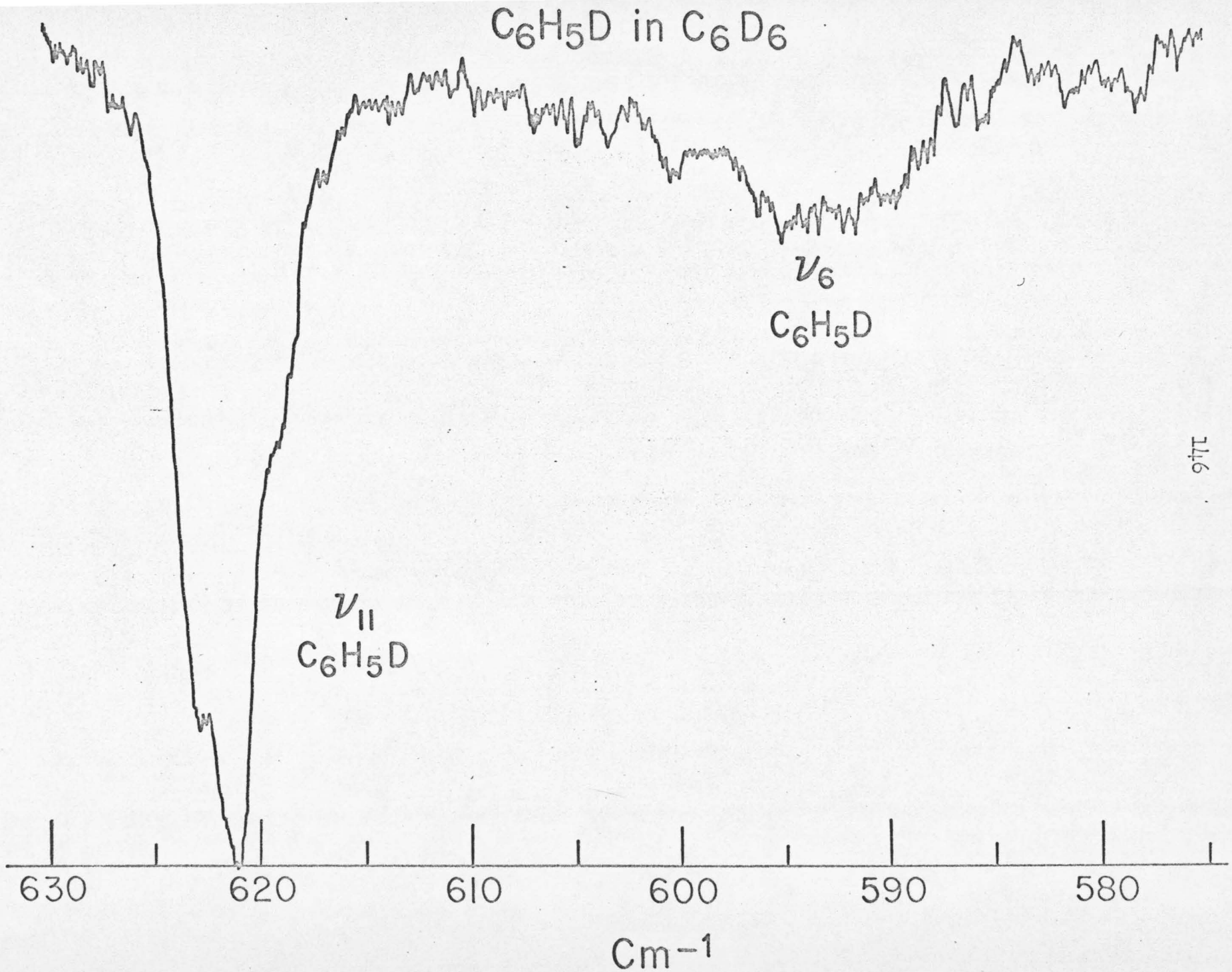
C_6H_5D in C_6D_6
ν_6
C_6H_5D
ν_{11}
C_6H_5D
630
620
610
600
590
580
Cm^{-1}

Fig. 16. Sym-$C_6H_3D_3$ ν_{11} does induce ν_6 of C_6D_6 but only weakly.

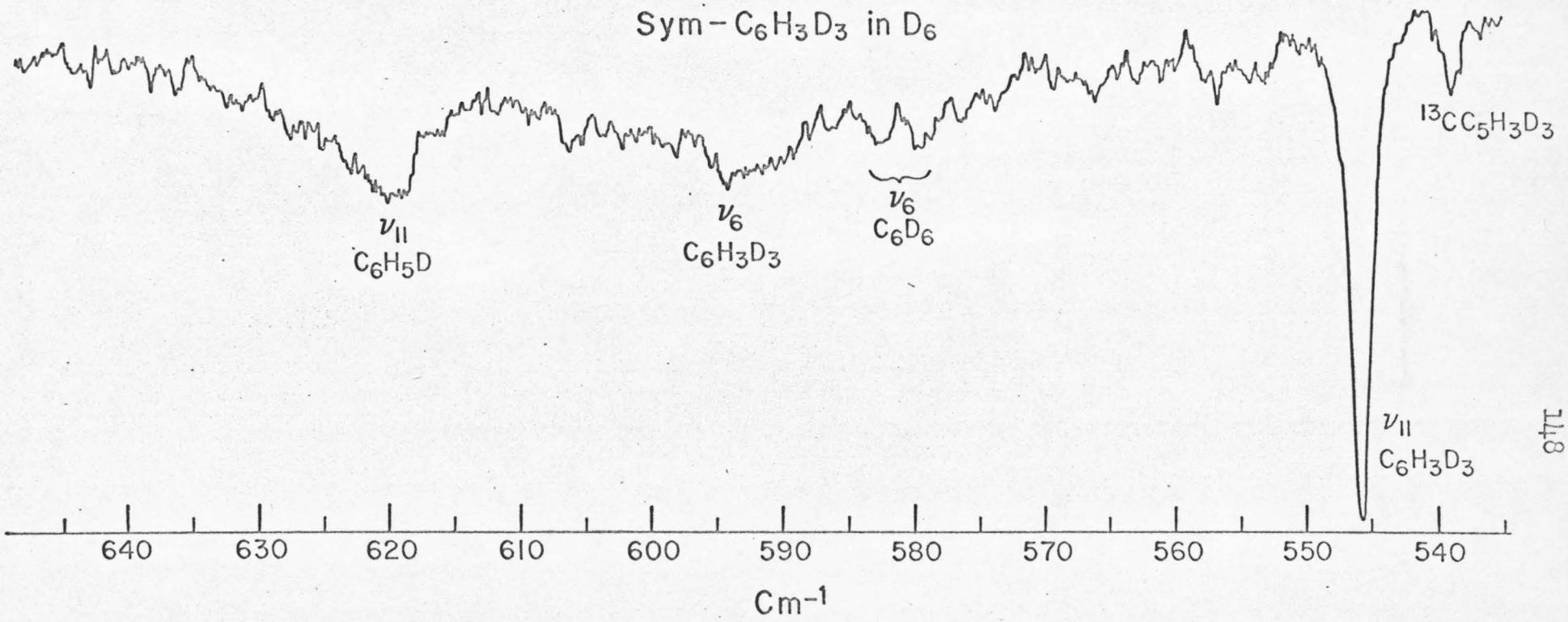
Sym-$C_6H_3D_3$ in D_6
ν_{11}
C_6H_5D
ν_6
$C_6H_3D_3$
ν_6
C_6D_6
$^{13}CC_5H_3D_3$
ν_{11}
$C_6H_3D_3$
640
630
620
610
600
590
580
570
560
550
540
Cm^{-1}

This is not a missing page. It is a result of page misnumbering.

Fig. 17. ν_{11} m-$C_6H_2D_4$ does not induce the ν_6 of C_6H_6. ν_{10} m-$C_6D_4H_2$ does show C_i orientational effect.

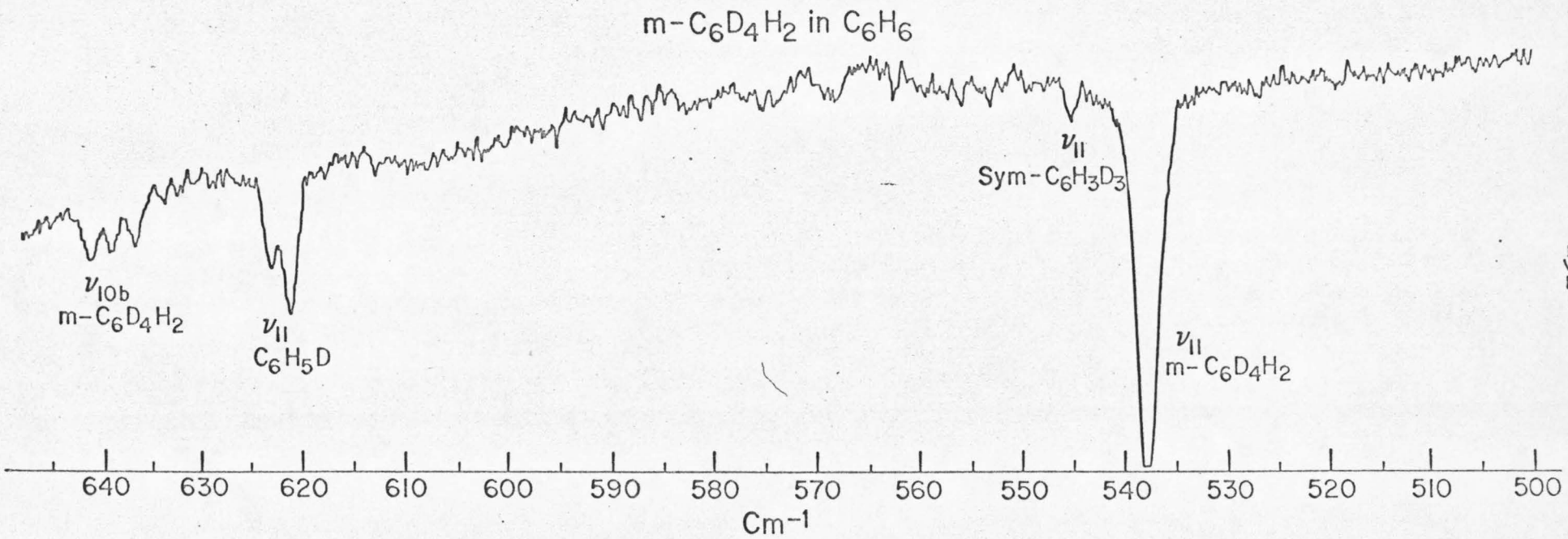
m-C6D4H2 in C6H6
ν10b
m-C6D4H2
ν11
C6H5D
ν11
Sym-C6H3D3
ν11
m-C6D4H2
640
630
620
610
600
590
580
570
560
550
540
530
520
510
500
Cm-1

Fig. 18. Geometrical representation of possible site symmetries for a benzene site. The crystal structure data (Ref. 13) gives site as $\underset{\sim}{C}_i$ but also a planar molecule. The approximate mirror through the two triangles of the $\underset{\sim}{C}_i$ configuration gives the $\underset{\sim}{C}_{2h}$ site. Making this site planar then gives the $\underset{\sim}{D}_{2h}$ site.

POSSIBLE "PHYSICAL SITES" FOR BENZENE CRYSTAL

C_{2h}

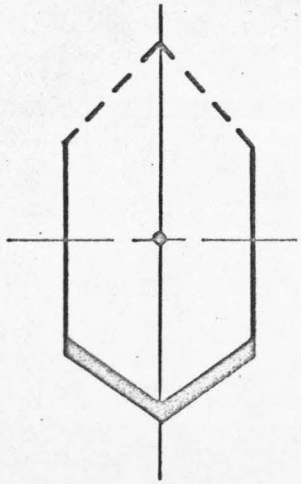

C_i

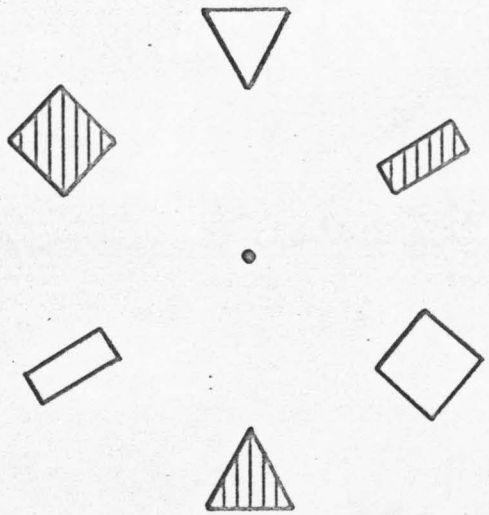

D_{2h}

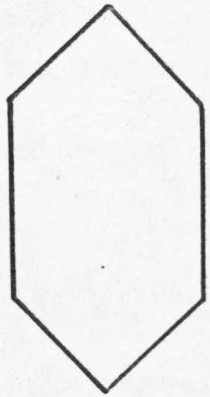

Fig. 19. C_6H_5D as an inpurify in m-$C_6H_4D_2$, showing ν_{11} (622.3 and 624.7 cm^{-1}), ν_{18} (855.2 and 858.4 cm^{-1}), and ν_{18} (1032.7 and 1035.6 cm^{-1}).

0.1% C_6H_5D in m-$C_6H_4D_2$

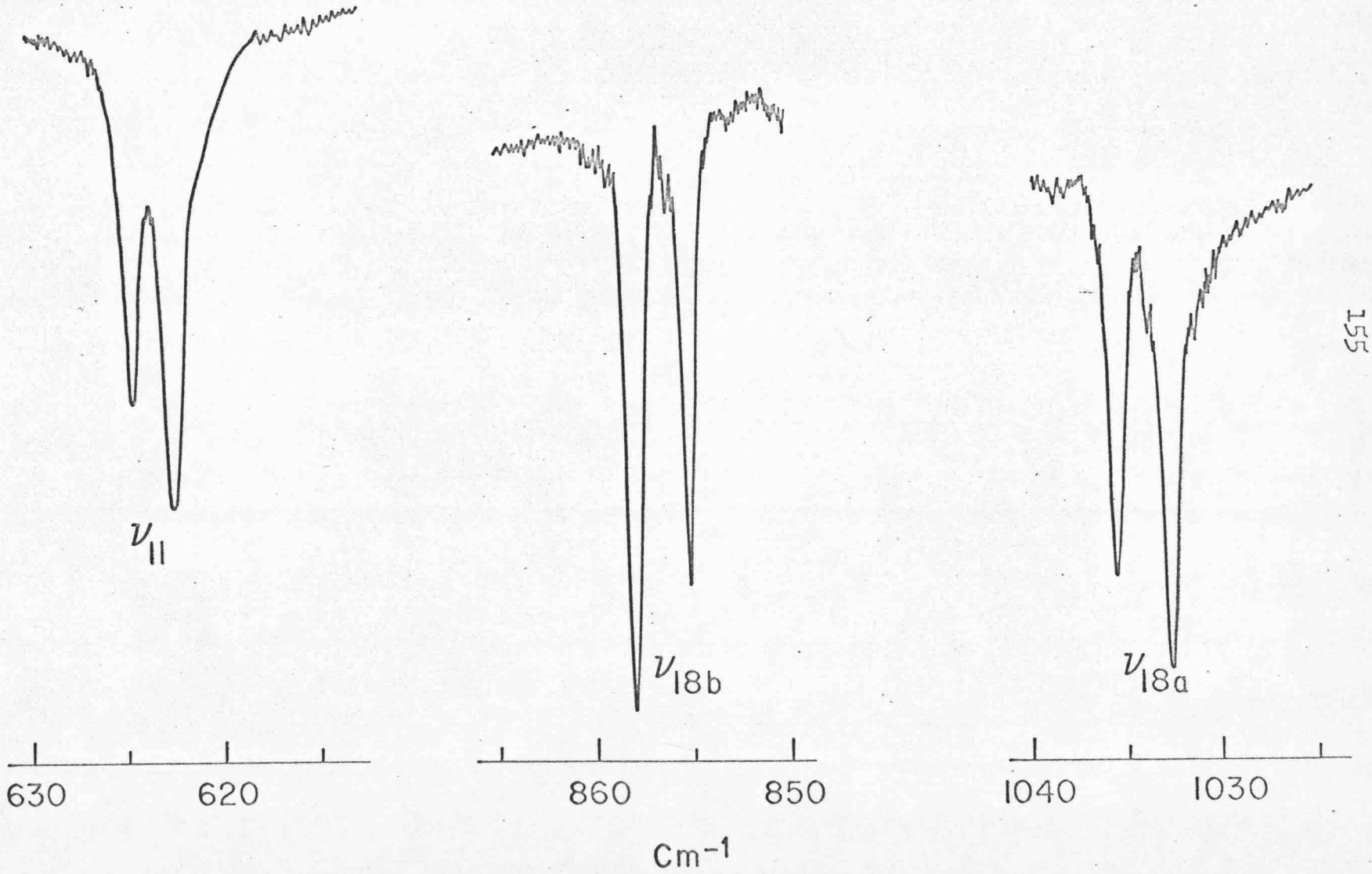

Static Crystal Effects on the Vibronic Structure of the Phosphorescence, Fluorescence, and Absorption Spectra of Benzene Isotopic Mixed Crystals†

E. R. BERNSTEIN, S. D. COLSON, D. S. TINTI, and G. W. ROBINSON

Gates and Crellin Laboratories of Chemistry,‡
California Institute of Technology, Pasadena, California 91109

ABSTRACT

The phosphorescence, fluorescence and absorption spectra of the isotopic benzenes C_6H_6, C_6H_5D, p-$C_6H_4D_2$, and sym-$C_6H_3D_3$, present as dilute guests in a C_6D_6 host crystal at 4.2°K, are obtained with sufficient spectral resolution to ascertain the magnitude of the crystalline site effects. Two such effects are emphasized: site splitting of degenerate fundamentals and orientational effects. The former can occur for the isotopes C_6H_6 and sym-$C_6H_3D_3$, while the latter is possible only for isotopes with less than a molecular three-fold rotation axis. The observations show that both site-splitting and orientational effects do occur as a general rule on vibronic and vibrational states in benzene isotopic mixed crystals. We conclude, therefore, that the site interactions are not negligible.

---

†Supported in part by the Air Force Office of Scientific Research, Contract No. AF 49(638)-1644.

‡Contribution No. 3546.

An empirical correlation of the magnitudes of the site splitting, orientation effect and site (gas-to-crystal) shifts for in-plane and out-of-plane modes is noted. Our results for the ground state vibrations are in good agreement with the findings of Bernstein from infrared spectra in those cases where levels can be observed by both techniques.

In order to characterize completely the above mentioned site effects it was necessary to analyze in some detail both the emission and absorption spectra of the isotopic guest molecules. The phosphorescence of C_6H_6 and sym-$C_6H_3D_3$ has been completely analyzed out to 0, 0-($\nu_8 + \nu_1$) while for that of C_6H_5D, the analysis of only the more intense bands near the electronic origin has been carried out. Some ground state vibrations of p-$C_6H_4D_2$ are presented but the phosphorescence spectrum, complicated greatly by both ground and excited state orientational effects, is not analyzed in this present work. The fluorescence of these isotopes was used only to corroborate and supplement the conclusions and assignments extracted from the phosphorescence analysis and is not presented in detail. The relative vibronic intensities in the fluorescence spectrum are compared to those in the phosphorescence. From the general analysis it is possible to conclude that the effect of the crystal site on the molecule, while spectroscopically measurable, is quite small.

On heavily exposed photographic plates it has been possible to assign the $^{13}CC_5H_6$ emission spectra in both the pure electronic and a few vibronic bands. Absorption spectra of these mixed crystals have yielded information concerning

the orientational effect on the first excited singlet state of C_6H_5D and p-$C_6H_4D_2$ as well as site splitting of the ν_6' vibrational levels of C_6H_6. The $^{13}CC_5H_{6-n}D_n$ 0, 0 absorption spectra have also been identified. New absorptions, in the region of the 0, 0 of C_6H_6 and C_6H_5D have been tentatively assigned to resonance pair lines and $^{13}C_2C_4H_{6-n}D_n$ on the basis of their intensity behavior as a function of guest concentration

I. INTRODUCTION

Since the classic work of Halford,[1] Hornig,[2] and Winston and Halford[3] in the late 1940's, the effect of the crystal environment on molecular spectra has been of much interest. These early works deal in part with the effect of the crystal site on the degenerate molecular states. More recently, Bernstein[4] and Strizhevsky[5] have considered further site interactions not limited only to degenerate states, viz., orientational effects,[4] gas-to-crystal shifts,[4] and enhanced Fermi resonance[4,5] in the solid. For experimental as well as historical reasons, most of these investigations concern the ground state vibrations observable by means of infrared spectroscopy. Since it is of theoretical importance to know whether or not such effects are present for all the vibration classes and types, in the present work we look for the above effects in the vibronic transitions of C_6H_6 and some of its deuterated isotopes: that is, the phosphorescence, fluorescence, and absorption spectra of various benzene isotopic mixed crystals. This allows us to study site interactions in vibrations which are not seen by infrared absorption.

For the case of a C_6H_6 guest in the $\underset{\sim}{C}_i^{\,6}$ site of a C_6D_6 host crystal, the molecular u, g classification of guest states is retained, imposing the u ↔ g dipole selection rule for the C_6H_6 transitions. Thus, in the infrared absorption spectra from the g-ground state, only u-vibrations are observed, while vibronic transitions involving u-excited states can be utilized to study g-vibrations. The emission spectra also supplement the vibrational data obtained employing the Raman effect. On the other hand, in an isotope that does not have inversion symmetry, the infrared absorption and the UV emission spectra can involve the same vibrations, and thus the data complement each other. For example, in the case of site splitting of degenerate fundamentals, the infrared and UV data for C_6H_6 should supplement one another due to the u ↔ g selection rule, while for the case of sym-$C_6H_3D_3$ these data should overlap and check one another. Similarly, for the orientation effect, the C_6H_5D data should overlap with both techniques while for p-$C_6H_4D_2$, there would be no direct overlap of data. It was from these considerations that C_6H_6, C_6H_5D, p-$C_6H_4D_2$, and sym-$C_6H_3D_3$ were chosen for this work. These were all studied as dilute guests in a C_6D_6 host crystal at 4.2 °K. By such a study we hope to provide a complete picture of crystal effects on vibrations of the benzene molecule for all classes and types and, therefore, furnish a good test for theoretical calculations of intramolecular and intermolecular force fields and potentials in solid benzene.

A vibrational analysis of the benzene phosphorescence spectrum in EPA at 77 °K was first published by Shull.[7] Sveshnikov and co-workers[8] and Leach and Lopez-Delgado[9] have compared the vibronic structure of phosphorescence and fluorescence, again in glasses at 77 °K. Nieman[10] and Nieman and Tinti (NT)[11] have analyzed the benzene phosphorescence under low resolution for many benzene isotopes in a C_6D_6 host crystal at 4.2 °K.

The benzene emission spectra in amorphous solids do not generally show resolvable crystal effects on the ground state vibrations. While a few of the larger of these effects were observed in the lower resolution crystal spectra of NT, it is only with the higher resolution employed here that the effects are discernible on nearly all vibronic bands as a general occurrence and can be quantitatively discussed with confidence.

II. THEORETICAL CONSIDERATIONS OF CRYSTAL EFFECTS ON VIBRATIONS

Crystal effects on vibrations have been considered in great detail previously both in our laboratory and others. We will only discuss the general results as needed here, referring the reader to the more detailed work when necessary. Site splitting [1,2] for a molecular energy state occurs if this level has a degenerate representation in the group of the molecule which maps into one or more nondegenerate representations in the group of the crystal site. Thus, the doubly degenerate vibrations of C_6H_6 and sym-$C_6H_3D_3$ are mapped into two nondegenerate components in the $\underset{\sim}{C}_i$ site of the benzene crystal. The energy difference between these two components in an "ideal mixed crystal" is defined as the site group splitting δ_{ss}.[4,12] The concept of an "ideal mixed crystal" implies the absence of all resonance and quasi-resonance intermolecular interactions, while all other interactions remain as in the pure crystal. Dilute (<1%) isotopic mixed crystals of benzene have been shown to be an excellent approximation to the "ideal mixed crystal" for ground state vibrations.[4] This is found not to be true, however, for the lowest excited singlet state of benzene.[13]

For benzene isotopes without a molecular threefold axis, a different effect occurs.[4] It is clear that in the $\underset{\sim}{C}_i$ site there are three possible

orientations with respect to rotation about the original C_6H_6 sixfold axis for the isotopic molecule that, at least in principle, could have different energies. Therefore, a nondegenerate molecular vibration could give rise in the spectrum to three lines, each of which is due to differently oriented molecules in three physically equivalent but distinct sites. For other site symmetries, in general a different number of physically distinct orientations are possible. Thus, the number of lines observed in the spectrum for a given vibration is an indication of the effective site symmetry. Table I summarizes the number of orientations group theoretically possible for benzene isotopes in various sites.

The observations of either effect measures the effect of the static field on the guest molecule. However, certain interaction terms present in one are absent in the other. In the orientational effect, which involves two or more guest molecules on different sites, the ground state terms do not necessarily cancel. These terms must cancel in transitions to the two site split components. Moreover, the two site split components have the same symmetry in the crystal site and can interact with each other, increasing the first-order splitting given by interaction with the static crystal field. This latter interaction can not, of course, occur for molecules on widely separated sites, i.e. for the orientational effect. Because of these differences, a direct comparison of the respective magnitudes of these effects is difficult at best and could be misleading.

III. EXPERIMENTAL

The benzenes were obtained from Merck, Sharp and Dohme, Ltd., of Montreal, Canada. The mixed isotopic solutions were purified by the method described by Colson and Bernstein[14] and directly vacuum distilled into modified "Bridgman type" growing tubes, of the type depicted in Fig. 1. Two

thicknesses of crystal were used: 3 mm and ~ 20 μ. The thick crystals were grown by lowering the optical cells through a temperature gradient of about 100°C/cm directly into a liquid N_2 cooled chamber at the rate of roughly 1 cm/day. These crystals, which are usually transparent and nearly free of cracks, are then cooled to 4.2°K with little decrease in quality. This same technique has been successful in growing crystals up to 3 cm in length. The thin crystals are grown in the same type tube by suspending the holder in a dewar approximately 20 cm above the liquid N_2 surface and subsequently cooling to helium temperatures. Once the crystal holder is completely submerged under the liquid helium, the cell is broken open above the graded seal to insure good thermal contact with the coolant. If this is not done, the sample temperature has been found to remain well above 4.2°K for some length of time and increases when the sample is irradiated.

The emission spectra of the guest triplet and singlet states were excited by absorbing into the C_6D_6 host singlet exciton band from which the excitation energy is rapidly transferred to the lowest excited singlet and triplet states of the guest. These lie approximately 30 cm^{-1} to lower energy for each hydrogen substituted into C_6D_6. The guests thus serve as effective energy traps from which emission is observed at low temperatures. Both low and high pressure Hg lamps were employed as excitation sources. Order sorting, where necessary, was accomplished by liquid Kasha or Corning glass filters in conjunction with 0.1m-atm Cl_2 and Br_2 filters. When high orders were used, a small Bausch and Lomb monochrometer was used as a predispersing element or as an order sorter.

The phosphorescence spectra of the mixed isotopic crystals were photographed at 4.2°K on a Jarrell-Ash 3.4 meter Ebert spectrograph. Two gratings were employed. The first had 15000 line/in yielding a plate

factor of roughly 1.62 Å/mm in the third order. Exposure times for the more intense vibronic lines were about 5 min with 20 μ entrance slits. The weaker lines required approximately one hour exposures. A second grating was used in the eighteenth order where the plate factor was 0.32 Å/mm. Only the more intense vibronic lines of C_6H_6 were photographed, requiring exposure times with 40 μ entrance slits of four hours.

All fluorescence and some of the survey phosphorescence spectra were obtained on a 2.0 meter Czerny-Turner spectrograph, constructed in our laboratory, with a 15000 line/in grating blazed at 1.0 μ. Spectra were taken in third order where the dispersions are 2.4 Å/mm and 3.7 Å/mm in the phosphorescence and fluorescence regions, respectively. The exposure times for 5 μ slits were roughly 5 min. Some of the very weak phosphorescence lines were measured from these plates.

Absorption spectra were taken on the 3.4 meter instrument utilizing the fourth order of the lower resolution grating which gives a dispersion of roughly 1.23 Å/mm at 2650 Å. A few spectra were also photographed with the higher resolution grating.

IV. EMISSION SPECTRA

Both fluorescence and phosphorescence emissions have been photographed for the isotopic guest in a C_6D_6 host crystal at 4.2 °K. Exposure times for the more intense features are roughly equal for the two emissions at lower dispersions, implying nearly equal quantum yields for the singlet and triplet emissions of the guest molecule for the isotopes studies. Furthermore, the measured phosphorescence lifetime of the guest molecule for C_6H_6, C_6H_5D, p-$C_6H_4D_2$, and sym-$C_6H_3D_3$ is independent of the isotopic composition of the guest and its concentration for less than about 1% guest by weight.

The phosphorescence intensity, followed over the first decade change for isolated vibronic lines, decayed exponentially within experimental error with an average lifetime of 8.7 sec. This constant triplet lifetime implies that the quantum yields remain approximately constant independent of the guest and thus appear to be crystal determined.

The phosphorescence does have somewhat sharper lines and is thus easier to photograph at higher dispersions. Due to this smaller linewidth and the greater cm^{-1} dispersion available in the phosphorescence spectral region, we have concentrated mainly on the phosphorescence spectrum as a means of studying ground state vibrations. The larger of the site splittings to be discussed is resolved in both emissions and we have used the fluorescence to complement the phosphorescence where possible.

The narrowest phosphorescence linewidth at the highest resolution employed was approximately 0.1 cm^{-1} and seemed to be limited by the quality of the crystal. This linewidth was observed only once in a very transparent, seemingly near perfect, crystal of 0.04% C_6H_6 in C_6D_6. The linewidth of 0.1 cm^{-1} was superimposed on a weaker background whose width was approximately 0.5 cm^{-1}. This latter width probably corresponds to residual crystal imperfections. It should be noted that the narrowest linewidth we obtained roughly equals the expected zero-field splitting in the triplet state. Thus, the vibronic linewidth which would result from the uncertainty broadening of the ground state excited vibrational level may be much less than 0.1 cm^{-1}, implying that the vibrational relaxation time in the ground state is $\gtrsim 5 \times 10^{-11}$ sec.

The lowest benzene triplet state most likely has B_{1u} symmetry in point group $\underset{\sim}{D}_{6h}$.[15] It is thus both spin and electronically forbidden. This double forbiddenness can be formally removed in a second-order perturbation scheme

by some combination of spin-orbit and vibronic mixing such that the active vibrations must have symmetries contained in $\Gamma_T \times \Gamma_S \times \Gamma_R$ where Γ_i is the irreducible representation in point group $\underset{\sim}{D}_{6h}$ of the phosphorescing triplet state, the dipole allowed singlet state, and the spin-orbit operator for i = T, S, and R, respectively. In this way e_{2g}, b_{2g}, and e_{1g} vibrations are group theoretically predicted to be active in the phosphorescence spectrum for the free $\underset{\sim}{D}_{6h}$ molecule.

Albrecht[16] has analyzed various first- and second-order mechanisms for bringing dipole-allowed singlet character into the triplet state. From the polarized phosphorescence spectrum in solid glass at 77 °K, he concludes that the bulk of the transition probability arises from vibronic mixing, utilizing the e_{2g} vibrations ν_8 and ν_9 [17] of the lowest triplet with the $^3E_{1u}$ state which is spin-orbit coupled to the dipole-allowed singlet states $^1A_{2u}$ and $^1E_{1u}$. Assuming this mixing route and that the lowest excited singlet has B_{2u} symmetry, the vibronic structure of the phosphorescence implies the $^3B_{1u}$ assignment for the lowest triplet state in point-group $\underset{\sim}{D}_{6h}$.

For the lowest excited benzene singlet state,[18] B_{2u} symmetry in point-group $\underset{\sim}{D}_{6h}$ has been established with greater certainty than the triplet symmetry. The spatial forbiddenness of the transition between the ground $^1A_{1g}$ state and the lowest excited $^1B_{2u}$ state can be formally removed by vibronic mixing with the dipole allowed $^1E_{1u}$ and $^1A_{2u}$ states. The latter route requires a b_{1g} fundamental of which benzene has none. However, e_{2g} vibrations can mix a B_{2u} and an E_{1u} state. Thus, vibrations of species e_{2g} are group theoretically predicted to be active in the fluorescence and singlet absorption spectra. Vibronic calculations[19] predict that the e_{2g} vibration ν_6 should dominate.

In the $\underset{\sim}{C}_i$ site of the C_6D_6 host crystal, only the u, g-classification of molecular states is retained and, therefore, the above group-theoretical arguments are no longer rigorously correct. However, it is found experimentally (vide infra) that the above scheme predicts the dominant features of the spectrum, implying that the molecular classification of states is still approximately valid. The effect of the site is demonstrated by the appearance in both the fluorescence and phosphorescence of a totally symmetric progression built on a relatively weak 0, 0 band.

One feature common to both emissions is the activity of a 72 cm^{-1} lattice phonon. This frequency is apparently determined primarily by the C_6D_6 host, independent of the guest, since the value does not measurably change for different isotopic guests. The phonon emission band is quite broad (~ 5 cm^{-1}) and is usually photographed only for the stronger molecular bands. Crystalline C_6D_6 does have two observed[20] optical phonons in this range with frequencies of 62 and 77 cm^{-1} at 4.2 °K. Some unobserved optical phonons are also estimated[20] to have very similar frequencies so that the species of the phonon is not known with certainty. Symmetry arguments require that it be a gerade type.

1. C_6H_6

The more active vibrations in the phosphorescence spectrum of C_6H_6 in a C_6D_6 host are the same as previously assigned in the solid glasses. However, the much sharper lines in the mixed crystal allow a more nearly complete analysis. For example, some of the fundamentals of $^{13}C^{12}C_5H_6$ can be assigned (vide infra). C_6H_6 has four degenerate fundamentals of e_{2g} symmetry in $\underset{\sim}{D}_{6h}$--ν_6, ν_7, ν_8, and ν_9--of which ν_8 dominates the phosphorescance in all solvents, being roughly a factor of five more intense than the

next strongest vibronic origin built on ν_9. In a C_6D_6 host many other weaker "false" origins are resolved and assigned. Progressions of the totally symmetric 990 cm^{-1} (a_{1g}, ν_1) quantum are also found built on ν_6, on the two b_{2g} fundamentals ν_4 and ν_5, the single degenerate e_{1g} fundamental ν_{10}, the electronic 0, 0 and combinations and overtones of overall symmetry e_{2g}, b_{2g}, and e_{1g}.

Figure 2 shows a microphotometer tracing of the phosphorescence spectrum of C_6H_6 from the 0, 0 to 0, 0 - 2500 cm^{-1}. The analysis of the C_6H_6 phosphorescence is given in Table II for energies greater than 0, 0 - ($\nu_8 + \nu_1$). Table III compares the relative intensity of the stronger vibronic origins in the C_6H_6 phosphorescence and fluorescence spectra as determined from microphotometer tracings of photographic plates.

Fig. 2 and Tables II and III show the general dominance of e_{2g} vibrations, and in particular of ν_8 and ν_9 in activating the triplet emission spectrum in qualitative agreement with vibronic theory.[16,19] The almost exclusive activation of the benzene phosphorescence by the modes ν_8 and ν_9 is partially carried over to all the lower symmetry isotopes with an increase in the activity of certain other vibrations qualitatively predictable from mixing of the normal coordinates in the other isotopes. The only e_{2g} fundamental not assigned in the phosphorescence is ν_7. The fundamental ν_6 is quite weak. However, when in combination with ν_1 it steals intensity from ν_8 by Fermi resonance. The totally symmetric progression built on the $\nu_{10}(e_{1g})$ origin is the weakest progression analyzed, being weaker than some progressions based on combinations or overtones of u-fundamentals of overall symmetry e_{2g}. The only g-fundamentals which were not assigned in the phosphorescence of C_6H_6 are $\nu_2(a_{1g})$, $\nu_3(a_{2g})$, and $\nu_7(e_{2g})$. However, ν_2 and ν_7 are assigned from the fluorescence spectrum. No u-vibrations are seen in either emission.

In general the same ground state vibrations are observed in the fluorescence spectrum as in the phosphorescence. However, the relative vibronic activity is substantially different, as can be seen from Table III . The relative intensities in the fluorescence also agree generally with the prediction of vibronic theory outlined earlier. In comparing the two emissions the following features seem noteworthy. The b_{2g} modes, both fundamentals and combinations, are relatively much more intense in the phosphorescence. The only b_{2g} mode we have assigned in the fluorescence is the fundamental ν_4, which appears very weakly. No vibrations of species b_{2g} are seen in the gas phase $^1B_{2u}$ - $^1A_{1g}$ spectrum.[18] However, its intensity is so much less than ν_1 and, therefore, the electronic 0, 0, that it is not possible to draw definitive conclusions from its appearance. The presence of a b_{2g} vibronic origin in the free molecule would support a B_{1u} assignment for the lowest singlet state, but in the crystal the b_{2g} origin could easily be due to crystal site interactions.

The intensity of the totally symmetric fundamental ν_1 relative to the most intense vibronic origin is much greater in the fluorescence than in the phosphorescence. It seems reasonable to attribute this to a greater enhancement of the 0, 0 in the fluorescence since the transition is only symmetry and not spin forbidden. However, the possibility that vibronic mixing by ν_8 in the phosphorescence is enhanced simultaneously with the 0, 0 in the crystal can not be eliminated.

Site splitting δ_{SS} defined in Sec. II is observed for the degenerate e_{2g} fundamentals ν_6, ν_7, and ν_9 amounting to 3.1 cm^{-1}, 5.5 cm^{-1}, and 0.54 cm^{-1}, respectively. The splitting of ν_9 is seen only with the highest resolution employed and is not shown in Table II. Fig. 3 is a densitometer tracing of ν_9 and ν_8 with this highest resolution. No distinct splitting is seen in ν_8, but, as seen in the Fig. 3, the ν_8 linewidth is roughly equal to the total bandwidth of the split ν_9 fundamental. ν_8 could be much more sensitive to

crystal quality than ν_9 so that its greater linewidth (0.5 cm^{-1}) need not completely represent unresolved site splitting. On the other hand, the absence of a splitting in ν_8 supports the assignment of the splitting in ν_9 as a genuine site splitting rather than a splitting due to different sites in a non-perfect crystal. A very weak line, which has not been assigned, is observed ca. 8.5 cm^{-1} to low energy of the very strong 0,0 - ν_9 - $n\nu_1$ progression. The intensity ratio of ν_9 to the unassigned line is > 100 and much larger that the intensity ratio ($\lesssim$ 10) for the two components of any other observed site-split fundamental. We thus feel that this weak feature does not represent the other component of ν_9.

The e_{1g} fundamental ν_{10} is also split (δ_{ss} = 6.8 cm^{-1}). The vibronic intensity of the two components is different in the fundamental (see Fig. 2), but in the observed combinations of ν_{10} with ν_5 ($e_{1g} \times b_{2g} = e_{2g}$) and with ν_9, ν_8 and $\nu_6 + \nu_1$ ($e_{1g} \times e_{2g} = b_{1g} + b_{2g} + e_{1g}$) the splitting repeats itself. The intensity of the components also tends to equalize in these combinations. For the totally symmetric progression built on ν_{10} the intensity difference remains. The mode ν_{10} is not observed in the fluorescence, apparently since it has e_{1g} symmetry in D_{6h}, but the overtone $2\nu_{10}$ (e_{2g}) is seen very weakly and a site splitting of 7 cm^{-1} can be inferred. Thus, even though the vibronic intensities of the site split components of ν_{10} in the phosphorescence is different, the reported site splitting and the frequencies of the components are certainly correct.

In the combination and overtone vibronic bands, site splitting in many u-fundamentals can be inferred. Consider for example the three lines at 808.3, 818.1, and 826.8 cm^{-1} removed from the 0,0 which are assigned as $2\nu_{16}$, $(e_{2u})^2 = e_{2g} + a_{1g}$ in D_{6h}. The observed splitting could arise by two different routes, both yielding three lines. The first mechanism assumes

the degenerate fundamental ν_{16} is not split, but that the site and intramolecular anharmonic terms removes the threefold degeneracy of the overtone $2\nu_{16}$. If this were the case, the expected splitting would be small and the pattern not necessarily symmetric. If, however, the fundamental ν_{16} is split in the site, then the overtone would be three symmetrically spaced lines for small anharmonicities with intensities determined by the binomial coefficients, i.e., 1:2:1, for equal vibronic activity among the three components. As seen from Fig. 2 and Table II the intensities are roughly in this ratio in the phosphorescence and the splitting nearly symmetrical. The fundamental ν_{16} is thus predicted to occur at 404.2 cm^{-1} and 413.0 cm^{-1} with a site splitting δ_{ss} of 8.8 cm^{-1}. In the infrared spectrum of C_6H_6 in a C_6D_6 host crystal,[4a] ν_{16} consists of a doublet at 404.8 cm^{-1} and 413.0 cm^{-1} (δ_{ss} = 8.2 cm^{-1}) in excellent agreement with the values inferred from the emission spectra. A small deviation is expected both from anharmonicities and from Fermi resonance among the trio of lines corresponding to $2\nu_{16}$ each of which rigorously has only symmetry a_g in the $\underset{\sim}{C}_i$ site. The same band observed in the fluorescence, however, does not show this intensity pattern, the high-energy component at 827 cm^{-1} being more intense relative to the other two.

Similarly, the doublet at 1101.6 and 1110.9 cm^{-1}, which is assigned to $\nu_{11} + \nu_{16}$, is the combination of ν_{11} with each of the site-split components of ν_{16}. Assuming no anharmonic corrections or resonances, the inferred value of ν_{11} is 697.4 cm^{-1} which compares with 696.9 observed in the infrared. The quartet assigned to $\nu_{16} + \nu_{17}$ at about 1390 cm^{-1} yields for the degenerate fundamental ν_{17} the frequencies 978.3 cm^{-1} and 982.8 cm^{-1} for an inferred site splitting of 4.5 cm^{-1}. This should be compared with 5.6 cm^{-1} observed in the infrared.

Table IV summarizes the fundamental ground state frequencies of C_6H_6 in a C_6D_6 host crystal and the site splittings for the degenerate fundamentals. The g-fundamentals were obtained directly from the emission spectra as false origins for totally symmetric progressions. For the u-fundamentals both the values inferred in this work from combinations and overtones and the values observed directly in the infrared are given. The latter should, of course, be taken for the frequencies of the u-fundamentals. Sixteen of the twenty benzene fundamentals are therefore accurately known and the site splitting of eight of the ten degenerate fundamentals is established for a crystalline benzene environment. For comparison, Table IV also includes the vapor and liquid phase fundamentals.

2. $^{13}C^{12}C_5H_6$

The isotope ^{13}C is present in natural abundance in the amount of 1.1%. Thus, roughly 6.6% of any benzene will contain at least one ^{13}C atom. For all the partially deuterated benzenes, more than one isomer with the chemical formula $^{13}C^{12}C_5H_nD_{6-n}$ exists. The corresponding vibrational frequencies of each of these isotopes will be very similar and difficult to resolve. However, only one isomer $^{13}C^{12}C_5H_6$ exists. Electronic spectra provide a means of obtaining some of the vibrational frequencies of $^{13}C^{12}C_5H_6$ as an "impurity" in the C_6H_6 guest in the C_6D_6 crystal. This may have a definite advantage over a conventional infrared spectrum since in an electronic transition the corresponding vibronic lines are separated not by the vibrational energy difference, but by the vibrational energy difference plus the zero-point energy contribution. Thus, even if a particular vibrational frequency is unchanged by introducing ^{13}C, the corresponding vibronic lines will be separated in energy by zero-point effects which may be much larger than any individual shift in a vibration. In actuality, however, the electronic

emission spectra have been only of limited usefulness in these mixed crystals for several reasons. Although ~ 6% of the isotopic guest is ^{13}C-benzene, the ^{13}C to ^{12}C phosphorescence intensity ratio is less than 6% since the transition energy for ^{13}C-benzene lies above that of ^{12}C-benzene. Thus, at low temperatures excitation energy transfer to the lowest lying trap, i. e., the ^{12}C-benzene, can reduce the relative intensity of emission from the ^{13}C-isotope. Definitive assignments of all but the more intense ^{13}C-lines are further hampered by the intense background of ^{12}C-lines along with phonon structure on very heavily exposed plates.

Since $^{13}C^{12}C_5H_6$ has vibrational symmetry $\underset{\sim}{C}_{2V}$, the degenerate vibrations of $^{12}C_6H_6$ are split into a and b components. In the $\underset{\sim}{C}_i$ site the vibrations of $^{13}C^{12}C_5H_6$ can be further perturbed by orientational effects and thus give rise to further apparent splittings or line broadening. However, the orientation effects due to one ^{13}C-atom should be much smaller than that for one D-atom since the guest-host interaction is more sensitive to changes on the periphery of the interacting molecules. The orientation effects for $^{12}C_6H_5D$, discussed in a following section, are in general $\lesssim 1$ cm^{-1} and, thus, are expected to be vanishingly small for $^{13}C^{12}C_5H_6$. Therefore, the only new vibrational structure anticipated is the removal of the $^{12}C_6H_6$ vibrational degeneracies.

A somewhat surprising result for $^{13}C^{12}C_5H_6$ is that the isotope shifts from $^{12}C_6H_6$ in the electronic origins of the phosphorescence and fluorescence are quite different, contrary to the observations for the deuterium substituted isotopes.[21,11] These shifts to high energy from the corresponding $^{13}C_6H_6$ transitions are 3.7 and 7.8 cm^{-1} in the $^1B_{2u}$ - $^1A_{1g}$ and $^3B_{1u}$ - $^1A_{1g}$ 0,0 lines, respectively. The electronic origin in the singlet transition, as will be discussed in Section V, is determined from the 0,0 line observed in

This is not a missing page. It is a result of page misnumbering.

absorption. The assignment is confirmed by the presence in the fluorescence spectrum of a progression built on this origin involving a known fundamental[22,23] of $^{13}C^{12}C_5H_6$, viz. ν_1 of species a_1. The mixed crystal value observed for this fundamental is 982.0 cm^{-1} compared to a liquid value[22] of 984 cm^{-1}.

The other $^{13}C^{12}C_5H_6$ fundamentals assigned with some certainty are ν_4, ν_5, ν_{9a}, and ν_{9b}. These were obtained from the phosphorescence wherein they serve as origins for progressions in ν_1. The 0,0 and 0,0-ν_4 lines are very weak and, thus, were only photographed with the faster, lower resolution spectrograph. The bands involving $\nu_{9a,b}$ are seen in Fig. 2 as a weak doublet to high energy of the very strong 0,0-ν_9-nν_1 progression of $^{12}C_6H_6$. The progressions built on ν_4 and ν_5 are too weak to see on the exposure corresponding to Fig. 2 as is the $^{13}C^{12}C_5H_6$ 0,0. The fundamental frequencies are presented in Table V. The observed ^{13}C-shifts are also tabulated and compared with the shift calculated from Whiffen's[24] force field employing the modifications of Albrecht.[25] The agreement between the predicted and observed shifts for the fundamentals ν_1, ν_4, ν_5, and $\nu_{9a,b}$ is excellent and generally within the experimental error limits of ±0.3 cm^{-1}. This range is imposed mainly by the uncertainty in the phosphorescence electronic origin. The vibronic bands terminating in the ground state fundamentals are nearly as sharp as the $^{12}C_6H_6$ lines at the same resolution, confirming our expectations of a very small orientation effect for $^{13}C^{12}C_5H_6$.

Other lines are observed in both emissions which seem due to ^{13}C-benzene, but the analysis leaves some doubt. For example, ν_6 is expected to be stronger than the assigned ν_1 in the fluorescence (cf. Table III). A single line of about the correct intensity relative to ν_6 of ^{12}C-benzene is seen 599.5 cm^{-1} from the ^{13}C-0,0. If the $\nu_{6a,b}$-splitting is greater than about 5 cm^{-1} and if the low energy component is the one observed, the other

component of ν_6 would be unresolved from the overexposed ν_6 band of ^{12}C-benzene. Two very weak lines are seen in the phosphorescence at 600 and 606 cm^{-1} from the ^{13}C-0, 0 and, thus, seemingly support the assignment to $\nu_{6a,b}$. However, this analysis can not be confirmed by a progression of ν_1 built on $\nu_{6a,b}$. Moderately intense lines are seen in the correct spectral region in both the fluorescence and phosphorescence emissions, but they are not easily assignable to $\nu_{6a,b} + \nu_1$. Because of the different ^{13}C-shifts in the phosphorescence and fluorescence electronic origins, the ^{13}C-lines are shifted relative to the ^{12}C-lines in the two emissions. Some lines show the correct shift, but a sufficient number do not or are absent, to make an analysis difficult. Moreover, $\nu_{6a,b} + \nu_1$ is most likely in Fermi resonance with $\nu_{8a,b}$ and possibly also $\nu_{6a,b} + \nu_{12}$. Therefore, we do not conjecture a possible assignment for $\nu_{8a,b}$, even though in the phosphorescence it is expected to be stronger than the assigned $\nu_{9a,b}$, and present the results for $\nu_{6a,b}$ only as tentative.

For the other $^{13}C^{12}C_5H_nD_{6-n}$ isotopes, which are of course present in the other isotopic benzenes, no assignments to ^{13}C-benzene are made. However, some of the unassigned weak lines, especially in the spectrum of sym-$C_6H_3D_3$, could easily be due to $^{13}C^{12}C_5H_3D_3$.

3. sym-$C_6H_3D_3$

From the correlation diagram shown in Fig. 4, the active vibrations in the phosphorescence of sym-$C_6H_3D_3$ (point group $\underset{\sim}{D}_{3h}$) are predicted to have symmetry a_2'', e', and e''. However, only vibrations which correlate directly to the active C_6H_6 vibrations given in Table III, viz. ν_4, ν_5, ν_6, ν_8, and ν_9, or are strongly mixed with them in the lower symmetry isotope are intense vibronic origins in the phosphorescence. For the mixing to be strong the vibrations must have similar frequencies and the same symmetry in the

free molecule. Thus, as shown by the normal coordinate analysis of Brodersen and Langseth,[26] relatively strong mixing occurs between ν_9 and ν_{18}, ν_4 and ν_{11}, and ν_8 and ν_{19}. Weaker mixing does occur to some extent among all vibrations of the same symmetry, and in particular in the $\underset{\sim}{C}_i$ site symmetry among all the vibrations of sym-$C_6H_3D_3$. This latter mixing, however, does not appear to be very strong since the predicted vibrations are the more intense. Figure 5 shows a microphotometer tracing of the phosphorescence spectrum of sym-$C_6H_3D_3$ in crystalline C_6D_6 near the electronic origin. All of the observed fundaments serve as false origins for totally symmetric ν_1 (a_1', 955 cm^{-1}) and ν_{12} (a_1', 1003 cm^{-1}) progressions. The analysis of the sym-$C_6H_3D_3$ phosphorescence out to $0,0-(\nu_8+\nu_1)$ is given in Table VI. Some of the lines shown in Fig. 5 are due to m-$C_6H_4D_2$ and m-$C_6H_2D_4$ impurities. These were identified from the phosphorescence of the corresponding isotopes in a C_6D_6 host. The frequencies are not included in Table VI. The possibility that some of the unassigned lines might be due to isotopic impurities other than the two above has not been investigated.

The vibrational degeneracies in sym-$C_6H_3D_3$, as in C_6H_6, can also be removed by the low symmetry crystalline field, giving rise to site splittings. Nine of the ten degenerate vibrations have been assigned from the phosphorescence and fluorescence spectra. Site splitting is directly observed on four e′ and two e″ (vide infra) fundamentals and inferred for the third e″ fundamental. ν_{20} was obtained from the fluorescence. Because of the greater linewidth in the fluorescence, the site splitting in ν_{20} could be as large as 3 cm^{-1} and not be resolvable. For ν_{19} the site splitting must be < 1 cm^{-1} assuming roughly equal intensities for the two components since only one line was observed. The results are summarized in Table VII.

None of the three possible a_2' vibrations -- ν_3, ν_{14}, and ν_{15} -- were assigned from the emission spectra. These were observed in the infrared for sym-$C_6H_3D_3$ in both C_6H_6 and C_6D_6 hosts and are reported in Ref. 4. For the ground state fundamentals that are seen both in the infrared spectrum and in the electronic emission spectra the agreement is within experimental error except for ν_{17}. The site split components of the fundamental ν_{17} in the phosphorescence have quite different intensities and the high energy component of the vibration is too weak to observe in most combinations. The two components are seen only in ν_{17} and in the doublets tentatively assigned to $\nu_{17} + \nu_8$ and to $\nu_{17} + \nu_5$, where the splitting repeats but the intensities become more nearly equal. This behavior is similar to ν_{10} in both C_6H_6 and sym-$C_6H_3D_3$, but for ν_{17} the intensity difference is greater. The more intense component of ν_{17} agrees with one of the infrared values in a C_6D_6 host, but the weaker component differs from the other infrared value by ca. 2 cm^{-1} which is outside the combined experimental errors. The infrared values for this sym-$C_6H_3D_3$ vibration in the two hosts C_6H_6 and C_6D_6 show larger than usual shifts (ca. 1 cm^{-1}), but this borders on the reported experimental error. Considering the weakness of the high energy component in the phosphorescence, the assignment to ν_{17} may be questioned, but, if this is not the correct assignment and the other component of ν_{17} is unobserved, then the vibronic intensities of the two components must be greatly different as ν_{17} is seen as a doublet in the mixed crystal infrared spectrum. An alternate assignment of the very weak 940.7 cm^{-1} component would be to ν_1 of either one (or both) of the two $^{13}C^{12}C_5H_3D_3$ species present. Brodersen and Langseth have assigned a Raman line at 947 cm^{-1}, observed in liquid sym-$C_6H_3D_3$, to $^{13}C^{12}C_5H_3D_3$. If the ^{13}C-isotope shift in the phosphorescence 0, 0 of $^{13}C^{12}C_5H_3D_3$ is roughly equal to the 7.8 cm^{-1} ^{13}C-shift seen for

$^{13}C^{12}C_5H_6$, then the line at $\Delta\nu = 940.7\ cm^{-1}$ becomes $\Delta\nu = 948.5\ cm^{-1}$ based on the unobserved ^{13}C-0, 0. This near agreement with the Brodersen and Langseth value and the weakness of the vibronic line suggests that perhaps the assignment to ^{13}C is correct. We choose to report in Table VII a site splitting of $4.1\ cm^{-1}$ based on (1) the few tentative combinations involving both components of ν_{17} in the phosphorescence and (2) the observation of a comparable site splitting in the infrared.

At $\Delta\nu \approx 1100\ cm^{-1}$ the fundamental $\nu_9(e')$ is in resonance with the combination $\nu_{10} + \nu_{16}$ $(e' + a' + a_2')$. The strongest two lines in this region, which might be assigned to ν_9 since this fundamental is expected to be strong in the phosphorescence, are degenerate with two of the harmonic values for $\nu_{10} + \nu_{16}$. Since six lines are observed, the ν_9 component of the Fermi multiplet is apparently responsible for two of these lines; however, unambiguous assignments can not be made. Similar problems occur $2270\ cm^{-1}$ to the red of the 0, 0. The fundamental ν_7 is expected to occur in this region, but again overlapping combinations make a unique assignment difficult especially from the phosphorescence (see Table VI). However, in the sym-$C_6H_3D_3$ fluorescence, as in that of C_6H_6, the relative vibronic intensity of ν_7 is increased and, therefore, the lines assigned to ν_7 stand out more clearly. Of course the higher the energy of the ground state vibration, i. e., the further it is removed from the 0, 0, the more severe these problems become. Furthermore, for all the isotopes the emission lines at the same time become broader and an underlying continuum appears. Thus, the assignments to ν_2 and ν_{20} in the $3050\ cm^{-1}$ region are the least certain. As seen by comparing Figs. 3 and 5, the density of lines is less in the C_6H_6 emissions and these complications are not so prevalent.

4. C_6H_5D

C_6H_5D has vibrational symmetry $\underset{\sim}{C}_{2v}$ for a hexagonal carbon framework. As seen from the correlation diagram in Fig. 4 , degenerate vibrations are split into a and b components in this lower symmetry and all vibrations group theoretically can be active in the phosphorescence spectrum. However, those vibrations which correlate directly to the more intense vibrations in the phosphorescence of C_6H_6 or are strongly mixed with one of these active vibrations[23] again dominate. For example, the b_2 vibrations ν_{11} and ν_{17b} are mixed with ν_4 and ν_5, respectively. For the b_1 vibrations strong mixing occurs among ν_{9b}, ν_{15}, and ν_{18b} and between ν_3 and ν_{14}. Thus, besides the strong vibrations corresponding to those shown in Table III, the vibrations ν_{11}, ν_{17b}, ν_{15}, and ν_{18b} also serve as relatively strong vibronic origins of totally symmetric progressions. The weakness of the remaining vibrations again suggests that the molecular symmetry classifications are still approximately valid in the $\underset{\sim}{C}_i$ site.

As a result of this mixing, the actual numbering of the fundamentals is somewhat arbitrary in a number of cases. We have generally followed Brodersen and Langseth, deviating from their labeling scheme only in one of the more arbitrary cases where the vibronic activity seemed to suggest a different assignment, i. e., ν_{9b} and ν_{15} are interchanged.

Since there are no degenerate species in point group $\underset{\sim}{C}_{2v}$, site splitting cannot occur. As pointed out in Section II an apparently similar and related effect can and does occur. The latter has been termed the orientational effect.[4] The expected line pattern is given in Table I for the different isotopes for different choices of the effective site symmetry.

The phosphorescence spectrum near the electronic origin for 0.5% C_6H_5D in a C_6D_6 host crystal is shown in Fig. 6. Table VIII gives the complete analysis for the measured bands out to $0,0-(\nu_{8\,a,b}+\nu_1)$. The electronic origin consists of a pair of lines separated by 6.5 cm^{-1} and all other vibronic bands are doublets or triplets with a total band width of approximately 7 cm^{-1}. These general features have been previously described by NT. They assigned the 0,0 doublet to different orientations of the guest in the crystal, the 6.5 cm^{-1} "splitting" representing the difference in zero-point energies among distinct guest molecules with different orientations of the deuterium atoms in the nearly $\underset{\sim}{C}_{2h}$ site. Thus, based on each member of the 0.0 band vibronic lines appear with energy separations corresponding to vibrational frequencies. Due to the complications of the reduced molecular symmetry and of the orientational effect, the overall density of lines is greatly increased in the C_6H_5D phosphorescence. Therefore, we have primarily concentrated on the lower energy fundamentals and the more intense combinations.

For example, consider the doublet assigned to $0,0-\nu_1(a_1)$ in Fig. 6. Each of these represents the subtraction of a quantum of the totally symmetric mode ν_1 from its respective 0,0 line. NT have been able to show from concentration studies that for some of the more intense lines, the high (low) energy member of a vibronic doublet corresponds to the high (low) energy member of the 0,0 band. Therefore, in the analysis for ν_1 presented in Table VIII the subtractions are made assuming this correlation holds for all vibronic bands. Two values are in this manner obtained for ν_1, 979.0 cm^{-1} and 979.4 cm^{-1}. The difference in these two values results from the inequivalence of the guest-host interactions when two guest molecules undergo the same vibration in two physically different crystal directions corresponding

to the two different guest orientations. This apparent splitting, namely 0.4 cm^{-1} for ν_1, is the orientational effect on this vibration for C_6H_5D in a C_6D_6 host crystal. If this vibration were observed in the infrared or by the Raman effect with sufficient resolution, it would appear as a close doublet with a splitting of 0.4 cm^{-1}, instead of the apparent 6.9 cm^{-1} splitting observed in the phosphorescence.

Since the crystallographic site symmetry is $\underset{\sim}{C}_i$ and not $\underset{\sim}{C}_{2h}$, triplets are predicted in Table I instead of the generally observed doublets. In fact, triplets are observed for some bands, e.g., ν_{18b} and ν_5 in Fig. 6, and inferred for many doublets since the high-energy line is broader. From this and the concentration studies of NT, two of the three electronic origins are assigned to the higher energy component of the 0,0. In Table VIII this nearly degenerate pair are designated as $0,0^1$ and $0,0^2$; the third origin 6.5 cm^{-1} to lower energy is called $0,0^3$.

For the vibronic bands which appear as doublets, the vibrational energy quantum corresponding to origins $0,0^1$ and $0,0^2$ are again nearly degenerate. If the vibronic band is a triplet, the two lines at higher energy are subtracted from the assumed degenerate electronic origins $0,0^1$ and $0,0^2$ to obtain the respective vibrational quantum for these two guest orientations. The vibrational energy in the third orientation is obtained by

subtracting the low-energy line of the triplet vibronic band from $0,0^3$. In this fashion, three different frequencies are generally obtained for a given vibrational mode as shown in Table VIII.

The results are summarized in Table IX which gives all the directly observed fundamental frequencies and the orientational effects determined. The near equivalence of the $0,0^1$ and $0,0^2$ orientations is demonstrated by the fact that only two of the fifteen observed fundamentals show a triplet structure and thus have non-zero entries in column 6 of Table IX. This indicates that the effective site symmetry is very nearly C_{2h}. However, the effect on the vibrational energy in these two cases is quite large, amounting to 1-3 cm^{-1}, compared to an average orientation splitting of 0.7 cm^{-1} between $0,0^3$ and $0,0^2$. It should be noted that both positive and negative energy shifts are observed for the orientational effect. Where the fundamentals reported here overlap with bands observed directly in the infrared the agreement is excellent. No orientation effect has been reported for ν_{9a} or ν_{8b} as it is difficult to conclusively assign all the lines in these regions (1170 and 1575 cm^{-1} removed from the 0,0 band, respectively). It appears that these fundamentals are in Fermi resonance with combinations (see Table VIII).

Since these orientational effects are all small, it is necessary to carefully analyze the sources and the magnitudes of the errors and their propagation in obtaining the final result. The first consideration is, of course, the validity of the subtractions. These have been made subject to the following restrictions: the concentration studies referred to earlier and the fact that where the assignments are unambiguous the orientational effects are usually small (vide infra and Ref. 4). These considerations lead to the method of subtraction given above. Besides this fundamental problem, experimental errors in line frequencies can distort the final result. Such an analysis leads to an uncertainty in the orientational effect of $\lesssim 0.5$ cm^{-1}.

This is a consequence mainly to the three differences involved and round-off error in the absolute energy of any given vibronic line which is reported only to $\pm 0.1\ cm^{-1}$.

5. p-$C_6H_4D_2$

For p-$C_6H_4D_2$, which has vibrational symmetry $\underset{\sim}{D}_{2h}$ for a hexagonal carbon framework, the correlation diagram in Fig. 4 shows that all the g-vibrations a_{1g}, b_{1g}, and b_{3g} can group theoretically be active in the phosphorescence spectrum. Besides those vibrations which correlate directly to the more active vibrations of C_6H_6, a significant activity is also seen of the vibrations $\nu_{10}\,b(b_{3g})$ and $\nu_3(b_{2g})$ which mix with $\nu_4(b_{3g})$ and $\nu_9\,b(b_{2g})$, respectively. As in C_6H_5D, no degeneracies remain in the vibrational manifold of p-$C_6H_4D_2$. However, inversion symmetry is preserved in the latter isotope so that in general the same fundamentals are not observed in the infrared and emission spectra.

As can be seen from the phosphorescence spectrum of 0.5% p-$C_6H_4D_2$ shown in Fig. 7, the electronic 0, 0 and apparently all other vibronic bands are triplets. Because of the complex nature of this spectrum, it was not completely analyzed. A partial analysis of the spectrum is given in the figure, where the average band width of the triplets is about 13 cm^{-1}. The origin of the electronic splittings and their relative magnitude for various isotopes has been discussed by NT. Proceeding as in C_6H_5D, in general three different frequencies corresponding to $0, 0^1$, $0, 0^2$, and $0, 0^3$ are observed for each vibrational mode summarized in Table X. These bands are the only ones for which an unambiguous assignment of the orientation effect could be made.

V. $^1B_{2u} \leftarrow {}^1A_{1g}$ ABSORPTION SPECTRA

The vibronic absorption spectra of the guest in an isotopic mixed crystal also provides a useful tool for studying the effects of the crystal environment on the molecular energy levels. Not only can some excited state vibrations be studied but the orientational structure of the 0, 0 band can be observed directly. Unlike the fluorescence, the guest singlet ← singlet absorption spectra can be very sharp in properly prepared crystals. Care must be exercised to avoid straining the crystal to obtain maximum sharpness.[27] In the thicker crystals of C_6H_6 in C_6D_6, absorption linewidths as narrow as 0.6 cm^{-1} have been measured. The structure of the guest 0, 0 absorption bands is given in Table XI for mixed crystals of C_6H_6, C_6H_5D, p-$C_6H_4D_2$, and sym-$C_6H_3D_3$ at $\lesssim 0.005\%$ in C_6D_6 at 4.2°K. This structure represents the differences in the orientational effects of the ground and lowest excited singlet states, including both the vibrational contribution to their zero-point energies and any electronic effect. That is, if the net contribution to the energy of the zeroth vibronic level for a given orientation were the same for both states and if this were true for all orientations, the 0, 0 band would consist of one line. From a comparison of Tables VIII, X, and XI one can see that this difference for the $^1B_{2u} \leftarrow {}^1A_{1g}$ transition is about 1/5 that of the $^3B_{1u} \leftarrow {}^1A_{1g}$ transition, but in both transitions the overall splitting for p-$C_6H_4D_2$ is about twice that for C_6H_5D. For a detailed discussion of the significance of these differences, see NT.

The thin crystals (~ 20 μ) are required to observe the higher vibronic guest transitions as such absorptions are completely masked by the host absorption in the thick samples. Such guest lines are usually sharper than the fluorescence lines even in these "poorer" crystals. The vibrational frequencies obtained from these absorption lines are less significant than

those of ground state vibrations as excited state levels are more apt to be shifted by interactions with the host. The excitation exchange interactions are typically larger for the singlet vibronic bands than for the ground state vibrational bands and thus quasiresonance interactions[28] with nearby host bands could cause a different shift in each vibronic level. A few C_6H_6 in C_6D_6 levels are given in Table XII from which it can be seen that the ν_6' site splitting (2.1 cm^{-1}) is less than that of the ν_6'' (3.1 cm^{-1}). This splitting should not necessarily be the same as that of the ν_6' in a pure C_6H_6 crystal, which has been reported[29] to be 9 cm^{-1}, since resonance interactions must contribute to the splitting in the pure crystal.

Absorptions due to ^{13}C-containing benzene have also been observed (see Table XI). In thick crystals of about 0.04% C_6H_6, considerable fine structure is seen surrounding the 0, 0 line. The spectrum is shown in Fig. 8 and analyzed in Table XIII. The additional absorptions are tentatively assigned to ^{13}C-benzene, $^{13}C_2$-benzene, and to pairs of guest molecules in adjacent sites ("dimers" or "resonance pairs"). The line at 37856.9 cm^{-1} is assigned to $^{13}C^{12}C_5H_6$ based on the presence of a 982 cm^{-1} (ν_1, a_1) progression built on this origin in the $^1B_{2u} \rightarrow {}^1A_{1g}$ emission spectrum, as described earlier, and on its intensity relative to the $^{12}C_6H_6$ 0, 0 absorption at very low concentrations. The $^{13}C_2$-benzene assignment is made from an analogy with the deuterium isotope effect;[11,21] that is, the $^{13}C_2$-line is expected to be shifted twice as much as the $^{13}C_1$-line. Also in analogy with the deuterium effect, the o-, m-, or p-$^{13}C_2$-shifts are expected to be nearly equal (within 10% of one another). The assignment of the line at 37848.6 cm^{-1} to a resonance pair is made on the basis of its concentration dependence; that is, its intensity decreases more rapidly than that of the C_6H_6 "monomer" absorption with decreasing C_6H_6 concentration. The line at 37851.2 cm^{-1}, which may also be due to a dimer on a different pair of crystalographic sites, has not been shown to have the expected concentration dependence since it is

too near the intense monomer absorption. At the highest resolution employed, additional absorption lines very near the monomer line are resolved. These are given in Table XIII, but are unresolved in the lower resolution spectrum shown in Fig. 8. Their concentration dependence and, therefore, their definite assignment is unknown. Similar lines were seen for the other deuterated isotopes. The C_6H_5D data is also given in Table XIII; note the consistency of the orientational effects.

It should be pointed out that polarized absorption spectra of pairs of molecules in isotopic mixed crystals allow the magnitudes and relative signs of pairwise intermolecular excitation exchange interactions to be determined directly, and therefore may be quite important in the interpretation of the pure crystal spectrum. Within the Frenkel limit, assuming short range terms dominate, these interactions are responsible for exciton mobilities and Davydor splittings, as well as for the full exciton band structures of molecular crystals.[30]

VI. DISCUSSION AND CONCLUSIONS

From the results presented in the summary Tables, both site splittings and orientational effects are seen to be a general occurrence in the benzene crystal. The magnitude of the effects are generally insensitive to isotopic substitution, u- or g-symmetry classification, or to the vibration type as long as the vibration is either in- or out-of-plane. Even the gas-to-crystal frequency shifts (*vide infra*) follow this general pattern. However, differences are seen comparing in-plane and out-of-plane vibrations. Apparent exceptions for the site shifts are the particular in-plane vibrations ν_2, ν_7, ν_8, and ν_{13}. However, the anomalously large gas-to-crystal shift for these vibrations parallels an anomalously large gas-to-liquid shift, while for the

other fundamentals the gas-to-liquid shifts are very small. This implies that the gas-to-solid shifts for these vibrations are due to environmentally induced interactions among the molecular vibrations, rather than, for example, repulsive interactions in the solid phase. The average site shift for the in-plane vibrations is very nearly zero and certainly within gas phase experimental error (2-3 cm^{-1}) for unresolved bands. For the out-of-plane vibrations the average site shift (solid-gas) is greater than 10 cm^{-1}.

This trend is followed in the site splittings (see Tables IV and VII). The average site splitting for the out-of-plane vibrations is $\sim$ 7 cm^{-1} while the in-plane vibrations have an average site splitting of roughly 3 cm^{-1}. For the orientational effect the distinction between in-plane and out-of-plane bands is less clear and it appears that the effect is more dependent on the particular vibrational mode. We note, however, that for $\nu_{16}(CC^{\perp})$ the orientational effect as seen in the infrared[4] in C_6H_5D and p-$C_6H_4D_2$ is the largest observed. Furthermore, the average maximum splitting among the orientational components is generally less than site splitting.

We suggest that the distinction between in-plane and out-of-plane modes is probably due to the greater vibrational amplitudes[24] for the out-of-plane displacements. This could imply that interaction with the crystal environment is greater and, therefore, larger site shifts, site splittings, and orientational effects result for larger vibrational displacements. For the lower symmetry isotopes which exhibit orientational effects, the mixing among vibrations, especially in the $\underset{\sim}{C}_i$ site, tends to equalize the vibrational amplitudes. Hence, one might not expect a clear distinction into certain vibrational classes or types, but rather a general effect larger only for certain motions with large vibrational amplitudes.

The site splitting observed in the fundamental ν_6 for C_6H_6 is 3.1 cm^{-1}.

When totally symmetric additions are made to ν_6, $(\nu_6+\nu_1) + n\nu_1$ comes into Fermi resonance with $\nu_8 + n\nu_1$ and the measured splitting decreases to roughly 1.2 cm^{-1} as shown in Table XIV. The assignment of the "ν_6 component" in the Fermi doublet is made by comparison of the intensities of the members of the Fermi couple with the ν_6 fundamental in the fluorescence and phosphorescence emissions (cf. Table III and Fig. 3). The decrease in the measured splitting of ν_6 for C_6H_6 in the Fermi couple is apparently due to the resonance. Note, however, that the "lost splitting" does not appear in the other half of the couple ν_8. In sym-$C_6H_3D_3$ this same resonance does not appear to be as strong since the observed value for $\nu_6+\nu_1$ is closer to the harmonic value. The site splitting in this progression is more nearly constant and equals 1.7, 1.9 and 1.5 cm^{-1} for n = 0, 1, and 2 respectively. Furthermore, ν_8 in sym-$C_6H_3D_3$ is split by 1.0 cm^{-1}.

Even though the site-split components of a degenerate fundamental usually have very nearly equal vibronic intensities, the fundamentals ν_{10} in both C_6H_6 and sym-$C_6H_3D_3$ and ν_{17} in sym-$C_6H_3D_3$ are exceptions. Exactly how to evaluate this difference in vibronic intensities is not clear at present. An unknown amount of mixing and Fermi resonance between the components contributes to the site splitting and, if substantial, these interactions would tend to equalize the vibronic intensities. Therefore, one might conclude that for the bands where significant intensity differences are seen such intra-site interactions are small. The inverse, however, need not be true; that is, nearly equal intensities does not necessarily imply strong intra-site interactions. It may just be that in these cases the site-split components are equally good "intensity stealers." In combination and overtone bands the relative intensity of the components is variable. For example, the components of $(\nu_{16} + \nu_{11})$ and $2\nu_{16}$ in C_6H_6 appear as expected in the phosphorescence,

but in the fluorescence $2\nu_{16}$ differs from this intensity pattern, whereas $(\nu_{11} + \nu_{16})$ does not. Other examples are evident both from the approximate intensities given in Tables IV and VII and Figs. 2 and 5. Some of these have been previously discussed.

One would also expect an increased mixing and interaction among different molecular vibrations. These effects are expected to show up most clearly where they are symmetry forbidden or weak in the molecule but allowed in the crystal site. For example, for the well known case of $(\nu_6 + \nu_1) + n\nu_1$ interacting with $\nu_8 + n\nu_1$, as given in Table XIV, crystal effects are not obvious. However, for sym-$C_6H_3D_3$ $\nu_{16} + \nu_{10}$ and ν_9 (see Fig. 5 and Table VI) and ν_{20} and ν_2 seem to be examples of crystal site induced interactions. A further possible indication of the magnitude of the crystal site induced effects can be obtained from anharmonicities. Observing $n\nu_1$ out to $n = 5$ in the C_6H_6 fluorescence, the anharmonic effects are small in accordance with the above observations. The only other vibrations whose overtones are observed are ν_{16} and ν_{10}, but in these cases Fermi resonance in the crystal site among the three components of the overtone complicates the analysis of the anharmonicities. Similar difficulties are encountered in the combination bands.

The general conclusion from the gross vibrational structure is that neither the energies nor the symmetry classifications of the vibrations are strongly perturbed by the crystal. This is specifically shown by the magnitude of the site shifts, splittings, and orientational effects and by the dominance of the e_{2g} vibrations in the singlet and triplet spectra. The most pronounced effect of the crystal is the appearance of the 0, 0 progressions in the two emissions. This, along with the observation of site splittings, indicates that the molecular symmetry is not strictly $\underset{\sim}{D}_{6h}$, but these effects could correspond to very small molecular distortions.

References

[1]R. S. Halford, J. Chem. Phys. 14, 8 (1946).

[2]D. F. Hornig, J. Chem. Phys. 16, 1063 (1948).

[3]H. Winston and R. S. Halford, J. Chem. Phys. 17, 607 (1949).

[4(a)]E. R. Bernstein, "Site Effects in Molecular Crystals--Site Shift, Site Splitting, Orientational Effect and Intermolecular Fermi Resonance for Benzene Crystals," J. Chem. Phys. (to be published). [(b)]E. R. Bernstein and G. W. Robinson, "Vibrational Exciton Structure in Crystals of Isotopic Benzenes," J. Chem. Phys. (to be published). [(c)]E. R. Bernstein, "Calculation of the Ground State Vibrational Structure and Phonons of the Isotopic Benzene Crystals," J. Chem. Phys. (to be published).

[5]V. L. Strizhevsky, Opt. i Spektroskopiya 8, 86 (1960).

[6]E. G. Cox, Rev. Mod. Phys. 30, 159 (1958); E. G. Cox, D. W. J. Cruickshank, and J. A. S. Smith, Proc. Roy. Soc. (London) A247, 1 (1958).

[7]H. Shull, J. Chem. Phys. 17, 295 (1949).

[8]B. Ya. Sveshnikov and P. P. Dikun, Dokl. Akad. Nauk SSSR 65, 637 (1949); Zhur. Eksperim. i Teor. Fiz. 19, 1000 (1949); T. V. Ivanova and B. Ya. Sveshnikov, Opt. i Spektroskopiya 11, 322 (1961).

[9]S. Leach and R. Lopez-Delgado, J. chim. phys. 61, 1636 (1964).

[10]G. C. Nieman, Thesis, California Institute of Technology, 1965.

[11]G. C. Nieman and D. S. Tinti, J. Chem. Phys. 46, 1432 (1967).

[12]E. R. Bernstein, S. D. Colson, R. Kopelman, and G. W. Robinson (manuscript in preparation).

[13]S. D. Colson, "Electronic Absorption Spectra of Isotopic Mixed Benzene Crystals," J. Chem. Phys. (to be published).

[14]S. D. Colson and E. R. Bernstein, J. Chem. Phys. 43, 2661 (1965).

[15]See, however, G. Castro and R. M. Hochstrasser, J. Chem. Phys. 46, 3671 (1967), who suggest that the lowest triplet is $^3B_{2u}$.

[16]A. C. Albrecht, J. Chem. Phys. 38, 1326 (1963).

[17]Here and elsewhere in this work, the normal coordinates are numbered after E. B. Wilson, J. C. Decius, and P. C. Cross, Molecular Vibrations, McGraw-Hill Book Co., Inc., New York, New York, 1955.

[18]J. H. Callomon, T. M. Dunn, and I. M. Mills, Phil. Trans. Roy. Soc. (London) A259, 499 (1966).

[19]A. C. Albrecht, J. Chem. Phys. 33, 156, 169 (1960); D. P. Craig, J. Chem. Soc. 1950, 59 2146; J. N. Murrell and J. A. Pople, Proc. Phys. Soc. (London) A69, 245 (1956); A. Liehr, Z. Naturforsch. A16, 641 (1961).

[20]M. Ito and T. Shigeoka, Spectrochim. Acta 22, 1029 (1966).

[21]F. M. Garforth, C. K. Ingold, and H. G. Poole, J. Chem. Soc. 1948, 508.

[22]A. Langseth and R. C. Lord, Jr., J. Chem. Phys. 38, 203 (1938); W. Gerlach, Ber. d. Bayr. Akad. d. Wiss. 1, 39(1932).

[23]A. R. Gee and G. W. Robinson, J. Chem. Phys. 46, 4847 (1967).

[24]D. H. Whiffen, Phil. Trans. Roy. Soc. (London) A248, 131 (1955).

[25]A. C. Albrecht, J. Mol. Spectry. 5, 236 (1960).

[26]S. Brodersen and A. Langseth, Danske Videnkab. Selskab, Mat. Fys. Skrifter Kgl. 1, No. 1 (1956).

[27]S. D. Colson, J. Chem. Phys. 45, 4746 (1966).

[28]G. C. Nieman and G. W. Robinson, J. Chem. Phys. 38, 1928 (1963).

[29]V. L. Bronde, Usp. Fiz. Nauk 74, 577 (1961) [English transl. Soviet Phys.- Usp. 4, 584 (1962)].

[30]A. S. Davydov, Usp. Fiz. Nauk. 82, 393 (1964) [English transl. Soviet Phys.-Usp. 6, 145 (1964)].

TABLE I. Number of possible orientations for benzene isotopes in sites of different symmetries.

Molecule	Molecular Symmetry	Site Symmetry C_1	C_i	C_{2h}	D_{2h}
C_6H_6 C_6D_6	D_{6h}	1	1	1	1
sym-$C_6H_3D_3$	D_{3h}	2	1	1	1
p-$C_6H_4D_2$	D_{2h}	3	3	3,[a] 2	2
C_6H_5D o-$C_6H_4D_2$ m-$C_6H_4D_2$ vic-$C_6H_3D_3$	C_{2v}	6	3	3,[a] 2	2
asym-$C_6H_3D_3$	C_s	12	6	6,[a] 3	3

[a]Plane of the site same as the molecular plane.

TABLE II. Analysis of the C_6H_6 phosphorescence.

λ_{air}(Å)	ν_{vac}(cm^{-1})	Relative intensity	$\Delta\nu$(cm^{-1})	Assignment[a]	Vibrational symmetry in D_{6h}	Predicted harmonic value (cm^{-1})
3369.90	29666.0	vvw		^{13}C 0,0		
70.79	658.2	m	0	0,0		
3441.13	051.9	mw	606.3	ν_6	e_{2g}	
41.49	048.8	mw	609.4			
52.85	28953.3	m	704.9	ν_4	b_{2g}	
65.22	849.9	w	808.3	$2\nu_{16}$	$e_{2g}+a_{1g}$	809.6
66.40	840.1	mw	818.1			817.8
67.45	831.4	w	826.8			826.0
71.75	795.7	w	862.5	ν_{10}	e_{1g}	
72.57	788.9	vw	869.3			
87.25	667.7	m	990.5	ν_1	a_{1g}	
87.90	662.4	vw	995.8	^{13}C ν_5		
89.00	653.3	s	1004.9	ν_5	b_{2g}	
3500.82	556.6	w	1101.6	$\nu_{11}+\nu_{16}$	e_{2g}	1101.7
01.96	547.3	w	1110.9			1109.9
08.58	493.4	w	1164.8	^{13}C $\nu_{9a,b}$		
08.83	491.4	w	1166.8			
09.79	483.6	vs	1174.6	ν_9	e_{2g}	
10.84	475.1	vw	1183.1	?		
18.63	412.0	w,b	1246.2	$\nu_9+71.6$		

TABLE II. (Cont'd)

λ_{air}(Å)	ν_{vac}(cm^{-1})	Relative intensity	$\Delta\nu$(cm^{-1})	Assignment[a]	Vibrational symmetry in D_{6h}	Predicted harmonic value (cm^{-1})
3535.51	28276.4	w	1381.8			1383.1
36.21	270.8	mw	1387.4	$\nu_{16}+\nu_{17}$	$e_{2g}+a_{2g}+a_{1g}$	1387.5
36.8	266.	vw	1392.			1391.3
37.25	262.5	w	1395.7			1395.7
58.53	093.4	mw	1564.8			
59.01	089.6	mw	1568.6			
59.65	084.6	mw, b	1573.6	^{13}C ?		?
60.43	078.4	mw, b	1579.8			
61.00	073.9	vs	1584.3	ν_8	e_{2g}	
62.56	061.7	mw, b	1596.5	^{13}C ?		
63.35	055.4	s	1602.8	$\nu_6+\nu_1$	e_{2g}	1596.8
63.51	054.2	s	1604.0			1599.9
64.32	047.8	vw	1610.4	$\nu_6+\nu_5$	e_{1g}	1611.2
64.52	046.2	vw	1612.0			1614.3
70.10	002.4	w, b	1655.8	$\nu_8+71.5$		
72.59	27982.9	w, b	1675.3	$\nu_6+\nu_1+71.3$		
74.99	964.1	m	1694.1	$\nu_4+\nu_1$	b_{2g}	1695.4
88.75	856.9	w	1801.3			1800.1
90.08	846.5	mw	1811.7	$2\nu_{16}+\nu_1$	$e_{2g}+a_{1g}$	1808.3
91.20	837.9	w	1820.3			1816.5
95.31	806.0	w	1852.2	$\nu_{10}+\nu_1$	e_{1g}	1853.0
96.24	798.8	vw, b	1859.4			1859.8

TABLE II. (Cont'd)

λ_{air}(Å)	ν_{vac}(cm^{-1})	Relative intensity	$\Delta\nu$(cm^{-1})	Assignment[a]	Vibrational symmetry in D_{6h}	Predicted harmonic value (cm^{-1})
3597.02	27792.8	w	1865.4	$\nu_{10} + \nu_5$	e_{2g}	1867.4
97.86	786.3	w	1871.9			1874.2
98.77	779.3	w	1878.9	$\nu_9 + \nu_4$	e_{1g}	1879.5
3611.63	680.4	vw, sh	1977.8	$^{13}C\ \nu_5 + \nu_1$		
11.89	678.4	m	1979.8	$2\nu_1$	a_{1g}	1981.0
12.42	674.4	vw	1983.8	?		
13.78	664.0	s	1994.2	$\nu_5 + \nu_1$	b_{2g}	1995.4
19.30	621.8	w	2036.4	$\nu_{10} + \nu_9$	$e_{1g} + b_{2g} + b_{1g}$	2037.1
20.35	613.8	w	2044.4			2043.9
26.75	565.1	w	2093.1	$\nu_{11} + \nu_{16} + \nu_1$		2092.2
28.00	555.6	w	2102.6			2100.4
29.39	545.0	vw	2113.2	?		
33.76	511.8	w	2146.4	$^{13}C\ \nu_{9a,b} + \nu_1$		
34.05	509.6	w	2148.6			
35.32	500.0	vw	2158.2	$\nu_{12} + \nu_{15}$?	a_{2g}	2158.2
36.13	493.9	vs	2164.3	$\nu_9 + \nu_1$	e_{2g}	2165.1
37.23	485.6	vw	2172.6	?		
38.20	478.3	w	2179.9	$\nu_9 + \nu_5$	e_{1g}	2179.5
38.35	477.1	w, sh	2181.0	$\nu_{15} + \nu_{18}$	e_{2g}	2181.7
38.90	473.0	w	2185.2			2185.5
45.57	422.7	w, b	2235.5	$\nu_9 + \nu_1 + 71.2$		
52.47	370.9	w	2287.3	$\nu_8 + \nu_4$	e_{1g}	2289.2

TABLE II. (Cont'd)

λ_{air}(Å)	ν_{vac}(cm^{-1})	Relative intensity	$\Delta\nu$(cm^{-1})	Assignment[a]	Vibrational symmetry in D_{6h}	Predicted harmonic value (cm^{-1})
3660.46	27311.2	vw	2347.0	$\nu_{14}+\nu_{18}$	e_{2g}	2347.4
60.98	307.3	w	2350.9			2351.2
63.87	285.8	w	2372.4	$\nu_{16}+\nu_{17}+\nu_1$	$e_{2g}+a_{2g}+a_{1g}$	2373.6
64.65	280.0	w	2378.2			2378.0
65.31	275.1	vw	2383.1			2381.8
65.83	271.2	w, b	2387.0	$2\nu_6+\nu_9$	$2e_{2g}+a_{2g}+a_{1g}$	2386.2, 2387.2
66.31	267.6	w	2390.6			2390.3
66.53	266.0	w	2392.2			2393.4
68.94	248.1	w	2410.1	?		
69.46	244.2	w	2414.0	?		
73.73	212.5	w	2445.7	$\nu_8+\nu_{10}$	e_{1g}	2446.8
74.58	206.2	w, b	2452.0			2453.6
76.39	192.8	w	2465.4	$\nu_6+\nu_1+\nu_{10}$	e_{1g}	2465.9
77.15	187.2	w, b	2471.0			2472.7
86.68	116.9	mw	2541.3	^{13}C ?		
87.24	112.8	mw	2545.4			
88.60	102.8	m	2555.4			
89.58	095.6	m	2562.6			
90.34	090.1	vs	2568.1	$\nu_8+\nu_1$	e_{2g}	2574.8
91.38	082.4	mw	2575.8	^{13}C ?		
92.27	075.9	mw	2582.3			
93.00	070.6	mw	2587.6	$\nu_8+\nu_5$	e_{1g}	2589.2

TABLE II. (Cont'd)

λ_{air}(Å)	ν_{vac}(cm^{-1})	Relative intensity	$\Delta\nu$(cm^{-1})	Assignment[a]	Vibrational symmetry in D_{6h}	Predicted harmonic value (cm^{-1})
3693.91	27063.9	s	2594.3	$\nu_6 + 2\nu_1$	e_{2g}	2587.3
94.07	062.7	s	2595.5			2590.4
95.54	052.0	vw	2606.2	$\nu_6+\nu_1+\nu_5$	e_{1g}	2601.7
95.70	050.8	vw	2607.4			2604.8
3700.06	018.9	w, b	2639.3	$\nu_8+\nu_1+71.2$		
05.92	26976.2	mw	2682.0	$\nu_4 + 2\nu_1$	b_{2g}	2685.9

[a]Bands in Fermi resonance are connected by square brackets.

TABLE III. Relative intensity estimates for the stronger vibronic origins in the C_6H_6 phosphorescence and fluorescence spectra.

Symmetry	Vibration	$^3B_{1u} \rightarrow {}^1A_{1g}$	$^1B_{2u} \rightarrow {}^1A_{1g}$
e_{2g}	ν_6	1	100
	ν_7	–	3
	ν_8[a]	100	20
	ν_9	25	3
	$2\nu_{16}$	1	3
	$\nu_{11}+\nu_{16}$	<1	5
b_{2g}	ν_4	1+	<1
	ν_5	6	–
a_{1g}	ν_1	1	22
	ν_2	–	1
e_{1g}	ν_{10}	<1	–
0, 0		1	b

[a]Uncorrected for Fermi resonance with $\nu_6 + \nu_1$.

[b]Due to appreciable reabsorption, no relative intensity estimate is given.

TABLE IV. Summary of C_6H_6 data (cm^{-1}).

D_{6h} symmetry class	Vibration number and type[a]	Fundamental frequency gas[b]	liquid[c]	solid[d]	Site splitting
a_{1g}	$\nu_1(CC)$	995.4	(993)	990.5	
		(3073)	(3062)	3063.3	
a_{2g}	$\nu_3(H^{\parallel})$	(1350)	1346		
b_{2g}	$\nu_4(C^{\perp})$	(707)	(707)	704.9	
	$\nu_5(H^{\perp})$	(990)	(991)	1004.9	
e_{2g}	$\nu_6(C^{\parallel})$	608.0	(606)	606.3, 609.4	3.1
	$\nu_7(CH)$	(3056)	(3048)	3042.0, 3047.5	5.5
	$\nu_8(CC)$[e]	(1590)	1586	1584.2	$\leqslant 0.3$
	$\nu_9(H^{\parallel})$	(1178)	1177	$1174.3_4, 1174.8_8$	0.5_4
e_{1g}	$\nu_{10}(H^{\perp})$	(846)	850	862.5, 869.3	6.8
a_{2u}	$\nu_{11}(H^{\perp})$	674.0	675	696.9	
				[697]	
b_{1u}	$\nu_{12}(C^{\parallel})$	(1010)	1010	1011.3	
				[1011]	
	$\nu_{13}(CH)$	(3057)	(3048)		
b_{2u}	$\nu_{14}(CC)$	(1309)	1309	1312.6	
				[1313]	
	$\nu_{15}(H^{\parallel})$	(1146)	1146	1146.9	
				[1147]	
e_{2u}	$\nu_{16}(C^{\perp})$	398.6	404	404.8, 413.0	8.2
				[404, 413]	
	$\nu_{17}(H^{\perp})$	(967)	969	978.3, 983.9	5.6
				[978, 983]	

TABLE IV. (Cont'd)

D_{6h} symmetry class	Vibration number and type[a]	Fundamental frequency gas[b]	liquid[c]	solid	Site splitting
e_{1u}	$\nu_{18}(H^{\parallel})$	1037	1035	1034.8, 1038.6 [1034, 1038]	3.8
	$\nu_{19}(CC)$	1482	1479		
	$\nu_{20}(CH)$[e]	3047	3036		

[a]The vibrational numbering for this and the other isotopes follows Refs. 17 and 26.

[b]Taken from summary given in Ref. 26. ( ) indicates calculated values.

[c]Ref. 18.

[d]The frequencies of the u-fundamentals are from Ref. 4. The values inferred from the u. v. spectra, rounded-off to the nearest cm^{-1}, are given in parentheses.

[e]Uncorrected for Fermi resonance.

TABLE V. Some observed and calculated fundamental frequencies of $^{13}C^{12}C_5H_6$.

$^{13}C^{12}C_5H_6$ fundamental frequency	(cm^{-1})[a]	$\Delta\nu$ (^{12}C - ^{13}C) observed[b]	predicted[c]
ν_1	982.0	8.5	8.4
ν_4	702.0	2.9	3.5
ν_5	1003.8	1.1	1.0
$\nu_{9a,b}$	1174.6	0.0	0.3
	1172.6	2.0	2.4

[a] The experimental error is ±0.3 cm^{-1}.

[b] The mean of the site-split fundamental ν_9 of $^{12}C_6H_6$ was used to calculate the $\Delta\nu$ observed.

[c] See text.

TABLE VI. Analyses of the sym-$C_6H_3D_3$ phosphorescence.

λ_{air}(Å)	ν_{vac}(cm^{-1})	Relative intensity	$\Delta\nu$(cm^{-1})	Assignment†	Vibrational symmetry in D_{3h}	Predicted harmonic value (cm^{-1})
3361.89	29,753.8	m	0			
3422.78	29,207.6	m	546.2	ν_{11}	a_2''	
28.14	162.0	m	591.8	ν_6	e'	
28.33	160.3	m	593.5			
41.33	050.2	m	703.9	ν_4	a_2''	
43.06	035.6	mw	718.2	ν_{10}	e''	
43.59	031.1	vw	722.7			
47.55	28,997.8	w	756.0			
48.65	988.6	mw	765.2	$2\nu_{16}$	$a_1' + e'$	
49.70	979.7	w	774.1			
56.55	922.3	ms	831.5	ν_{18}	e'	
56.97	918.8	ms	835.0			
68.10	825.9	m	927.9	ν_5	a_2''	
69.17	817.1	mw	936.7	ν_{17}	e''	
69.66	813.1	vvw	940.7			
71.33	799.2	m	954.6	ν_1	a_1'	
77.15	750.9	mw	1002.9	ν_{12}	a_1'	
86.06	677.5	m	1076.3	$\nu_4 + \nu_{16}$?	e'	1081.9
86.80	671.3	ms	1082.5			1090.9
87.89	662.4	vw	1091.4	$2\nu_{11}$?	a_1'	1092.4

TABLE VI. (Cont'd)

λ_{air}(Å)	ν_{vac}(cm^{-1})	Relative intensity	$\Delta\nu$(cm^{-1})	Assignment	Vibrational symmetry in $\underset{\sim}{D}_{3h}$	Predicted harmonic value (cm^{-1})
3488.02	28,661.4	vw	1092.4	?		
88.35	658.6	m	1095.2			
88.60	656.5	m	1097.3		e′	
88.99	653.4	ms	1100.4	ν_9 and		
89.35	650.4	ms	1103.4	$\nu_{10}+\nu_{16}$	$e'+a_1'+a_2'$	
89.65	848.0	m	1105.8			
90.19	643.5	vw	1110.3			
3508.92	490.6	mw	1263.2	$\nu_{11}+\nu_{10}$	e′	1263.0
09.46	486.3	mw	1267.5			1267.5
14.70	443.8	vw	1310.0		e′	
15.22	439.6	w	1314.2	$\nu_{16}+\nu_5$, $\nu_{10}+\nu_6$,	$e''+a_1''+a_2''$	
15.44	437.8	vw	1316.0	$\nu_{16}+\nu_{17}$		
15.97	433.5	vw	1320.3		$e'+a_1'+a_2'$	
16.88	426.2	vw	1327.6			
27.23	342.8	ms	1411.0	ν_{19}	e′	
28.63	331.5	mw	1422.3	$\nu_6+\nu_{18}$	$e'+a_1'+a_2'$	
29.02	328.3	w	1425.5			
29.52	324.4	m	1429.4	$\nu_4+\nu_{10}$	e′	
35.07	279.9	vvw	1473.9	$\nu_{11}+\nu_5$	a′	1474.1
36.18	271.0	vvw	1482.8	$\nu_{11}+\nu_{17}$	e′	1482.9
38.32	253.9	mw	1499.9	$\nu_{11}+\nu_1$	a_2''	1500.8

TABLE VI. (Cont'd)

λ_{air}(Å)	ν_{vac}(cm^{-1})	Relative intensity	$\Delta\nu$(cm^{-1})	Assignment	Vibrational symmetry in $\underset{\sim}{D}_{3h}$	Predicted harmonic value (cm^{-1})
3542.63	28,219.5	w	1534.3	?		
43.90	209.5	s	1544.3	$\nu_6 + \nu_1$	e′	1546.5
44.13	207.6	s	1546.2			1548.2
44.67	203.3	w	1550.5	$\nu_{11} + \nu_{12}$	a_2''	1549.1
45.00	200.7	mw	1553.1	$\nu_{18} + \nu_{10}$?	$e'' + a_1'' + a_2''$	
45.98	192.9	m	1560.9	?		
46.43	189.3	w	1564.5	?		
47.28	182.6	vs	1571.2	ν_8 ‡	e′	
47.41	181.6	vs	1572.2			
48.39	173.7	w	1580.1	?		
49.12	168.0	vw	1585.8	?		
56.44	110	m, vb	1644	$\nu_8 + 72$		
57.24	103.6	w	1650.2	$\nu_5 + \nu_{10}$?	e′	1646.0
57.82	099.1	vw	1654.7			1650.5
58.22	095.9	mw	1657.9	$\nu_4 + \nu_1$	a_2''	1658.5
60.09	081.2	w	1672.6	$\nu_{10} + \nu_1$	e″	1672.8
60.68	076.5	vw	1677.3			1677.3
61.01	073.9	w	1679.9	?		
64.26	048.3	w	1705.5	$\nu_4 + \nu_{12}$	a_2''	1706.8
65.09	041.8	w	1712.0			1710.6
66.29	032.3	mw	1721.5	$2\nu_{16} + \nu_1$	$a_1' + e'$	1719.8
67.42	023.5	w	1730.3			1728.7

TABLE VI. (Cont'd)

λ_{air}(Å)	ν_{vac}(cm^{-1})	Relative intensity	$\Delta\nu$(cm^{-1})	Assignment	Vibrational symmetry in D_{3h}	Predicted harmonic value (cm^{-1})
3570.96	27,995.7	vvw	1758.1			1758.9
72.14	986.4	vw	1767.4	$2\nu_{16}+\nu_{12}$	$a_1' + e'$	1768.1
73.28	977.5	vvw	1776.3			1777.0
74.54	967.6	m	1786.2	$\nu_{18} + \nu_1$	e'	1786.1
75.00	964.0	m	1789.8			1789.2
80.71	919.6	mw	1834.2	$\nu_{18} + \nu_{12}$	e'	1834.4
81.14	916.1	mw	1837.7			1837.5
83.19	899.9	vw	1853.9	$2\nu_5$?	a_1'	1855.8
84.27	891.7	vw	1862.1	$\nu_5 + \nu_{17}$	e'	1864.5
84.93	886.6	vw	1867.2			1868.6
86.83	871.8	m	1882.0	$\nu_5 + \nu_1$	a_2''	1882.4
87.97	863.0	w	1890.8	$\nu_{17} + \nu_1$	e''	1891.3
90.45	845.3	w	1908.5	$2\nu_1$	a_1'	1909.2
93.05	823.5	mw	1930.3	$\nu_5 + \nu_{12}$	a_2''	1930.8
94.18	814.8	vw	1939.0	$\nu_{17} + \nu_{12}$	e''	1939.5
96.52	796.7	w	1957.1	$\nu_{12} + \nu_1$	a_1'	1957.5
3604.60	734.4	vvw	2019.4	?		
06.13	722.6	mw	2031.2	$\nu_4 + \nu_{16} + \nu_1$?	e'	2036.0
06.91	716.6	m	2037.2			2043.5
08.03	708.0	vvw	2045.8	?		

TABLE VI. (Cont'd)

λ_{air}(Å)	ν_{vac}(cm^{-1})	Relative intensity	$\Delta\nu$(cm^{-1})	Assignment	Vibrational symmetry in $\underset{\sim}{D}_{3h}$	Predicted harmonic value (cm^{-1})
3608.59	27,703.7	mw	2050.1			
08.88	701.5	mw	2052.3	$\nu_9 + \nu_1$	e′	
09.27	698.8	m	2055.0	$\nu_{10} + \nu_{16} + \nu_1$	e′ + a′$_1$ + a′$_2$	
09.67	695.8	m	2058.0			
09.92	693.5	m	2060.3			
12.23	675.8	vw	2078.0	$\nu_4 + \nu_{16} + \nu_{12}$?	e′	2084.8
13.08	669.3	w	2084.5			2093.8
13.74	664.3	vvw	2089.5	?		
14.12	661.4	vw	2092.4	?		
14.62	657.5	vvw	2096.3			
14.95	655.0	vvw	2098.8	$\nu_9 + \nu_{12}$	e′	
15.45	651.2	w	2102.6			
15.80	648.5	mw	2105.3	$\nu_{10} + \nu_{16} + \nu_{12}$	e′ + a′$_1$ + a′$_2$	
16.05	646.6	w	2107.2			
17.42	636.1	vvw	2117.7	?		
23.59	589.1	vvw	2164.7	?		
24.33	583.4	vvw	2170.4	?		
26.60	566.2	vvw	2187.6	?		
27.37	560.3	vvw	2193.5	?		
28.83	549.2	vvw	2205.6	?		

TABLE VI. (Cont'd)

λ_{air}(Å)	ν_{vac}(cm^{-1})	Relative intensity	$\Delta\nu$(cm^{-1})	Assignment	Vibrational symmetry in $\underset{\sim}{D}_{3h}$	Predicted harmonic value (cm^{-1})
3630.37	27,537.6	w	2216.2	$\nu_{11} + \nu_{10} + \nu_1$	e′	2219.0
30.93	533.3	vw	2220.5			2223.5
36.21	493.3	vvw	2260.5	$\nu_{11} + \nu_{10} + \nu_{12}$; $\nu_{10} + \nu_6 + \nu_1$		
36.69	489.7	vw	2264.1	ν_7; $\nu_{16} + \nu_5 + \nu_1$		
37.32	484.9	w	2268.9	$\nu_8 + \nu_4$; $\nu_{16} + \nu_{17} + \nu_1$		
38.09	479.1	w,b	2274.4			
39.14	471.2	vw	2282.6	ν_{13}		
40.08	464.1	w,b	2289.7	$\nu_8 + \nu_{10}$	e″ + a″$_1$ + a″$_2$	
40.64	459.9	w,b	2293.9			
41.80	451.1	vw	2302.7			
43.14	441.1	vw,b	2312.7	$\nu_6 + \nu_{12} + \nu_{14}$		
44.41	431.5	vvw	2322.3	$2\nu_{16} + \nu_{12} + \nu_{11}$		
44.97	427.2	vvw	2326.6	$2\nu_{16} + \nu_8$		
45.93	420.0	vvw	2333.8	$\nu_{19} + \nu_{17}$		
47.40	409.0	w	2344.6			
47.55	407.1	w	2346.6			
48.44	401.2	vw, b	2352.6			
50.02	389.3	m	2364.5	$\nu_{19} + \nu_1$	e′	2365.4
50.82	383.3	w	2370.5	$\nu_6 + \nu_{18} + \nu_1$;	e′ + a′$_1$ + a′$_2$	
51.81	375.9	w	2377.9	$\nu_4 + \nu_{10} + \nu_1$	e′	
52.40	371.5	mw	2382.3			

TABLE VI. (Cont'd)

λ_{air}(Å)	ν_{vac}(cm^{-1})	Relative intensity	$\Delta\nu$(cm^{-1})	Assignment	Vibrational symmetry in D_{3h}	Predicted harmonic value (cm^{-1})
3656.52	27,340.6	mw	2413.2	$\nu_{19} + \nu_{12}$	e′	2413.7
57.86	330.6	vw	2423.2	$\nu_6 + \nu_{18} + \nu_{12}$	e′ + a′$_1$ + a′$_2$	
58.50	325.8	vw	2428.0	$\nu_4 + \nu_{10} + \nu_{12}$	e′	
59.04	321.8	vw	2432.0	$\nu_{11} + \nu_5 + \nu_1$	a′$_1$	
60.84	308.4	vvw, b	2445.4	?		
61.79	301.3	vw	2452.5	$\nu_{11} + 2\nu_1$	a″$_2$	2455.4
64.49	281.2	vw, vb	2472.6	?		
65.85	273.0	vvw	2480.8	?		
65.96	270.2	vvw	2483.6	$\nu_{11} + \nu_{12} + \nu_{17}$	e′	2484.4
67.63	257.8	ms	2496.0	$\nu_6 + 2\nu_1$	e′	
67.83	256.3	ms	2497.5	$(\nu_8 + \nu_5)$	e″	
68.71	249.7	vw	2504.1	?		
69.15	246.4	mw	2507.4	$\nu_8 + \nu_{17}$(?)	e″ + a″$_1$ + a″$_2$	2508.3
69.89	241.0	vw	2512.8			2512.4
70.49	236.6	mw, vb	2517.2	?		
71.54	228.8	vs, b	2525.0	$\nu_8 + \nu_1$	e′	2525.8
72.56	221.2	vw	2532.6	?		
73.46	214.5	vw	2539.1	?		
74.04	210.2	vw	2543.6	?		

TABLE VI. (Cont'd)

λ_{air}(Å)	ν_{vac}(cm^{-1})	Relative intensity	$\Delta\nu$(cm^{-1})	Assignment	Vibrational symmetry in $\underset{\sim}{D}_{3h}$	Predicted harmonic value (cm^{-1})
3677.84	27,182.2	s	2571.6	$\nu_8 + \nu_{12}$	e′	2574.1
81.34	156.3	mw, vb	2597.5	$\nu_8 + \nu_1 + 72.0$		
82.77	145.7	vw	2608.1	$\nu_4 + 2\nu_1$	a_2''	2613.1
85.19	127.9	vw	2625.9	$\nu_{10} + 2\nu_1$?		2632.0
86.44	118.7	vw	2635.1	$\nu_6 + 2\nu_{11} + \nu_1$	e′	2638.9
86.66	117.1	vw	2636.7			2639.6
87.5	111.3	w, vb	2643.5	$\nu_8 + \nu_{12} + 71.9$		
88.67	102.4	vvw	2651.4	?		
89.22	098.3	vvw	2655.5	?		
89.71	094.7	vvw	2659.1	?		
90.32	090.3	m-b	2663.5	$\nu_8 + 2\nu_{11}$	e′	2664.1

†Square brackets connect possible Fermi resonances.

‡Splitting only resolved at higher resolution.

TABLE VII. Summary of the sym-$C_6H_3D_3$ data (cm^{-1})

D_{3h} symmetry class	Vibration number	Fundamental frequency gas[a]	liquid[a]	solid[b]		Site splitting
a_1'	ν_1	(956)	955	954.6		
	ν_2	(3074)	(3062)	3046.3		
	ν_{12}	(1004)	1003	1002.9		
	ν_{13}	(2294)	2282	2281.4		
a_2''	ν_4	697	697	703.9		
	ν_5	917	918	927.8		
	ν_{11}	531	533	546.2		
e'	ν_6	594	594	591.8	593.5	1.7
	ν_7	2282	2274	2269.0	2274	5
	ν_8	1580	1575	1571.2	1572.2	1.0
	ν_9	1101	1101	FR		
	ν_{18}	833	833	831.5	834.6	3.1
	ν_{19}	1414	1412	1410.8		<1
	ν_{20}	3063	3553	3060.6		<3
e''	ν_{10}	(707)	711	718.2	722.7	4.5
	ν_{16}	(370)	375	[378]	[387]	[8.5]
	ν_{17}	(924)	(926)	936.6	940.7	4.1[c]

[a] Ref. 26. Values in parentheses are calculated.

[b] Not corrected for possible Fermi resonance (FR). Values in brackets are inferred from combinations.

[c] See text.

TABLE VIII. Analysis of the C_6H_5D phosphorescence

λ_{air} (Å)	ν_{vac} (cm^{-1})	Relative intensity	$\Delta\nu$ (cm^{-1})	Assignment[a]				Vibrational symmetry in C_{2v}	Predicted harmonic value (cm^{-1})
3367.85	29690.3	w	0	$0,0^1$	$0,0^2$				
67.11	683.8	w	6.5			$0,0^3$			
3436.53	090.8	vw, b	599.5	599.5			ν_{6a}	a_1	
37.37	083.7	vw, b	606.6			600.1	ν_{6b}	b_1	
39.14	068.8	vw, b	621.5	621.5			ν_{11}	b_2	
40.11	060.6	vw, b	629.7			623.2			
48.81	28987.2	w	703.1	703.1			ν_4	b_2	
49.60	980.6	w	709.7			703.2			
66.88	836.1	vw	854.2	854.2			(ν_{10a})	a_2	
67.23	833.2	w	857.1		857.1				
68.15	825.6	w	864.7			858.2	ν_{18b}	b_1	
76.86	755.3	vw	937.0	937.0			ν_{17b}	b_2	
77.56	747.5	vw	942.8			936.3			
81.95	711.3	w	979.0	979.0			ν_1	a_1	
82.78	704.4	w	985.9			979.4			
84.09	693.7	w	996.6	996.6			ν_5	b_2	
84.21	692.7	w	997.6		997.6				
84.99	686.2	mw	1004.1			997.6			

TABLE VIII. (Cont'd)

λ_{air} (Å)	ν_{vac} (cm^{-1})	Relative intensity	$\Delta\nu$ (cm^{-1})	Assignment[a]				Vibrational symmetry in C_{2v}	Predicted harmonic value (cm^{-1})
3493.76	28614.3	w	1076.0	1076.0			ν_{15}	b_1	
94.76	606.1	w	1084.2			1077.7			
3503.58	534.1	m	1156.2	1156.2			ν_{9b}	b_1	
04.39	527.5	mw	1162.8			1156.3			
05.09	521.8	mw	1168.5	1168.5			$3\nu_{16}$	b_2	
05.43	519.0	mw	1171.3		1171.3		ν_{9a}	a_1	
06.07	513.8	w	1176.5	1176.5			$(\nu_{16b}+\nu_{10a})$	b_1	
06.21	512.2	m	1178.1			1171.6	ν_{9a}	a_1	
07.51	510.3	w	1180.0	1180			$3\nu_{16}$	b_2	
07.90	499.0	vw	1191.3			1184.8	$(\nu_{16b}+\nu_{10a})$	b_1	
21.08	392.3	vvw	1297.5	1297.5			ν_3	b_1	
21.95	385.3	vvw	1305.0			1298.5			
23.88	369.7	vw	1320.6	1320.6			ν_{14}	b_1	
24.43	365.2	vw	1325.1			1318.4			
39.72	242.8	vw	1447.5				ν_{19b}	b_1	
40.56	236.1	vw	1454.2			1417.7			
53.27	135.0	vw, b	1555.3	1555.3			$\nu_{11}+\nu_{17b}$	a_1	1558.6
54.15	128.1	vw, b	1562.7			1555.7			1566.0

TABLE VIII. (Cont'd)

λ_{air} (Å)	ν_{vac} (cm^{-1})	Relative intensity	$\Delta\nu$ (cm^{-1})	Assignment[a]			Vibrational symmetry in C_{2v}	Predicted harmonic value (cm^{-1})
3555.41	28118.1	s	1572.2	1572.2		$(\nu_6+\nu_1)$	b_1, a_1	
55.68	115.9	s	1574.4	1574.4		$\nu_8 b$	b_1	
56.39	110.3	s	1580.0		1573.5	$(\nu_6+\nu_1)$	b_1, a_1	
56.55	109.1	s	1581.2		1574.7	$\nu_8 b$	b_1	
57.67	100.2	s	1590.1	1590.1		$\nu_8 a$	a_1	
58.52	093.5	s	1596.8		1590.3			
64.38	047.3	vw, b	1643.0			$\nu_8 b+69.7$		
66.52	030.5	vw, b	1659.8			$\nu_8 a+69.7$		
69.31	008.6	w	1681.7	1681.7		$\nu_4+\nu_1$	b_2	1682.1
70.19	001.7	w	1689.6		1683.1			1689.1
81.91	27910.1	vw	1780.2	1780.2		$(\nu_{10}b+\nu_1)$	b_2	
82.57	905.0	vw	1785.3		1778.8			
89.19	853.5	vw, b	1836.8	1836.8		$\nu_{18}b+\nu_1$	b_1	1833.2 1836.1
90.13	846.2	vw	1844.1		1837.6			1844.1
99.29	775.4	vw	1914.9	1914.9		$\nu_{17}b+\nu_1$	b_2	1916.0
3600.21	768.3	vw	1922.0		1915.5			1922.0
04.73	733.4	vw	1956.9	1956.9		$2\nu_1$	a_1	1958.0
05.68	726.1	vw	1964.2		1957.3			1965.3

TABLE VIII. (Cont'd)

λ_{air} (Å)	ν_{vac} (cm^{-1})	Relative intensity	$\Delta\nu$ (cm^{-1})	Assignment[a]				Vibrational symmetry in C_{2v}	Predicted harmonic value (cm^{-1})
3607.12	27715.0	w	1975.3	1975.3					1975.6
07.25	714.0	w	1976.3		1976.3		$\nu_5+\nu_1$	b_2	1976.6
08.09	707.6	w	1982.7			1975.7			1983.5
17.50	635.5	vw	2054.8	2054.8			$\nu_{15}+\nu_1$	b_1	2055.0
18.62	627.0	vw	2063.3			2056.8			2063.6
28.03	555.3	m	2135.0	2135.0			$\nu_{9b}+\nu_1$	b_1	2135.2
28.92	548.6	mw	2141.7			2135.2			2142.2
29.67	542.9	mw	2147.4	2147.4			$3\nu_{16}+\nu_1$	b_2	
30.04	540.1	m	2150.2		2150.2		$\nu_{9a}+\nu_1$	a_1	
30.86	533.9	vw	2156.4				$(\nu_{16a}+\nu_{10a})+\nu_1$	b_1	
30.95	533.2	m	2157.1			2149.2	$\nu_{9a}+\nu_1$	a_1	
31.30	530.5	vw	2159.8				$3\nu_{16}+\nu_1$	b_2	
49.54	392.9	vvw	2297.4	2297.4			$(\nu_3+\nu_1)$, ν_{7a}	b_1	
49.87	390.4	vw	2299.9	2299.9			$\nu_{14}+\nu_1$	b_1	2299.6
50.38	386.6	vw	2303.7			2297.7			2304.3
66.64	265.0	vw	2425.3	2425.3			$\nu_{19b}+\nu_1$	b_1	2426.5
67.60	258.1	vw	2432.2			2425.7			
83.06	143.6	s	2546.7	2546.7			$\nu_{8b}+\nu_1$	b_1	
83.34	141.5	s	2548.8		2548.8		$\nu_6+2\nu_1$	b_1, a_1	
84.18	135.3	s	2555.0			2547.5			

TABLE VIII. (Cont'd)

λ_{air} (Å)	ν_{vac} (cm^{-1})	Relative intensity	$\Delta\nu$ (cm^{-1})		Assignment[a]		Vibrational symmetry in C_{2v}	Predicted harmonic value (cm^{-1})
3686.20	27120.5	s	2569.8	2569.8		$\nu_8a+\nu_1$	a_1	2569.1
87.18	113.3	s	2577.0		2570.5			2582.7

[a] Bands in Fermi resonance are connected by square brackets.

TABLE IX. Summary of C_6H_5D data (cm^{-1})

C_{2v} symmetry class	Vibration number	Gas[a]	Liquid[a]	Solid sites 1	2	3	Orientational effect (arbitrary) 2-1	3-2	Comments[b]
a_1	ν_1	(983)	(983)	979.0		979.4		+0.4	FR: ν_5
	ν_{8a}	(1600)	1593	1590.1		1590.3		+0.2	FR: ν_{8a}, ν_{8b} and $(\nu_6+\nu_1)$
	ν_{9a}	(1177)	1177	1171		–			FR: $(\nu_{10}+\nu_{16b})$ and 3 ν_{16b}; F
b_1	ν_3	(1295)	1291	1297.5		1298.5	0	+1.0	
	ν_{6b}	(607)	602	599.5		600.1	0	+0.6	ν_{6a} and ν_{6b} in resonance
	ν_{8b}	(1590)	1576	1575.2		–	0		FR: ν_{8a}, ν_{8b} and $(\nu_6+\nu_1)$; F
	ν_9	(1157)	1158	1156.2		1156.3	0	+0.1	
	ν_{14}	(1327)	(1325)	1320.6		1318.4	0	-2.2	
	ν_{15}	1077	1077	1076.0		1077.7	0	+1.7	
	ν_{18b}	858	857	854.2	857.1	858.2	+2.9	+1.1	FR: ν_{10a}
	ν_{19b}	1440-1490	1448	1447.5		1447.7	0	+0.2	FR: ν_{19a}

TABLE IX. (Cont'd)

C_{2v} symmetry class	Vibration number	Gas[a]	Liquid[a]	Solid sites 1	2	3	Orientational effect (arbitrary) 2-1	3-2	Comments
b_2	ν_4	698	699	703.1		703.2	0	+0.1	
	ν_5	(984)	978	996.6	997.6	997.6	+1.0	0	FR: ν_1
	ν_{11}	607	602	621.4		623.6	0	+2.2	FR: ν_6 in liquid
	ν_{17}	924	925	937.0		936.3	0	-0.7	

[a] Ref. 26 ( ) indicates calculated values.

[b] FR = Fermi resonance; F = frequency observed in the fluorescence.

Table X. Summary of p-$C_6H_4D_2$ Data (cm^{-1})

D_{2h} symmetry class	Vibration number	Gas[a]	Liquid[a]	Solid sites 1	2	3	Orientational effect (arbitrary) 2-1	3-2
b_{3g}	ν_4	(633)	633	637.9	641.2	643.6	+3.3	+ 2.4
	ν_{10b}	(739)	736	744.3	742.4	742.9	-1.9	+ 0.5
	ν_3	(1307)	1311	1310.2	1311.5	1308.1	+1.3	- 3.4
a_{1g}	ν_{9a}	(1177)	1173	1171.4	1172.9	1171.8	+1.5	- 1.1
b_{2g}	ν_{9b}	(913)	908	908.4	906.5	909.1	-1.9	+ 2.6
$^1B_{3u}$	0, 0			29721.4	29723.3	29734.9	+1.9	+12.6

[a]Ref. 26 ( ) indicates calculated values.

Table XI. $^1B_{2u} \longleftarrow {}^1A_{1g}$ Electronic Transition Energy for Isotopic Guests in a C_6D_6 Host Crystal at 4.2°K.

	mixed crystal[a] (cm^{-1})		gas[b] (cm^{-1})
	$^{12}C_6H_nD_{6-n}$	$^{13}C\,^{12}C_5H_nD_{6-n}$	$^{12}C_6H_nD_{6-n}$
C_6H_6	37853.3	37856.9	38086.1
C_6H_5D	37885.2 37884.0	37888.8 37887.7	38124
p-$C_6H_4D_2$	37915.7 37912.9		38154
sym-$C_6H_3D_3$	37947.9	37951.4	38184

[a] Uncorrected for interaction with the C_6D_6 host.

[b] The C_6H_6 value is from Ref. 18. For the other isotopes the 0,0 is taken from Ref. 21.

Table XII. Analysis of the $^1B_{2u} \longleftarrow {}^1A_{1g}$ Absorption Spectrum of 1% C_6H_6 in C_6D_6 at 4.2°K.

λ_{air}	ν_{vac}	$\Delta\nu$	Assignment	Gas $\Delta\nu$
2641.00	37,853.3	0	0-0	
2605.34	38,371.3	518.0	ν_6'	522.4[a]
2605.20	38,373.4	520.1		
2577.89	38,779.8	926.5	ν_1'	923[b]
2543.9	39,297(b)	1444	$\nu_1' + \nu_6'$	

[a] Ref. 18.

[b] F. M. Garforth and C. K. Ingold, J. Chem. Soc., 1948, 417

Table XIII. Structure Observed Near the Electronic Origin for C_6H_6 and C_6H_5D at Higher Concentrations in a C_6D_6 Host.

	C_6H_6†			C_6H_5D†		
	ν cm^{-1}	I	Assignment	ν cm^{-1}	I	Assignment
a‡	37,860.9	w	$^{13}C_2{}^{12}C_4H_6$	37,892.5	w	$^{13}C_2{}^{12}C_4H_5D$
				37,891.6	w	
b	37,856.9	s	$^{13}C\,C_5H_6$	37,888.8	s	$^{13}C^{12}C_5H_5D$
				37,887.7	s	
c	~37,854.1	w,sh		—		
d	37,853.3	vs	Monomer	37,885.2	vs	Monomer
				37,884.0	vs	
e	37,852.3	w		—		
f	37,851.2	w		37,882.7	w	
				37,881.8	w	
g	37,848.6	w	Resonance Pair	37,880.0	w,b	Resonance Pair

†0.04% guest in a ~ 2 mm C_6D_6 host crystal.

‡See Fig. 8.

Table XIV. Change in the 1600 cm^{-1} ν_8 and $\nu_6 + \nu_1$ Fermi Couple Splitting with Totally Symmetric $n\nu_1$ Additions

n	$\nu_8 + \nu_1$ (cm^{-1})	$(\nu_6 + \nu_1) + n\nu_1$ (cm^{-1})	Site splitting (cm^{-1})	Fermi splitting (cm^{-1}) solid[a]	gas[b]
0	1584.3	1602.8	1.2	19.1	20
		1604.0			
1	2568.1	2594.3	1.2	26.8	26
		2595.5			
2	3551.6	3583.5	1.3	32.5	31
		3584.8			
3	4534.1	4571.5[c]		37.4	37
ν_6		606.3	3.1		
		609.4			

[a]The mean of the split $(\nu_6 + \nu_1) + n\nu_1$ component is used to calculate the Fermi splitting.

[b]F. M. Garforth, C. K. Ingold and H. G. Poole, J. Chem. Soc., 1948, 427.

[c]This band is too weak to observe any splitting.

Caption for Fig. 1.

Modified "Bridgman-type" sample cell.

SAMPLE CELL

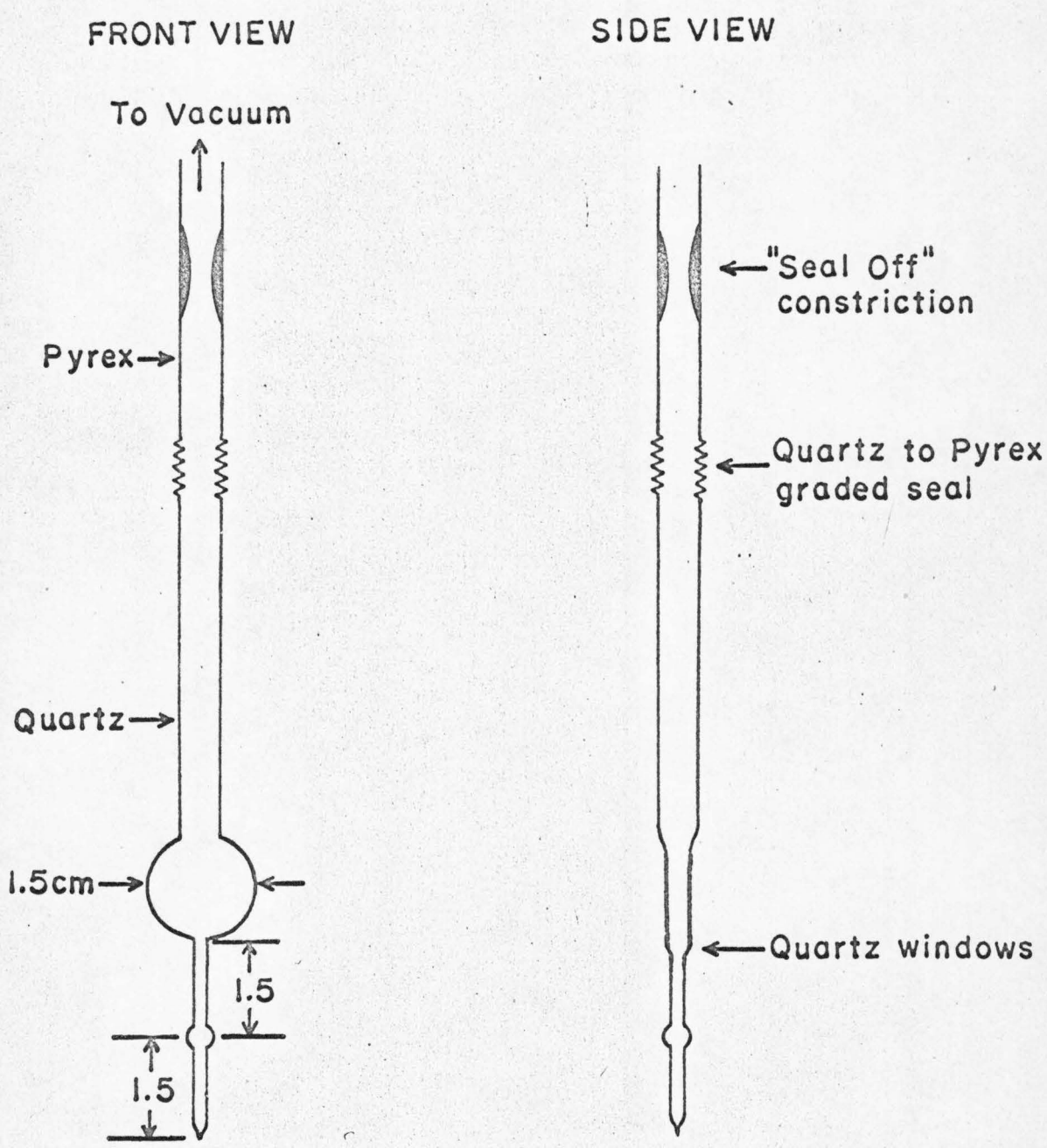
FRONT VIEW
SIDE VIEW
To Vacuum
Pyrex
Quartz
1.5cm
1.5
1.5
"Seal Off" constriction
Quartz to Pyrex graded seal
Quartz windows